Public Works Canada
Travaux publics Canada

Architectural and Engineering Services
Services d'architecture et de génie

AES/SAG 1-2:88-12

FEASIBILITY STUDY OF FULL SCALE ICEBERG IMPACT TESTS

July 1988

Canada

89-01822/

Public Works Canada
Architectural and Engineering Services
Technology

AES/SAG 1-2:88-12

FEASIBILITY STUDY OF FULL SCALE ICEBERG IMPACT TESTS

July 1988

Preparation Agency:
Center for Cold Ocean Resources Engineering
Memorial University of Newfoundland

Sponsoring Agency:
Panel for Energy Research
and Development (PERD)
Marine Product Line, Headquarters
Project Manager: M.S. Cheung

The contents of this document represent the views of the authors and are not necessarily the views or policies of the Department of Public Works.

The Minister of Public Works makes no representation or warranty, express or implied, with respect to this publication or the programs or information described in this publication, their quality, merchantability, or fitness for any particular purpose, or their adequacy to produce any particular result. In no event shall the Minister or Her Majesty the Queen in right of Canada, Her employees, servants or agents be legally liable to any person or persons for any damage, whether direct, indirect or consequential, resulting from the use of said publication or the programs or the information contained herein.

Published by Architectural and Engineering Services
Public Works Canada

© Minister of Supply and Services Canada 1988

Cat. No. W62-11/88-12E

ISBN 0-662-16559-4

Public Works Canada / Travaux publics Canada

DOCUMENT DATA

1. Document Title FEASIBILITY STUDY OF FULL SCALE ICEBERG IMPACT TESTS	2. Control Number AES/SAG 1-2:88-12
	3. Date JULY 1988
4. Author(s) D. Duthinh, J. Newell, A. Steel, W. Winsor	5. Consultant's Ref. No.
6. Project Manager M.S. Cheung	7. Discipline Series No.
8. Preparation Agency and Address Centre for Cold Ocean Resources Engineering Memorial University of Newfoundland St. John's, Newfoundland A1B-3X5	9. Document Type Technical Report
	10. No. of Pages 164
11. Sponsoring Agency and Address Panel for Energy Research and Development (PERD) and Public Works Canada, Marine Product Line Sir Charles Tupper Bldg., Riverside Drive Ottawa, Ontario K1A 0M2	12. PWC File No. 6200-31
	13. PWC Project No. 603534
14. Supplementary Notes	15. SSC Publication No. W62-11/88-12E
	16. ISBN 0-662-16559-4

17. Abstract

This report establishes that full scale large iceberg impact experiments are feasible. Such experiments would be an advance in ice mechanics and in the prediction of iceberg impact forces on offshore structures.

The report identifies potential sites complying to specified criteria. In all twenty-one possible locations have been identified along the coast of Newfoundland and Labrador. The recommended location is Deep Water Point, near St. Anthony, on the northern tip of Newfoundland. This location meets the required criteria having a relatively predictable iceberg population, steep cliffs, deep water alongshore and is in close proximity to a roadway and a local settlement.

Hydraulic model tests were used to determine the most practical and efficient method of conducting the experiment, while ensuring iceberg impact on the target area. Various towing/winching configurations were tested while simulating alongshore ocean currents. The recommended experimental method is to tow an iceberg into the cliff with two tugboats. Model tests confirm that this method provides the best control, stability and reliability to impact the iceberg on target.

The report also discusses the phenomena that should be monitored and instrumentation requirements. The predicted cost of such a project is broken down into various project phases, rough cost estimations have been made but may fluctuate significantly depending on the location that is selected and the extent of instrumentation.

18. Distribution Statement Copies are available from: Documentation Centre Public Works Canada Sir Charles Tupper Bldg. Riverside Drive Ottawa, Ontario K1A 0M2	19. Keywords Iceberg impacts; ice forces; ice/structure interaction	
	20. Documentation Centre Catalogue No. MA111	21. Price no charge

DPW 2398 (86/09)

Travaux publics Canada | Public Works Canada

FICHE SIGNALÉTIQUE DE DOCUMENT

1. Titre du document FEASIBILITY STUDY OF FULL SCALE ICEBERG IMPACT TESTS	2. Numéro de contrôle AES/SAG 1-2:88-12
	3. Date Juillet 1988
4. Auteur (s) D. Duthinh, J. Newell, A. Steel, W. Winsor	5. No de réf. du conseil
6. Chargé de projet M.S. Cheung	7. No de la collection technique
8. Nom et adresse de l'organisme rédacteur Centre for Cold Ocean Resources Engineering Memorial University of Newfoundland St. John's, Newfoundland A1B 3X5	9. Type de document Rapport technique
	10. Nombre de page 127
11. Nom et adresse de l'organisme promoteur Comité de la recherche et du développement énergétiques et Travaux publics Canada, Travaux maritimes, Immeuble Sir-Charles-Tupper, Promenade Riverside, OTTAWA (Ontario) K1A 0M2	12. No de dossier de TPC 6200-31
	13. No de projet de TPC 603534
14. Notes	15. No de publication de ASC W62-11/88-12E
	16. ISBN 0-662-16559-4

17. Résumé

On démontre dans ce rapport la faisabilité d'expérience à grande échelle pour l'étude de l'impact des icebergs. De telles expériences feraient progresser les sciences de la mécanique des glaces et de la prévision de la force d'impact des icebergs sur les structures au large des côtes.
On indique dans le rapport des endroits qui conviendraient, suivant des critères précis, pour la réalisation de ces expériences. On en a reconnu au total 21 sur les côtes de Terre-Neuve et du Labrador. L'emplacement recommandé est la pointe Deep Water, près de St. Anthony, à l'extrémité nord de Terre-Neuve. Il satisfait aux critères établis, puisqu'on y trouve une population d'icebergs relativement prévisible, des falaises abruptes ainsi que des zones d'eau profonde le long du rivage et que l'emplacement est à proximité d'une route et d'une agglomération.
Des essais sur modèle hydraulique ont été effectués afin de déterminer la méthode d'essai la plus pratique et la plus efficiente. On a essayé diverses configurations de remorquage-tirage des icebergs tout en simulant les courants océaniques près de la côte. La méthode recommandée consiste à tirer l'iceberg vers la falaise au moyen de deux remorqueurs. Des essais sur modèle ont confirmé la supériorité de cette méthode en ce qui concerne le contrôle, la stabilité et la fiabilité de l'impact sur la cible.
Le rapport traite des phénomènes qui devraient être suiviset des instruments requis. Le coût d'un tel projet a été calculé pour les diverses phases; des estimations approximatives sont fournies, mais les fluctuations peuvent être importantes suivant l'emplacement choisi et les instruments employés.

18. Diffusion Exemplaires disponibles du: Centre de documentation Travaux publics Canada Imm. Sir-Charles-Tupper, Prom. Riverside, OTTAWA, Ontario K1A 0M2	19. Mots clés Impacts des icebergs; mécanique des glaces; interactions glace structure.	
	20. No de catalogue du centre de documentation MA111	21. Prix Gratuit

MTP 2398 (86/09)

4*S/R-NOV/99.1

PREFACE

This report is one of several reports on the research work in the field of marine engineering, identified and managed by the Marine Product Line and Technology Resources groups of Public Works Canada, with funds provided by the Interdepartmental Panel on Energy Research and Development (PERD).

PERD was established in 1974 to coordinate research on energy by the Federal Government with objectives to provide, in conjunction with efforts in the private sector and the provinces, the technical basis for:

- maintaining oil self-sufficiency over the short term, in view of dwindling conventional supplies;
- developing a diversified energy economy, less dependant on oil and gas in the mid-term; and
- making Canadians less reliant on non-renewable energy sources in the long term.

The research work undertaken by Public Works Canada in Marine Engineering with funds from PERD has been directed particularly toward the following two main topics:

1. Ice/Structure Interaction
2. Construction and Towing of Reinforced Concrete Caissons in the Arctic.

This report is being published with a view to enhancing the technology in the field of Marine Engineering and contributing toward the objectives of PERD.

TABLE OF CONTENTS

PREFACE		i
LIST OF TABLES		v
LIST OF FIGURES		vi
LIST OF MATHEMATICAL NOTATIONS		viii
CONCLUSIONS AND RECOMMENDATIONS		x
1.	LARGE SCALE ICEBERG IMPACT EXPERIMENT	1
	1.1 Background	1
	1.2 Relation to Energy Development	1
	1.3 Requirements for Large Scale Iceberg Impact Experiments	2
	1.4 Instrumentation Requirements	4
	1.5 Overall Program and Cost Estimate	6
2.	SITE SELECTION FOR A FULL SCALE ICEBERG IMPACT EXPERIMENT	10
	2.1 Introduction	10
	2.2 Iceberg Availability	10
	2.3 Identification of Potential Sites	19
	2.4 Logistical Considerations	22
	2.5 Recommended Site	26
	2.6 Preliminary Site Survey	26
	2.7 Further Work Required	36
3.	METHODS OF TOWING ICEBERGS	38
	3.1 Tow Boats	38
	3.2 Winches	39
	3.3 Track-type Tractors	42
	3.4 Towing Lines	44

TABLE OF CONTENTS (cont...)

4.	MECHANICAL REQUIREMENTS FOR ICEBERG TOWING	47
5.	HYDRODYNAMICS OF ICEBERG MOTION AND HYDRAULIC MODEL TESTING	51
	5.1 Drag Force	51
	5.2 Added Mass	56
	5.3 Theory of Similarity	57
6.	MODEL TESTS	61
	6.1 Introduction	61
	6.2 Model Design	61
	6.3 Experimental Arrangement	63
	6.3.1 Wave Tank and Carriage	63
	6.3.2 String and Pulley Arrangement	68
	6.3.3 Data Acquisition System	69
	6.4 Drag Force Tests	69
	6.4.1 Free Moving Model	69
	6.4.2 Rigid Model	70
	6.5 Iceberg Impact Tests	73
	6.5.1 Continuous Towing, Double Pulley	74
	6.5.2 Drift, Double Pulley	78
	6.5.3 With Current, Double Pulley	83
	6.5.4 Modified Pendulum, Single Pulley	91
	6.5.5 Pendulum Constant Line Length	91
	6.5.6 Vertical Cliff Tests	98
	6.5.7 Additional Tests	102
	6.6 Iceberg Free Drift Tests	102
	6.7 Summary of Results and Conclusions	103

APPENDIX

I	Mechanical Requirements for Large Scale Ice Indentation	109
II	Calculation of Towing Force Caused by Falling Weights	112
III	Statement of Work From DSS, Canada	113

LIST OF TABLES

1.1	Required Velocity and Drag	2
3.1	ETW-350 Mooring Winch	40
3.2	DTW-100 Towing Winch	41
3.3	Rates Based on 8 Hour Day	42
3.4	Wire Rope Characteristics	44
3.5	Polypropylene Rope Characteristics	45
6.1	Drag Coefficients at Various Model Velocities	74
6.2	Test Summary Sheets	75
6.3	Test Summary Sheets	76
6.4	Model Velocity	77

LIST OF FIGURES

1.1	Ice Strength, Maximum Force and Impact Energy vs. Contact Area	3
2.1	Iceberg Limits for May (source Markham, 1980)	12
2.2	Monthly Average Fluxes of Icebergs Across Each Latitude from Newfoundland to Cape Dyer	14
2.3	Iceberg Density and Sea Ice Frequency for May	15
2.4	Iceberg Density and Sea Ice Frequency for June	17
2.5	Average Iceberg Density July-October	18
2.6	Key to Hydrographic Charts for Newfoundland	20
2.7	Key to Hydrographic Charts for Labrador	21
2.8	Sites Investigated and Recommended Site	23
2.9	Section of Hydrographic Field Sheet Showing Deep Water Point Near St. Anthony	24
2.10	Newfoundland and Labrador Road Network	25
2.11	Site Evaluation	27
2.12	Section of Hydrographic Chart for St. Anthony Showing Potential Sites	29
2.13	Topographic Maps for St. Anthony Area	30
2.14	Aerial Photograph of St. Anthony Area	31
2.15	Aerial Photograph of Big Cove Area	32
2.16	Deep Water Point, Newfoundland - A Potential Site for Full Scale Iceberg Impact Tests	34
2.17	Iceberg Near St. Anthony Point	35
3.1	Performance of D8N Tractor	43
3.2	Performance of D11N Tractor	43
5.1	Drag Coefficient	55
6.0	Elevation and Plan View of Wave/Tow Tank	64

LIST OF FIGURES(cont...)

6.1	Side View of Iceberg Impact Experimental Set Up	65
6.2	Plan View of Iceberg Impact Experimental Set Up	66
6.3	Double Pulley Configuration	67
6.4	Resistance Curve for Sphere With Free Moving Model	71
6.5	Resistance Curve for Cube and Sphere With Rigid Model	72
6.6	(Test #6, 10, 12) Continuous Towing, Double Pulley Selspot Data	79
6.7	(Test #6, 10, 12) Continuous Towing, Double Pulley Selspot Data	80
6.8	(Test #6, 10, 12) Continuous Towing, Double Pulley Selspot Data	81
6.9	Selspot Co-ordinate System	82
6.10	(Test #13, 14, 18) Drift, Double Pulley, Selspot Data	84
6.11	(Test #13, 14, 18) Drift, Double Pulley, Selspot Data	85
6.12	(Test #13, 14, 18) Drift, Double Pulley, Selspot Data	86
6.13	(Test #22, 23, 50, 29) With Current, Double Pulley, Selspot Data	87
6.14	(Test #22, 23, 50, 29) With Current, Double Pulley, Selspot Data	88
6.15	(Test #22, 23, 50, 29) With Current, Double Pulley, Selspot Data	89
6.16	(Test #22, 23, 50, 29) With Current, Double Pulley, Selspot Data	90
6.17	(Test #63, 53, 64, 37, 58, 57) Modified Pendulum, Single Pulley, Selspot Data	92
6.18	(Test #63, 53, 64, 37, 58, 57) Modified Pendulum, Single Pulley, Selspot Data	93
6.19	(Test #63, 53, 64, 37, 58, 57) Modified Pendulum, Single Pulley, Selspot Data	94

LIST OF FIGURES(cont...)

6.20	(Test #63, 53, 64, 37, 58, 57) Modified Pendulum, Single Pulley, Selspot Data	95
6.21	(Test #63, 53, 64, 37, 58, 57) Modified Pendulum, Single Pulley, Selspot Data	96
6.22	(Test #63, 53, 64, 37, 58, 57) Modified Pendulum, Single Pulley, Selspot Data	97
6.23	Plan View of Pendulum. Constant Line Length Selspot Data	99
6.24	(Test #41, 45) Pendulum, Constant Line Length Selspot Data	100
6.25	(Test #41, 45) Pendulum, Constant Line Length Selspot Data	101
6.26	(Test #76, 77, 78) Free Drift Test, Selspot Data	104
6.27	(Test #76, 77, 78) Free Drift Test, Selspot Data	105
6.28	(Test #76, 77, 78) Free Drift Test, Selspot Data	106

LIST OF MATHEMATICAL NOTATIONS

Chapter 4

B^2 - $(B_0^2 + B_1^2) / M$

B_0^2 - Linear (with velocity) component of towing force

B_1^2 - Linear (with velocity) component of drag force

C^2 - C_1^2 / M

C_1^2 - Quadratic (with velocity) component of drag force

D^2 - $T + B^4 / 4C^2$

DR - Drag force - $B_1^2 V + C_1^2 V^2$

M - Iceberg mass

T - T_0 / M

T_0 - Constant component of towing force

T* - Bollard pull or towing force - $T_0 - B_0^2 V$

V - Iceberg velocity

Chapter 5

A - a measure of the area of the body.

$F_{Friction}$ - $k \rho A V^2 R^{-1/2}$

k depends on the shape of the body

L - characteristic length

R_e - LV/ν - Reynolds number

V - flow velocity

ρ - fluid density

ν - dynamic viscosity

CONCLUSIONS AND RECOMMENDATIONS

This work was undertaken to establish the feasibility of large scale (10-100m^2) iceberg impact experiments with the ultimate aim of improving the estimation of iceberg impact forces. This would be an improvement over the present calculations based on small (0.01-0.1m^2) and medium scale (0.1 - 10m^2) tests.

Site Selection

The discovery of a potential site for such experiments is one of the goals of this study. Criteria for site selection are threefold: iceberg availability, site topography and bathymetry and logistics. Twenty one possible sites were selected on the coast of Newfoundland and Labrador. The best three are in the vicinity of St. Anthony, on the northern tip of Newfoundland. The recommended site is Deep Water Point. A preliminary field survey confirmed the desirability of the site: the coast is steep, with cliffs of 45 to 60 degrees extending to 60m below water and beyond. The town of St. Anthony provides easy accommodation and easy access to the site. The iceberg density is relatively high and stable (0.39 iceberg per 100 km^2 in June). It is estimated that a search area of 23 km radius would suffice to find a suitable iceberg in June.

Towing Schemes

Various iceberg towing methods and associated equipment were looked at. Powerful winches used in construction projects and for vessel mooring have the force and speed required to tow icebergs from shore. The disadvantages are high cost, unavailability and difficult transportation to the site. Tractors on tracks are also a possibility. A pair of the largest in existence, D11N, could be used to advantage in this project. The disadvantage is poor availability. The recommended towing method is

the conventional one which uses tugboats. The advantages are crew experience, proven technology and availability. It is recommended that the tow ropes be looped through onshore pulleys so the tugs can tow seaward. Improvements in ice anchors may be necessary.

Hydraulic Model Tests

A series of model tests were performed in a tow tank to compare various towing schemes in the presence or absence of alongshore currents. The recommended scheme uses two towlines attached to pulleys on either side of the impact target. With sufficient towing force and coordination between the two towboats, impacts on target can be achieved reliably. This coordination is especially crucial when a current exists. The towlines should be released about one berg length from shore. The "pendulum" concept, which uses a single pivot point upcurrent of the target, a constant length line and the force of the current, does not work. The iceberg would hover at an angle to the cliff and not touch it. However, a modified pendulum concept works, in which the towline is pulled in, thus shortening the pivot arm during the iceberg drift. Although impacts can be generated, impacts on target cannot be assured by this method, which also requires a constant current.

Experiments were also performed in current with two towlines of unequal pull. This is essentially a combination of pendulum and winching where the line with weaker pull can be considered as the adjustable pendulum arm. This can also be considered a variation on the two equal towlines method. It worked well with experience, showing again that coordination between the towboats is essential.

Recommendations

This study shows that full scale iceberg impact experiments are

feasible. The recommended site is Deep Water Point, near St. Anthony, Newfoundland, and the recommended method is towing by two towboats with towlines looped around pulleys on either side of the instrumented impact target.

It is recommended that the next phase of this study be undertaken this summer. This phase includes a detailed site survey and current measurement. Detailed engineering and planning, including measurement and recording techniques should also be carried out.

The third phase would consist of equipment procurement, installation and the first season experiments. In these experiments the iceberg motions and deformations will be measured, but the cliff will not be instrumented. Thus hitting on target is not crucial.

The fourth and final phase would see the instrumentation of the cliff face and further impacts. Following is a preliminary schedule and cost estimate:

		Cost
Phase II: (1988)	Site survey	25K
	Detailed engineering and planning	75K
Phase III: (1989)	Equipment procurement and installation	500K
	First season tests	500K
Phase IV: (1990)	Test site construction	600K
	Full scale tests	600K
	TOTAL	2300K

The cost estimate for Phase Two is reasonably certain. However, Phases Three and Four and their costs will be better defined in Phase Two.

Chapter 1

Large Scale Iceberg Impact Experiment

1.1 Background

At present iceberg impact forces are calculated using iceberg strength values based on small scale tests. Industry's latest work using indentor equipment on a grounded iceberg in Pond Inlet only tested crushed areas up to three square metres. Experience with the loading of sea ice on arctic structures, however, indicates that the effective strength of ice is reduced as the contact area is increased. It is very plausible that iceberg ice would be affected in the same manner. If a large iceberg were to strike a fixed platform, the contact area of the crushed ice would be in the range of 300 to 600 square metres. The effective strength of this large contact area would probably be much lower than the results from small scale tests suggest. But before an engineering team can use this information in the design of platforms, real loads resulting from large scale iceberg failures must be measured.

1.2 Relation to Energy Development

Iceberg impact force is one of the main design considerations for offshore structures located in the East Coast and Grand Banks area. It is critical in terms of its impact on the safety and cost of the individual structures. Up to now, accurately predicting iceberg impact force on offshore structures is one of the major uncertainties in the safe and efficient desing of such structures. Therefore, this work was undertaken to establish the feasibility of large scale iceberg impact experiments with the ultimate aim of improving the estimation of iceberg impact forces.

1.3 Requirements For Large Scale Iceberg Impact Experiments

The following are rough estimates of the requirements for large scale iceberg impact tests. Details can be found in Appendix I.

Water depth requirements

For a cubical berg, the water depth required is approximately proportional to the cubic root of the mass. For a 100,000 tonne berg, the required water depth is 43m. If the iceberg is twice as long as wide or deep, the above draft can be halved.

Energy Requirements

Figure 1.1 shows the kinetic energy required to generate a given area of impact and the corresponding maximum impact force. These results assume an ice strength that decreases linearly with contact area. The maximum impact force is useful in the design of, say, a ship-mounted indentor of the required size.

Towing Requirements

Table 1.1 shows the required velocity and associated drag force necessary to generate various contact areas for a 100,000 tonne iceberg. Again, ice strength is assumed to follow the line shown in Fig. 1.1.

Area (m^2)	Velocity (m/s)	Drag (MN)
30	.81	0.70
90	1.30	1.75
300	2.00	4.37

Table 1.1

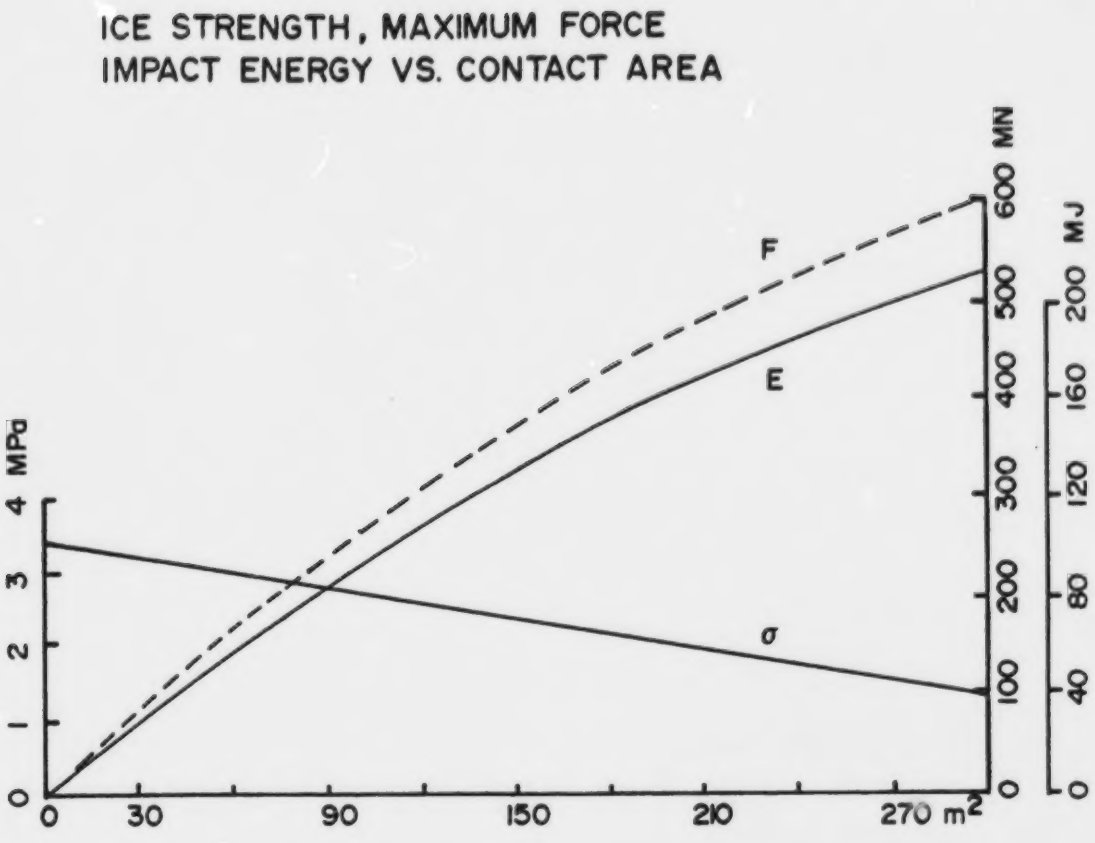

Figure 1.1 Ice Strength (σ - MPa), maximum force (F - MN), and impact energy (E - MJ) versus contact area (m^2).

1.4 Instrumentation Requirements

In preliminary full scale tests instruments will be deployed that do not require accurate guidance of the iceberg for their successful use: accelerometers and strainmeters on the iceberg, high speed photography, electronic distance meter from shore, etc... In the final tests, load panels will be deployed, once accurate guidance of the colliding iceberg can be ensured.

Iceberg Motion Sensors

Four 6 degree-of-freedom motion sensor packages have been developed at C-CORE/MUN (Lever et al. 1986). These units were specifically designed to be placed on icebergs and growlers to measure their behaviour under wave action or on contact with the seabed, depending on the circumstances. Both high capacity internal data logging and telemetry options are available. The units are of rugged construction and are designed to float free when an iceberg rolls over. These sensor packages have been successfully deployed over 30 times during the past 4 years from both helicopters and vessels, on ice masses ranging in size from a few hundred to 18 million tonnes.

One set of deployments of these instruments, during the 1985 Dynamics of Icebergs Grounding and Scouring (DIGS) experiment, captured the only full scale iceberg seabed interactions known to date, including the splitting and grounding of a multi-million tonne tabular iceberg on the Makkovik Bank (Lewis et al, 1987). The analysis of this latter event yields an estimate of the average iceberg impact pressure over an area of contact 3 orders of magnitude larger than any experiment yet conducted.

Monitoring the deformation of the ice

Even though it is probably impossible to read the stresses and strains at the failure zone, it would be interesting to embed sensors in the vicinity of the impact area in order to follow the stress distribution in the berg. The type of sensor envisaged could be of the strainmeter type or of the flat jack type. The main characteristic of the sensor which will be selected is the easiness of installation which ideally should be done remotely (dropped from an helicopter, for instance).

Instrumentation of the cliff

This is probably the most important part of the instrumentation. The first sensor candidate is a load panel similar to those used on offshore structures to monitor the ice loads (medof type or electric resistance type panels). The position and the size of each of the panels are very important in order to obtain the maximum information from one impact. A combination of several panels with various areas is one of the possible patterns. If a total area of 12 m x 12 m is instrumented, the impact zone could be covered with:

* 3 6x6 panels
* 3 3x3 panels
* 3 1.5x1.5 panels
* 4 .75x.75 panels

Since these sensors usually have a slow response to the impact, it would probably be necessary to enhance the reading with a high capacity load cell which could pick up the eventual high frequency variations of the load.

Monitoring the velocity of the berg

Besides the motion sensors which will sit on the berg, a direct reading of the displacement of the berg will also be made with EDM

equipment. Reflectors will be placed on the berg and followed by a time-pulsed EDM during the whole experiment. This equipment can be directly connected to a data acquisition terminal. Ideally, the monitoring of three points on the berg from three points on the shore will give the exact position of the berg at any moment.

Monitoring the towing load

In the eventuality of the berg being towed, the winches can be instrumented with load cells in order to estimate the towing force required to overcome the drag forces.

Photography and filming

The volume and the mass of the berg will be evaluated from aerial photography and underwater side scan sonar.

The impact zone will be filmed with a high speed camera in order to allow a good approximation of the contact area and to properly document the failure mechanisms.

1.5 Overall Program and Cost Estimate

A three-year research program has been developed. Each succeeding phase will only be undertaken depending on the recommendations of the preceding phase.

1988 Phase 1: Feasibility Study

The following chapters of this feasibility study cover the selection of a potential site for the experiment. They also discuss various possible means of towing an iceberg to a cliff with the required speed and control and the availability of such means. Finally, they describe a series of small scale experiments designed to test the various towing

schemes.

1988 Phase 2:

Phase 2 includes a detailed site survey, bathymetry and current measurements. Detailed engineering and planning, including measurement and recording techniques, are carried out.

The site survey includes an evaluation of roadwork construction and cost. The bathymetric survey fans out several kilometers from the proposed impact site, notes the presence of underwater obstructions and defines possible approach channels. Current measurements take place during May and June, the best time for the experiments.

The pulleys and their anchoring system are designed with due consideration given to grouting to the cliff and other geotechnical aspects. The sensors are basically known technology. Load panels, other stress sensors, strain arrays, accelerometers, electronic distance meters and cameras are evaluated with respect to performance and cost. Upward or side looking radars or sonars are investigated to determine the underwater profile and predict the zone of contact.

1989 Phase 3:

Phase 3 consists of equipment procurement, installation and the first season experiments which will be designed to be implemented at minimum cost. Instrumentation and recording devices will be low cost, possibly consisting of motion packages on the iceberg and distance meters (to measure deceleration), plus high-speed cameras to capture the iceberg failure process. In addition, field work on ice properties, ice anchor tests and towing trials will be performed.

The tasks to be performed in Phase 3 include:

- site preparation: road construction, pulley installation.
- mobilization: hiring of tugboats (equipped with winches and ropes), helicopter, accelerometers, cameras, radar, sonar, etc...
- experiment: deployment of instruments, towing icebergs into the cliff.

1990 Phase 4:

Phase 4 will involve instrumenting the cliff face over a large enough area to be reasonably sure of an actual impact and to obtain ice strength over large contact areas. The tasks of mobilization and experimentation are identical to Phase 3.

Cost Estimate (in thousands of dollars)

A preliminary cost estimate follows.

		Cost
Phase II: (1988)	site survey	25
	detailed engineering & planning	75
Phase III: (1989)	equipment procurement & installation	500
	first season tests	500
Phase IV: (1990)	test site construction	600
	full scale tests	600
	TOTAL	2300

The cost estimate for Phase Two is reasonably certain. However, Phases Three and Four and their costs will be better defined in Phase Two.

References

1.1 Lever, J.H. Klein, K. and Diemand, D. (1986). Design Development and Deployment of Instrument Packages to Monitor the Motion of Glacial Ice Masses at Sea. Ice Technology, Proc. of 1st Int. Conf., Springer-Verlag, New York, pp. 225-236.

1.2 Lewis, C.F.M., Parrott, D.R., Lever, J.H., Josenhans, H.W., Barrie, J.V., Woodworth-Lynas, C.M.T., Diemand, D., Carter, W. and Bass, D. (1987). The Dynamics of Iceberg Grounding and Scouring (DIGS) Experiment: Engineering Implications. Proceedings of 9th Int. Conf. on Port and Ocean Engineering under Arctic Conditions, Fairbanks, Alaska.

Chapter 2

Site Selection for A Full Scale Iceberg Impact Experiment

2.1 Introduction

This chapter details work carried out in selecting a potential site for a large scale iceberg impact experiment. The objective of the site selection process is to identify potential sites for conducting an experiment in which an iceberg of approximately 100,000 tonnes would be made to impact an instrumented underwater cliff face. The site selection criteria that were developed *a priori* can be divided into three categories; the first of which deals with the availability of icebergs, the second with the physical site selection and the last with logistical considerations. The criteria used in each of these categories are outlined below:

Iceberg availability criteria:

- the iceberg must exceed 50,000 tonnes to provide the required impact surface area and force for the experiment;
- the iceberg should be less than 300,000 tonnes to allow for towing, nearshore maneuverability and to limit the water depth required;
- the distance icebergs must be towed to reach the site should be minimized;
- the study area must have a relatively constant iceberg population, therefore, sites that occasionally experience seasons with low iceberg populations should be avoided;
- the study area should be free of sea ice during the period of the experiment.

Physical site selection criteria:

- an underwater cliff with a face as near vertical as possible;
- sufficient water depth at the base of the cliff to prevent

the iceberg from grounding prior to impact;

- an approach to the open ocean that is well charted and clear of obstructions, such as shoals, that would interfere with towing the iceberg to the site;
- a cliff face composed of consolidated material suitable for instrumenting;
- a sheltered site with relatively weak ocean and tidal currents. However, a consistent current may be used to advantage to bring the iceberg in.

Logistical criteria:

- easy access to the site from the land;
- availability of small (10-20 m) boats for hire in the vicinity;
- availability of accommodations in the vicinity;
- availability of other equipment and services in the area.

The following sections of this report outline the procedures followed in evaluating sites based on the above criteria and the results obtained to date.

2.2 Iceberg Availability

The icebergs found off the east coast of Canada are calved from the glaciers of Greenland and Ellesmere Island and are carried south by the cold Labrador Current. This current carries the icebergs south along the coast of Labrador and the east coast of Newfoundland to the southern Grand Banks where they melt. Therefore, the area of the east coast where icebergs are normally found, and where this experiment can be conducted, extends north from Cape Race (Figure 2.1). The Gulf of St. Lawrence is not suitable for the experiment since only a few icebergs penetrate the Strait of Belle Isle (Markham, 1980).

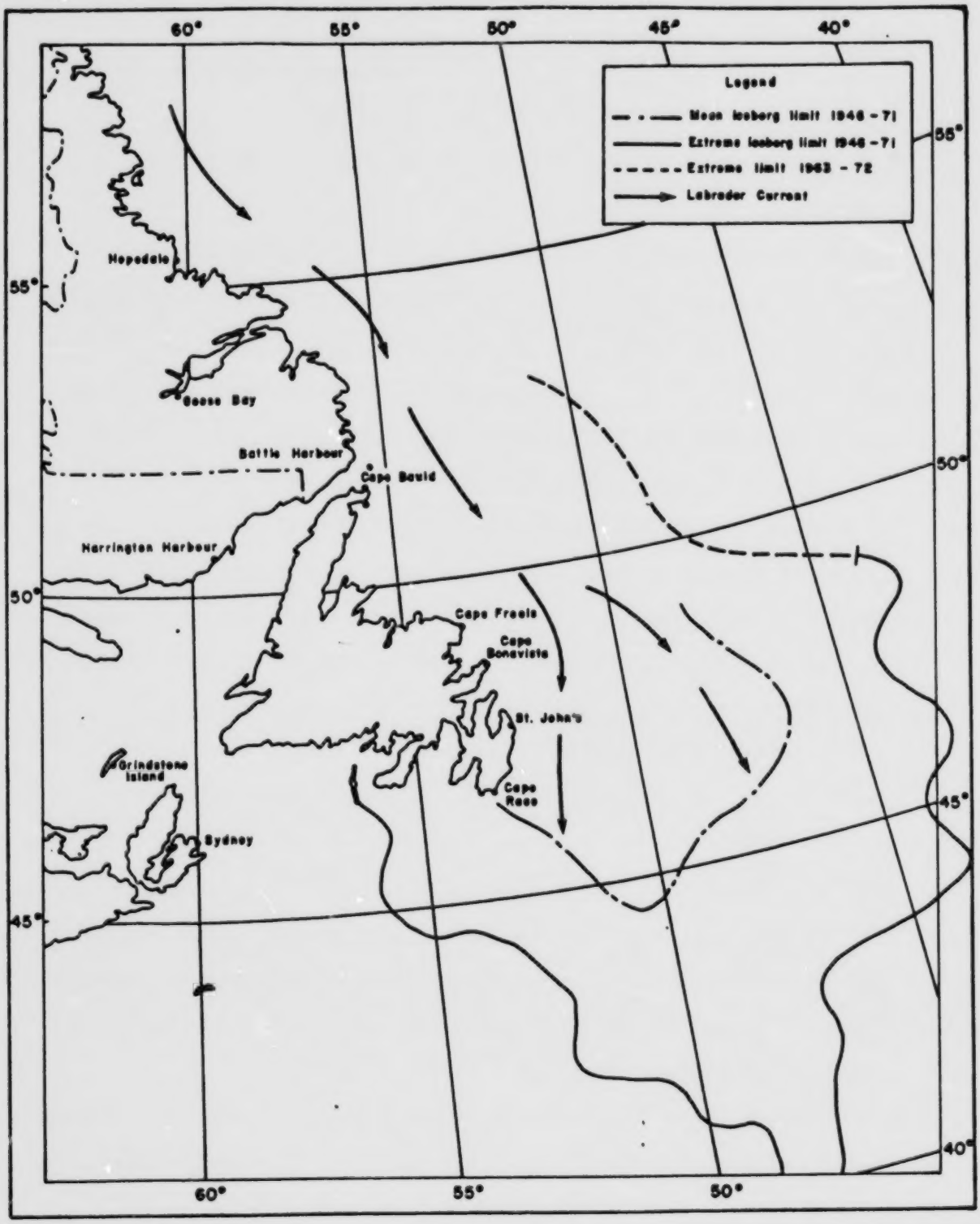

Figure 2.1 Iceberg Limits for May (source Markham, 1980).

The International Ice Patrol (IIP) has compiled statistics on the flux of icebergs south of 48N for the years since 1900 (Ketchen, 1977). These statistics indicate that the average monthly flux across 48N increases from near zero in December to over 90 in April and May then decreases to near zero again by September. Iceberg flux statistics for the Labrador coast compiled by Anderson (1971) indicate that for the area north of 53N the peak flux occurs in May and June (Figure 2.2). Based on this data it would appear that the ideal time to conduct this experiment would be between April and June.

To determine the relative favorability of various sites for conducting the experiment iceberg density statistics are required for the area from Cape Race to 60N. Gustajtis and Buckley (1977) have produced maps of average seasonal iceberg density for the Labrador coast using a data set of iceberg maps from IIP pre-season flights carried out during the 1960's and 1970's. This data set was reanalyzed by Miller and Hotzel (1984) and new maps produced. Unfortunately, similar maps are not available for the areas south of 52N. To overcome this problem iceberg statistics for the nearshore areas of eastern Newfoundland from 47N to 52N were compiled from a variety of sources to produce maps of iceberg density for May and June (Figure 2.3 and 2.4). Prior to May, sea ice and winter storms would preclude conducting the experiment off eastern Newfoundland while after June the majority of icebergs are found off Labrador and the existing data sets can be used.

Examination of ice conditions in May (Figure 2.3) indicates that sea ice normally extends south to near 49N and during 20 percent of years extends south to Cape Bonavista (48.6N). South of 49N the density of

Monthly average fluxes of icebergs across each latitude from Newfoundland to Cape Dyer (from Anderson, 1971)

FLUX ACROSS	JAN	FEB	MAR	APR	MAY	JUN	JUL	AUG	SEP	OCT	NOV	DEC	TOTAL
67N	134	118	147	143	155	156	165	161	128	123	128	139	1697
66N	134	117	150	137	153	154	165	154	120	110	117	139	1651
65N	134	117	142	140	152	153	163	154	126	102	104	137	1624
64N	134	117	141	138	149	152	161	153	113	99	97	130	1584
63N	134	117	139	137	147	149	157	146	107	95	91	123	1542
62N	107	95	139	135	145	134	124	84	61	53	57	93	1227
61N	106	95	134	135	145	138	122	86	60	49	49	87	1206
60N	103	95	128	131	144	142	124	87	51	40	40	74	1159
59N	97	94	122	130	142	141	129	90	53	26	36	59	1119
58N	87	92	115	129	139	140	135	95	62	21	26	43	1084
57N	73	88	112	128	132	137	127	99	56	20	16	31	1019
56N	49	77	112	112	133	134	122	106	68	28	10	19	966
55N	31	59	99	105	126	130	120	118	75	35	11	10	909
54N	17	39	82	98	116	118	91	81	49	32	15	6	744
53N	12	30	73	93	111	107	64	54	33	23	11	2	613
52N	9	23	62	89	106	102	42	34	22	14	9	0	512
51N	4	14	40	76	86	67	37	11	2	5	5	0	347
50N	3	8	35	66	75	32	22	5	1	2	3	0	263
49N	2	5	25	53	67	29	15	1	0	0	0	0	197
48N	0	5	18	46	57	23	8	0	0	0	0	0	157
48N 1963-69 AVERAGE/reported by International Ice Patrol	0	1	19	74	47	24	4	1	1	0	0	0	171

Figure 2.2

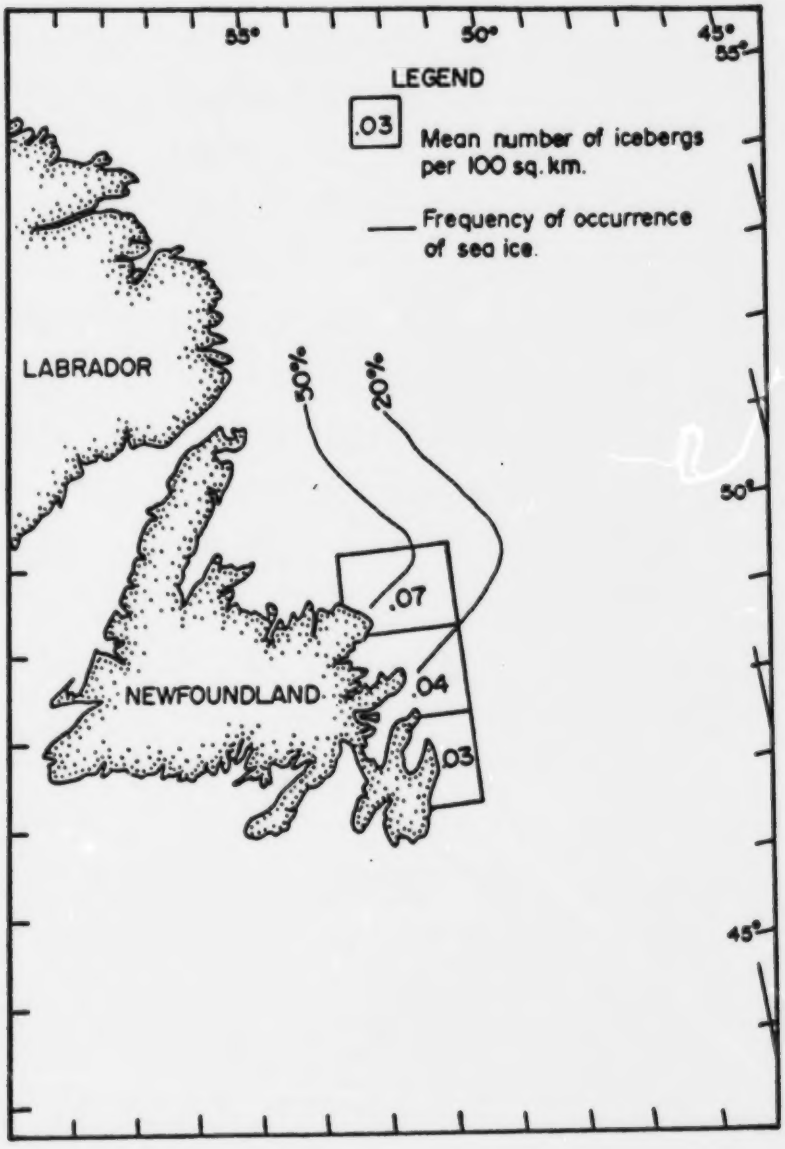

Figure 2.3 Iceberg Density and Sea Ice Frequency for May.

icebergs is relatively low (less than 0.05 per 100 sq. km). These conditions make May a relatively unattractive month for conducting the experiment. By mid-June (Figure 2.4) the southern limit of sea ice is normally north of 54N and extends south to 52N during 20 percent of years. Nearshore iceberg densities in June are greatest north of 51N with a peak near Cape Bauld (51.5N). Iceberg densities near Cape Bauld in June are nearly four times those for the Cape Freels area (49.2N). The data sets used to construct Figure 2.4 do not cover the Strait of Belle Isle area, however, other sources indicate that while average iceberg densities are relatively high in the eastern section of the Strait there is considerable year to year variability in density.

Figure 2.5 presents average iceberg densities for the Labrador coast during the months July to October (Miller and Hotzel, 1984). It is not practical to produce maps for individual months during this period due to the limited number of flights. The considerable spatial variability in density found on this map is a result of the limited data base and the high degree of variability from year to year in this area. A smoothing of the data would give more realistic values. In general, the map indicates that the highest densities are found near 55N. The map also indicates that northern Labrador is not as attractive a site for the experiment as might be supposed.

Based on the previous discussion it would appear that from the point of view of iceberg density the ideal locations and times for the experiment would be near Cape Bauld in June or any of a number of sites along the Labrador coast south of 56.5N later in the summer.

Based on the size criteria outlined previously it is clear that only

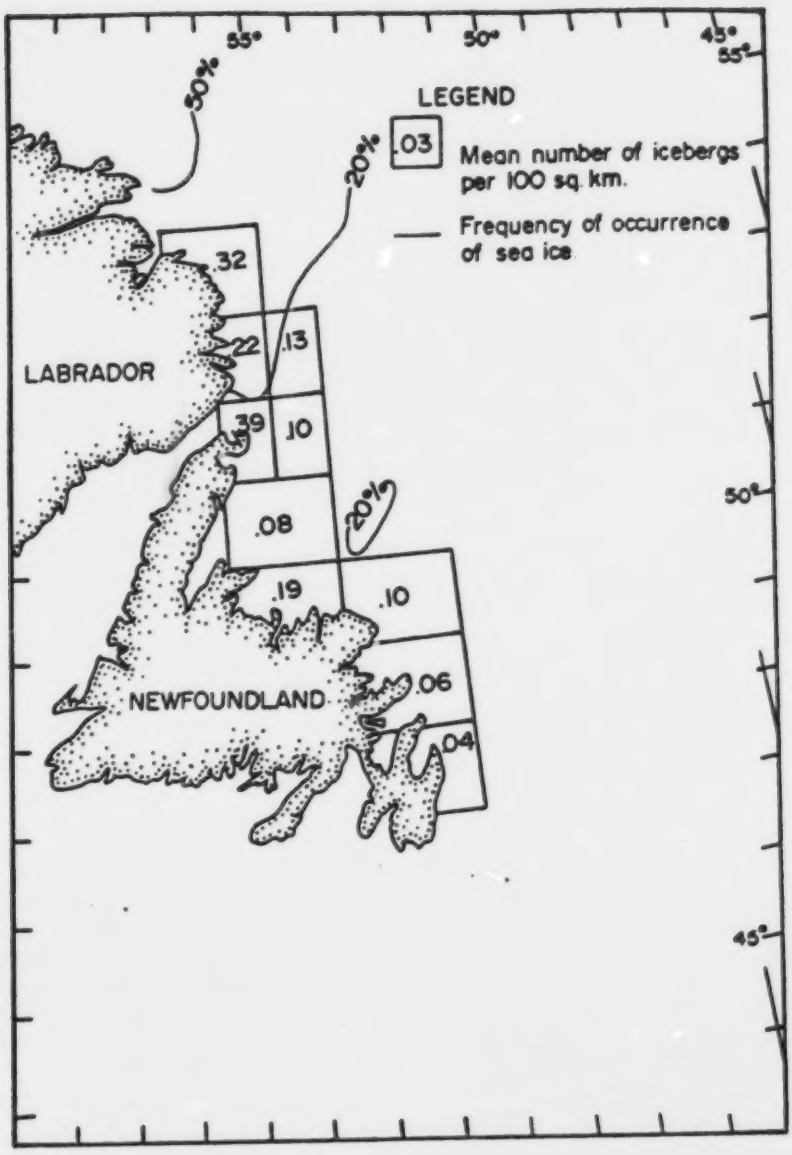

Figure 2.4 Iceberg Density and Sea Ice Frequency June.

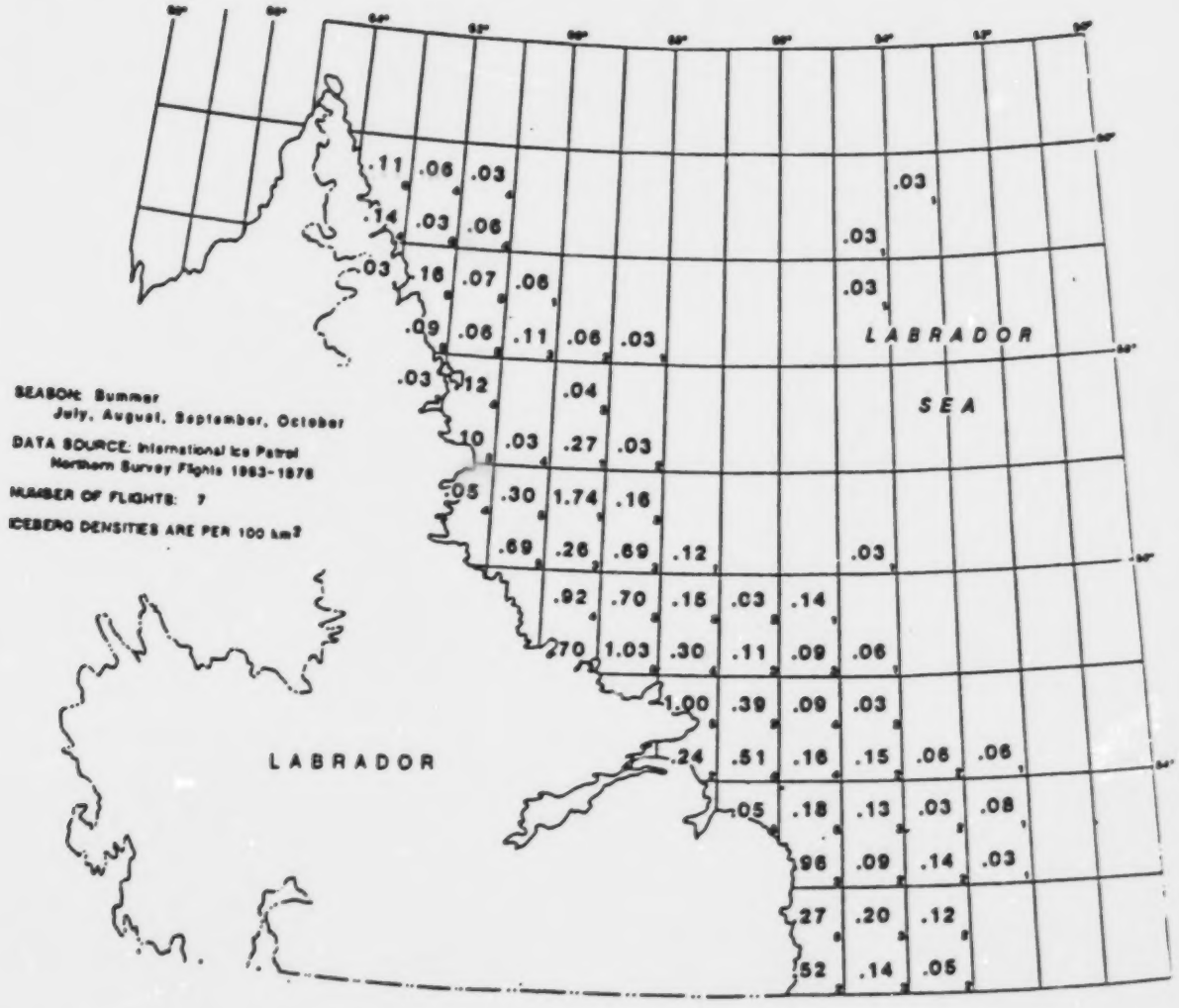

Figure 2.5 Average Iceberg Density July - October (source Miller & Hotzel 1984).

a proportion of the icebergs found in these areas will be suitable for the experiment. Statistics on the size (mass) distribution of icebergs off the east coast are available from a number of sources including: Lewis and Benedict (1981); Warbanski et. al. (1987); and Hotzel and Miller (1983). These sources indicate that approximately 30 percent of icebergs will meet the size criteria outlined previously.

Given an iceberg density similar to that found near Cape Bauld in June (0.39 icebergs per 100 sq. km) and assuming that 30 percent of icebergs meet the size criteria an area of 830 sq. km would have to be searched to find a suitable iceberg. If the search area extends in a semicircle from the coast it would have a radius of 23 km, which would also represent the maximum towing distance.

Plots of iceberg mass versus draft provided by El-Tahan and Davis (1982) indicate that an iceberg with a mass of 100,000 tonnes will have a draft of approximately 50 m. The same source also indicates that this iceberg would have an approximate length of 80 m. Given these values the site selected should have water depths of 50 m less than 40 m from shore.

2.3 Identification of Potential Sites

The identification of potential sites to conduct the experiment was based on a search of the navigation charts for Newfoundland waters produced by the Canadian Hydrographic Service (CHS). Figures 2.6 and 2.7 show the areas covered by these charts which vary in scales from 1:75,000 to 1:12,000. The most detailed charts are only available for the approaches to selected harbours. For a number of areas of the coast the charts are based on relatively old surveys and lack the detail of modern

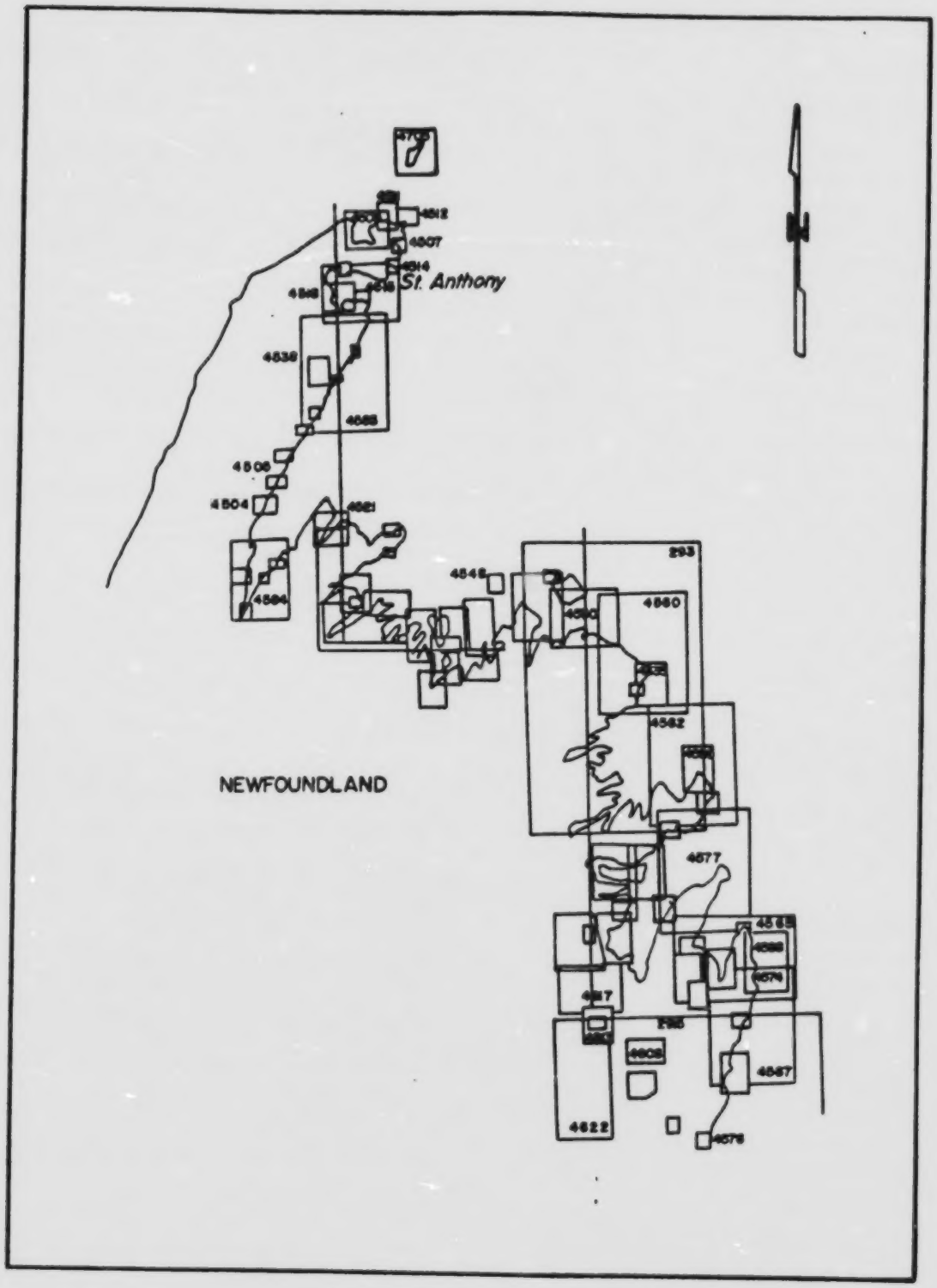

Figure 2.6 Key to Hydrographic Charts for Newfoundland

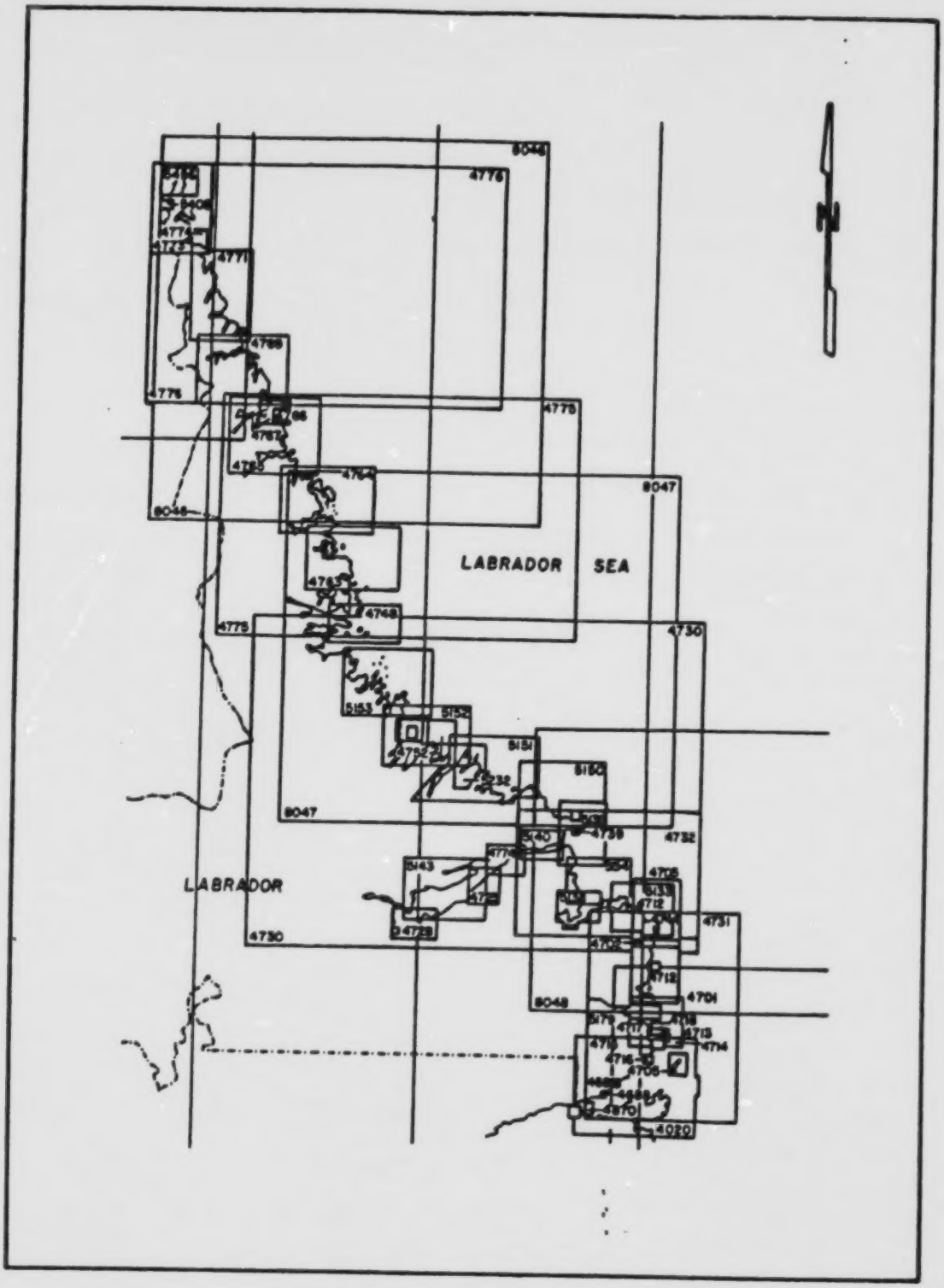

Figure 2.7 Key to Hydrographic Charts for Labrador.

charts.

The search was conducted for the east coast of Newfoundland north of St. John's and the Labrador coast. Sites with deep water near shore and good approaches to the open ocean were identified. The areas searched and the sites identified were then noted on 1:250,000 plotting charts. Due to the scale of the available charts the identification of sites was in most cases tentative. The potential sites identified are shown on Figure 2.8. In general the most promising sites were found north of 51N. Field plotting sheets used by CHS to produce the published charts were ordered for a number of the most promising sites. Examination of these field sheets indicates that the required water depths and approach conditions do exist at several of the sites. The most favorable site in terms of slope, water depth and approaches is Deep Water Point, which is situated near St. Anthony (51:20N). At this site the CHS field sheets indicate that water depths of approximately 60 m are found 30 m offshore (Figure 2.9).

2.4 Logistical Considerations

Access to the provincial road network (Figure 2.10) is one of the principal logistical considerations for this study. If a site is located near an existing road it would facilitate the site preparation work by allowing equipment and supplies to be easily transported to the site. Almost all of the sites on the island of Newfoundland are situated within a few kilometers of a road, however, this will exclude almost all the sites in Labrador. From the point of view of logistics the sites near St. Anthony appear to be the most favorable since they are close to roads, a good harbour, an airport and most other services.

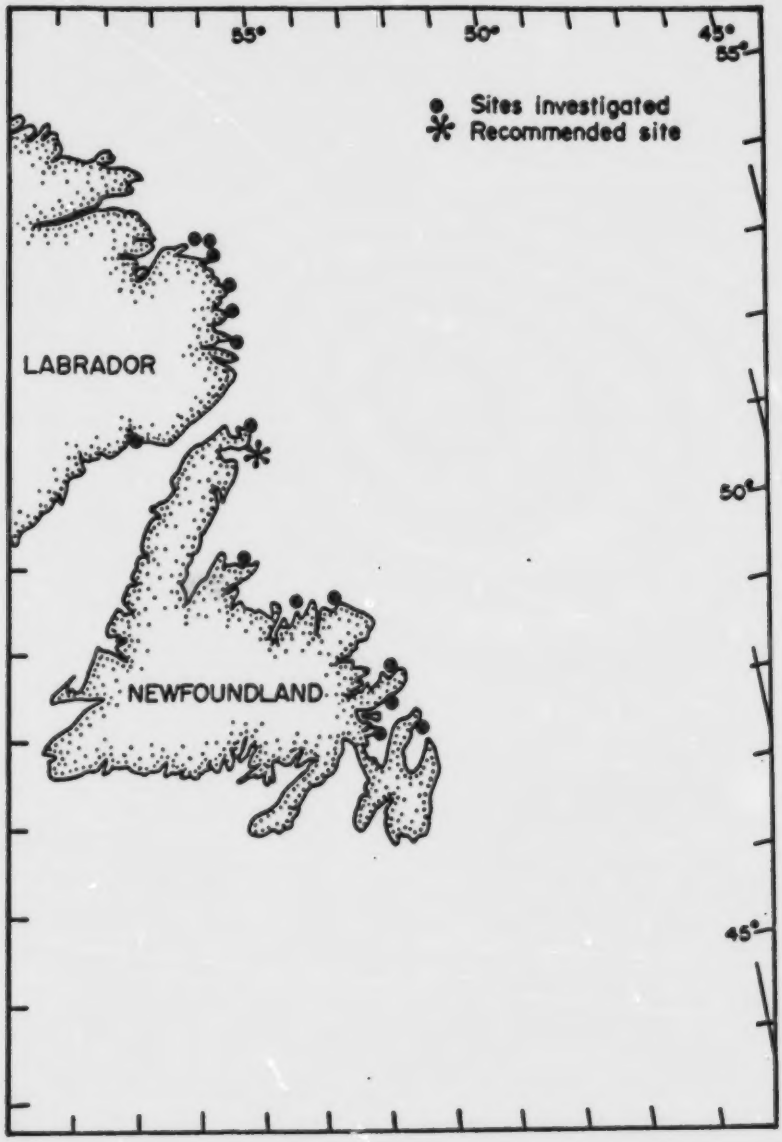

Figure 2.8 Sites Investigated and Recommended Site

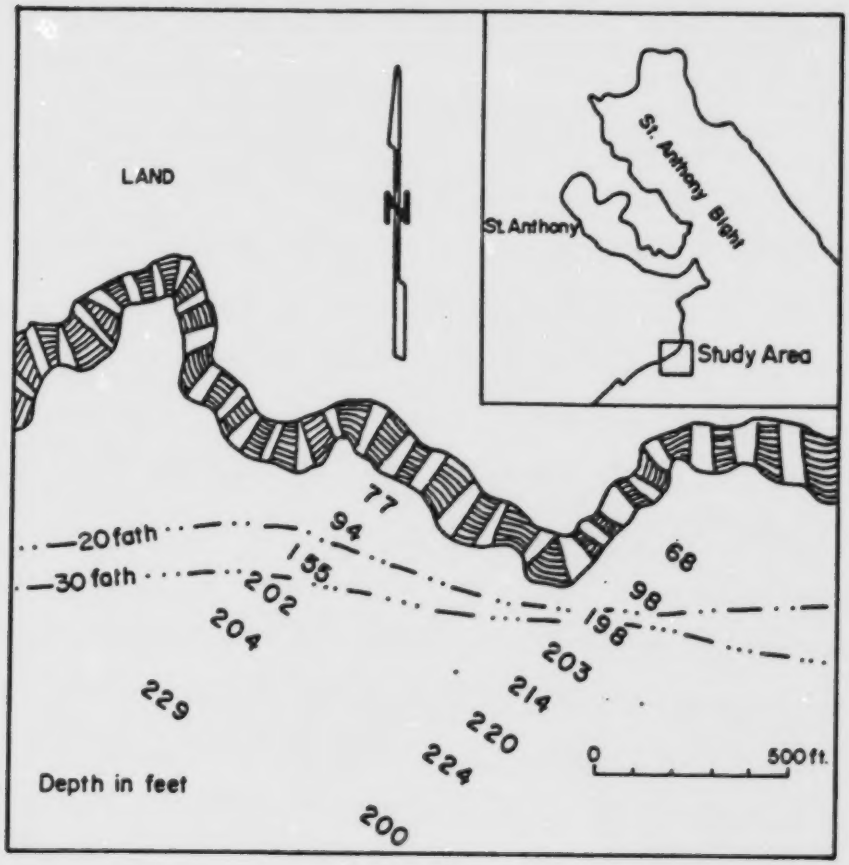

Figure 2.9 Section of Hydrographic Field Sheet Showing Deep Water Point Area Near St. Anthony.

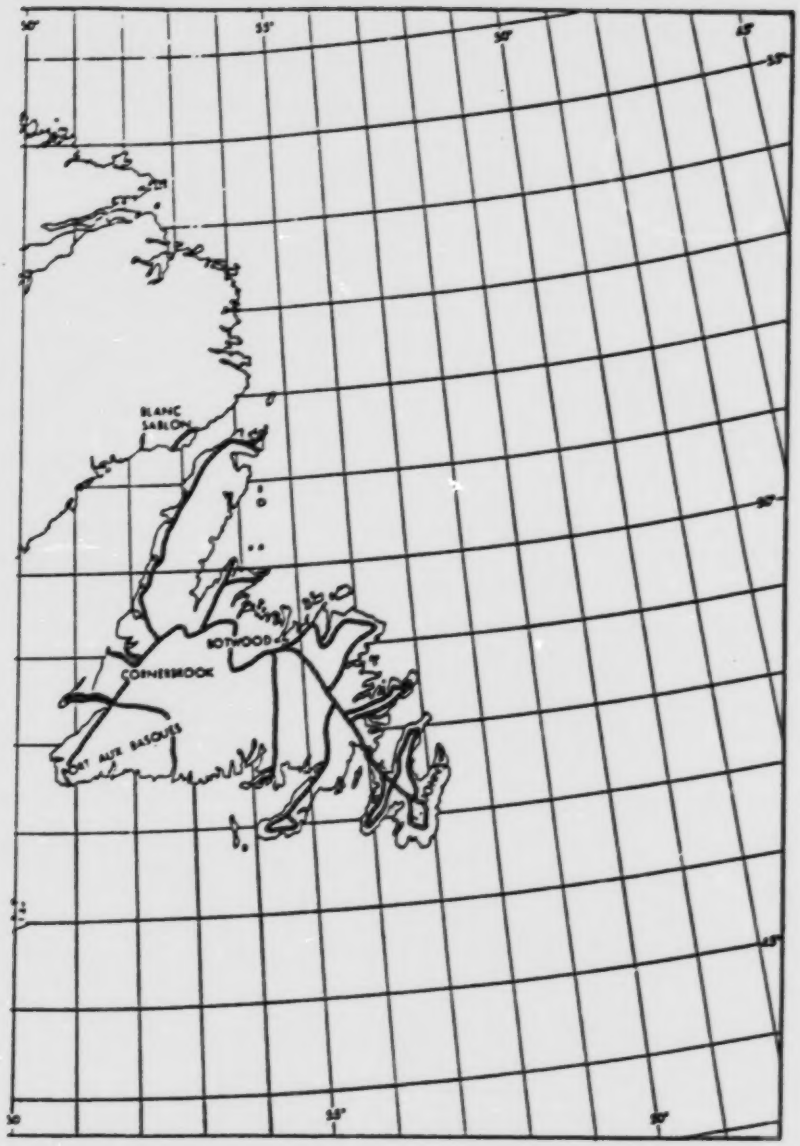

Figure 2.10 Newfoundland and Labrador Road Network.

2.5 Recommended Site

The final site selection was based on a cross tabulation of sites with a ranking of their suitability under various criteria (Figure 2.11). Based on all three types of criteria considered (icebergs, physical site and logistics) the sites near St. Anthony appear to offer the most favorable conditions. The optimum time to conduct the experiment at these sites would be from middle to late June.

Figure 2.12 presents a portion of the CHS chart for the St. Anthony area showing the Deep Water Point site and the two other sites identified in this area. While water depths and sub-surface slopes are not as great at the Savage Point site, compared to Deep Water Point, it does have a different type of shoreline which may be an advantage for setting up equipment. Figure 2.13 presents a portion of the 1:50,000 topographic map for the St. Anthony area. This map indicates that the cliffs at the Deep Water Point site are considerably steeper than at Savage Point. It also shows that both sites are within a few kilometers of the road network. Figures 2.14 and 2.15 present aerial photographs showing the three potential sites. Again the differences in topography between the Deep Water Point and Savage Point sites are evident. Other sources of data such as geological reports and planning reports for the town of St. Anthony were searched for additional data on these sites; unfortunately no other data was located. Only a detailed site inspection can provide the data required.

2.6 Preliminary Site Survey

A preliminary survey of the St. Anthony sites was conducted Feb. 3-7,

Figure 2.11

Site Evaluations

Site	Iceberg Availability	Site Considerations	Logistical Considerations
Random Sound (48° 03' N)	D	B	A
Bay de Verde (48° 05' N)	D	C	A
Bonaventure Head (48° 18' N)	D	C	A
Blackhead Bay (48° 33' N)	C	C	A
Black Is., NDB (49° 34' N)	C	B?	C
Herring Head (49° 40' N)	C	B	B
La Scie (49° 58' N)	C	C/B	B
Savage Pt. (St A) (51° 20' N)	A	B	A
Deep Water Pt (St A) (51° 21' N)	A	A	A
Big Cove (St A) (51° 22' N)	A	B	A
Amour Pt. (51° 29' N)	B	A/B	B
Cape Bauld (51° 39' N)	A	B	C
Cape St Lewis (52° 20' N)	A	B?	C/D
Double Is (52° 29' N)	A	B?	D
Hare Is (52° 35' N)	A	B?	D

Figure 2.11 Cont'd

Site Evaluations

Site	Iceberg Availability	Site Considerations	Logistical Considerations
Square Is (52° 44' N)	A	B?	D
Roundhill Is (53° 26' N)	A	B?	D
Halfway Is (53° 41' N)	A	B?	D
E. Gannet Rk (53° 56' N)	A	B?	D
Gannet Is (53° 57' N)	A	B?	D
Outer Gannet Is (54° 00' N)	A	B?	D

Keys

A - no apparent problems

B - some problems

C - serious problems

D - marginal site

? - insufficient data

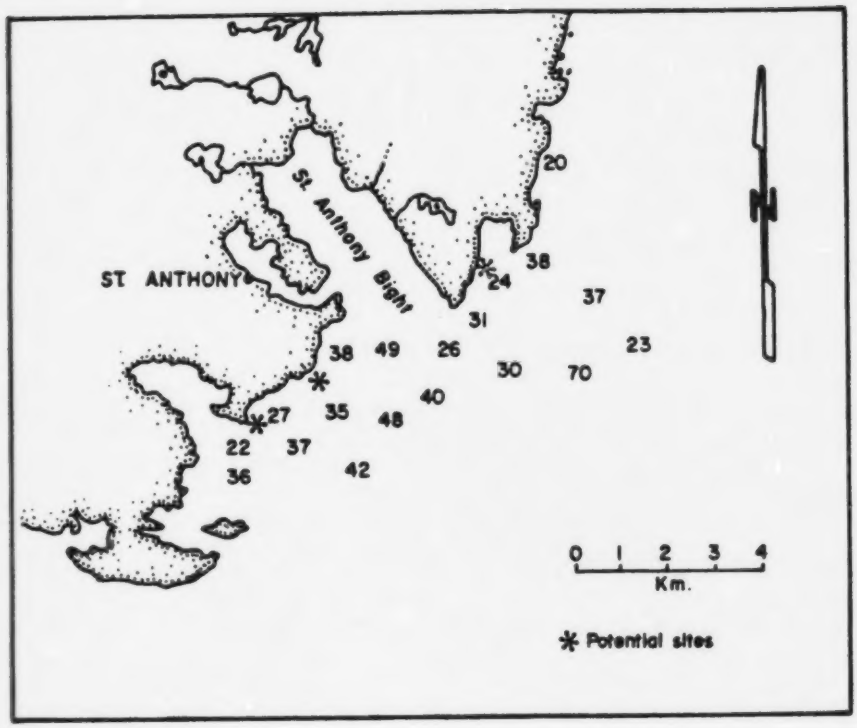

Figure 2.12 Section of Hydrographic Chart for St. Anthony Showing Potential Sites.

Figure 2.13 Topographic Maps for St. Anthony Area.

NF 79022 184
NEWFOUNDLAND & LABRADOR - DEPARTMENT OF FOREST RESOURCES & LAN
Mapping Division, Howley Building, Higgins Line, St. John's, Newfoundland

Figure 2.14 Aerial Photograph of St. Anthony Area.

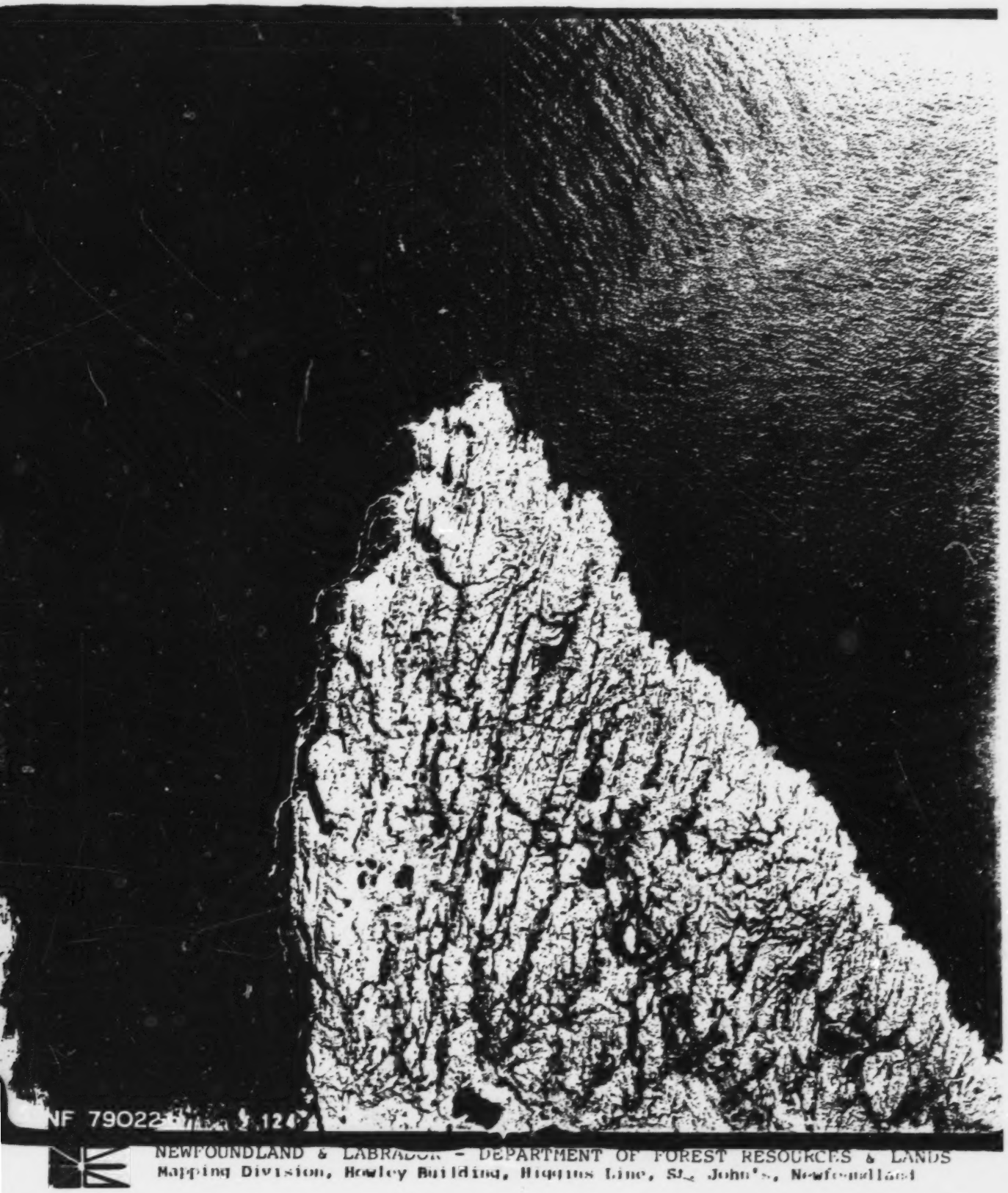
NF 79022
NEWFOUNDLAND & LABRADOR - DEPARTMENT OF FOREST RESOURCES & LANDS
Mapping Division, Howley Building, Higgins Line, St. John's, Newfoundland

Figure 2.15 Aerial Photograph of Big Cove Area.

1988. The objectives were:

- to inspect visually and record photographically the cliffs
- to inspect the terrain to assess suitability for road construction
- to assess accessibility of the sites
- to measure the water depth close to the cliffs
- to talk to the local people about iceberg sightings in the area.

The site survey confirmed that Deep Water Point is the most attractive site (Fig. 2.16). It is easily accessible from the road (the road to St. Anthony Hill is not shown on the topographic map Fig. 2.13) by a short walk or snowmobile ride. The cliff slopes into the water at about 45°. The terrain on top is relatively level and made up of hard schist. It should thus be easy to construct an access road. The second site, Savage Point is not as attractive. The water is not as deep as off Deep Water Point and the terrain is much more rugged.

There was no good viewpoint to observe the cliff of the third site near Big Cove. However, the topographic map shows that it is similar to Deep Water Point. A walk on top of the cliff also shows that the terrain is similar to Deep Water Point. From the gravel road between St. Anthony Bight and St. Carols, the access to the Big Cove site is significantly longer than from St. Anthony Hill to Deep Water Point. Big Cove is therefore definitely second to Deep Water Point.

The local people confirmed numerous iceberg sightings in late spring. They claim that some icebergs come very close to the cliffs, as shown in a postcard (Figure 2.17).

Unfortunately, the bathymetric part of the expedition could not be realized because of extreme wind and cold temperatures. After waiting

Figure 2.16 Deep Water Point, Nfld. - A Potential Site For Full Scale Iceberg Impact Test.

Figure 2.17 Iceberg Near St. Anthony Point.

five days for the weather to improve, the survey team returned to C-CORE.

2.7 Further Work Required

Prior to making the final site selection within the St. Anthony area further work is required to determine:

- the near shore water depths in more detail;
- the nature of the bottom;
- the nature of the currents at each site;
- the work required to prepare each site for the experiment.

Further field work, which would include using divers to investigate the bottom and deploying current meters, should be carried out in June.

References

2.1. Anderson, C. (1971) The Flow of Icebergs Along the Canadian East Coast, Proceeding of the Canadian Seminar on Icebergs, Halifax, NS, Dec. 6-7, 1971, pp. 52-61.

2.2. Miller, J.D. and I.S. Hotzel (1984) Iceberg Flux Estimation in the Labrador Sea, Proceedings of the Third International Offshore Mechanics and Arctic Engineering Symposium, New Orleans, LA, Feb. 12-17, 1984, Vol. III, pp. 298-304.

2.3. Gustajtis, K.A. and T.J. Buckley, (1977) A Seasonal Iceberg Density Distribution Along the Labrador Coast, Proceedings of the Fourth International Conference on Port and Ocean Engineering Under Arctic Conditions, POAC 77, St. John's, Sept. 26-30, 1977, Vol. II, pp. 972-983.

2.4. Lewis, J. and C.P. Benedict (1971) Icebergs on the Grand Banks: Oil and Gas Considerations, World Oil, January 1981, pp. 109-114.

2.5. Hotzel, I.S. and J.D. Miller (1983) Icebergs: Their Physical Dimensions and the Presentation and Application of Measured Data, Annals of Glaciology, 4, pp. 116-123.

2.6. El-Tahan, M. and H.L. Davis (1982) Correlation Between Iceberg Draft and Above Water Dimensions, NRCC Workshop on Ice Scouring, Paper #11, Montebello, P.Q., Feb. 15-19, 1982.

2.7. Warbanski, G., D. Strong and D. Burley (1987) Iceberg Management and the Water Cannon, paper presented at the Ice Management Workshop, St. John's, Nfld.

2.8. Shea, D. (1983) Marine Traffic Analysis Project Cape Norman, Strait of Belle Isle, project report No. MOB 82-2, prepared by Vessel Traffic Services, Aids and Waterways Newfoundland, Canadian Coast Guard, TP3870E.

2.9. Arctic Pilot Project (198-) Icebergs in the Strait of Belle Isle and Approaches, 21 p.

2.10. Ketchen, H.G. (1977) Iceberg Populations South of 48°N Since 1900, Appendix C, Report of the International Ice Patrol Service in the North Atlantic Ocean, Season 1977, Bulletin No.63, CG-188-32.

Chapter 3
Methods of Towing Icebergs

3.1 Tug Boats

The offshore supply boats designed and built for Grand Bank service are the best equipment for towing and maneuvering icebergs. The masters and crews of these vessels have considerable practical experience in handling icebergs. A supply boat master who has fourteen years experience towing icebergs provided some valuable insight. He pointed out that such a tow trial would be significantly different from the usual rig protection work. The researchers would ideally have some choice in selecting candidate icebergs and suitable weather. Therefore it would be prudent to select a stable iceberg and one which would hold the tow line. One clue to watch for when attempting to select a stable iceberg is a rough above water profile indicating that the iceberg has not rolled recently. A good wave melted water line groove serves to keep the tow line from slipping and protects the line from abrasion it might receive from freshly broken ice. The Master stated there would not be much concern about handling the ship at close quarters with some of the deep water sea cliffs, a feature commonly found along the coast of Newfoundland. He was very positive about the value of a single point mooring. He had visited Ice Engineering Ltd. when they were developing a single point mooring and was impressed with the possibilities of some of their concepts. If a secure anchor point could be made on the iceberg, it would allow attaching the wire towing hawser close to the iceberg without having to deal with the long leads of a fixed length polypropylene rope. This short lead is especially valuable if the tow line has to pass over a pulley close to the impact point. He was not discouraged by the necessity of having to work

on the iceberg to set the single point attachment. He expressed the opinion such work could be done with a helicopter for a large iceberg and from the tugboat's crane for smaller icebergs and growlers.

The typical Grand Banks supply boat can develop 11,200 SHP (shaft horse power), maximum power at 110 % of the engine's power rating. These boats have Bollard Pull ratings around 125,000 kg (140 tons). Supply boat operators stress, it is important not to attempt to overpower an iceberg because too much force might cause the iceberg to roll and slip its tow line. The conventional practise is to start out slowly and monitor what happens as power is applied. If the iceberg shows a tendency to tip then ease back on the power to keep the lines attached. When working with a stable iceberg with a good rope attachment, it is possible to tow the iceberg with full power. A modern supply boat can move a 100,000 tonne iceberg at 2 to 3 knots (1 to 1.5 m/s) depending on the form of the iceberg and incident wind, sea and current conditions. Normal procedure for an iceberg tow is to tow the 1,400 m (4,500 ft) polypropylene floating tow line around the iceberg steaming in a loop to pick up the other end of the tow line. This class of supply boat charters for $8,000 per day for short term charter and $8,000 per day plus fuel on a longer term charter.

3.2 Winches

There exist high hauling force winches used in construction projects and for mooring of offshore vessels. SKAGIT Winches made by Continental-Emsco Co. of Houston, Texas are some of the largest made. Product information on these winches has been provided. The largest winch

ETW-350 Mooring Winch
Weighs 130,000 kg (285,000 lbs)

Performance - average drum			
Gear	Line speed m/s	Line Pull kg	tons
Low Gear	0.1	180,000	200
	0.2	180,000	200
	0.3	175,000	190
	0.4	165,000	180
	0.5	130,000	145
High Gear	0.25	79,000	87.5
	0.5	77,000	85
	0.75	72,000	80
	1.0	66,000	72.5
	1.25	45,000	50

Table 3.1

advertised by Continental-Emsco is the SKAGIT EWT-350. Table 3.1 gives a summary of the performance as a function of line speed.

An affiliate of Atlantic Towing Limited in Saint John, New Brunswick has a SKAGIT Winch. It was quoted as a SKAGIT RB-100 *(this model number does not appear in the SKAGIT Equipment Catalog)*, a two drum winch; it can handle two separate drums of cable. The Atlantic Towing General Manager quoted the following capabilities but they don't correspond to any winch information of the SKAGIT Catalog. The SKAGIT RB-100 has an anchor pull *(bare drum at stall)* of 200,000 lbs. and a line pull of 59,000 kg (130,000 lbs. or 65 tons) at 60 RPM. The drum is about 750 mm (30 in) which would mean a linear pull of 2.4 m/s (470 fpm). None of the winches in the

product literature gives anything like this hauling force at this high speed. The Catalog performance figures for the SKAGIT DTW-100 are given in Table 3.2. Cable capacity of the winch is about 1000 m (3300 ft). This unit is fitted with a 2 in. wire cable. It is not known if it is fitted with marine hawser cable. This stationary winch was originally purchased for hauling the 36 in. pipeline into position during the construction of CAN-PORT in Saint John. This is a very heavy piece of equipment the SKAGIT DTW-100 weighs 24,000 kg (52,000 lbs.). The quoted rental rate for this winch is $25,000 per month.

A winch operation would require considerable site preparation to anchor the winch into position to develop its maximum hauling force. It could be brought on location with the same type of float and truck tractor required to move heavy construction equipment.

Performance - average drum			
Gear	Line speed m/s	Line Pull kg	tons
Low Gear	0.15	50,000	55
	0.3	35,000	39
	0.45	29,000	32
	0.6	24,000	26
Second Gear	0.25	23,000	26.0
	0.5	18,000	19.5
	0.75	13,000	15.0
	1.0	10,000	11.0
	1.25	6,000	7.5
	1.5	5,000	6.0

Table 3.2: DTW-100 Towing Winch - Weighs 24,000 kg (52,000 lbs)

3.3 Track-Type Tractors

The performance specification of track-type tractors were investigated to see if mobile machinery might be employed to pull an iceberg into a collision with a sea cliff. The Caterpillar Tractors are considered to provide an example of typical machines available. The D8 Caterpillar track-type tractor is the largest unit available from any construction firm in Newfoundland. Its performance is shown in Figure 3.1.

The operation rates for a D8L Caterpillar machine are cited to provide relative cost figures (Table 3.3). The rates include an operator and consumables. A float and truck tractor would be required to haul the tractors to the site and remove them at the end of the job. The rate for a float and truck tractor is also given.

	Rates based on 8 hour day			
Unit	hourly	daily	weekly	monthly
D8L Tractor	$175	$2,150	$8,700	$27,000
D8L Tractor with winch	$184	$2,257	$9,135	$28,350
Float with truck Tractor	$120	$1,200	$5,000	$15,600

Table 3.3

The largest track-type machine built by Caterpillar is the D11N. Its hauling capacity is provided in Figure 3.2. None of these machines is presently available in Newfoundland. These machines may be too large to be transported as single units by highway or railway and may have to be

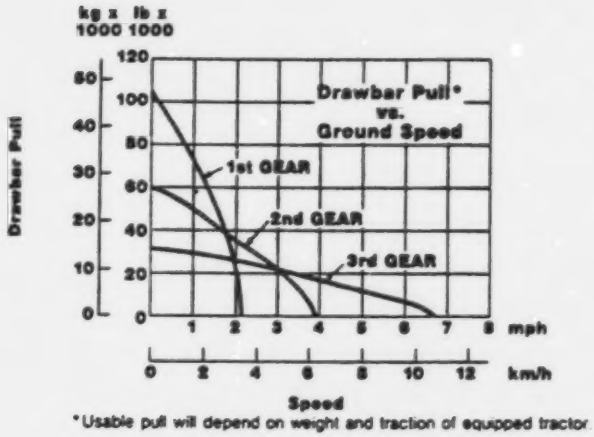

*Usable pull will depend on weight and traction of equipped tractor

Figure 3.1 Performance of D8N Tractor

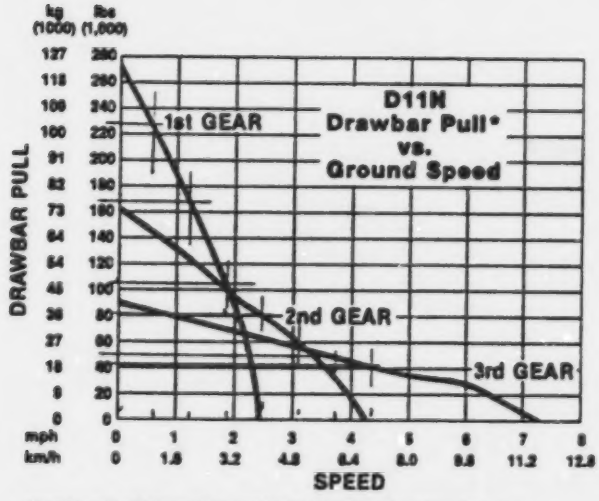

*Usable pull will depend on weight and traction of equipped tractor.

Figure 3.2 Performance of D11N Tractor

carried on site in pieces and assembled.

Diameter (in Inches)	Approx. Circum.	Average Breaking Strg. (in Pounds) (1)	Approx. Wgt. Per 100 Ft. (in Pounds)
1 - 7/8"	5 - 7/8"	258,000	545.0
2"	6 - 1/4"	284,000	620.0
2 - 1/4"	7"	364,000	785.0

(1) Tensile strength based on tests of new and unused rope under laboratory conditions.

Wire Rope Characteristics

Table 3.4

3.4 Towing Lines

There is a wide range of wire rope and synthetic line strength available. Prices and availability are quoted for the types of lines required for a 65 ton Bollard Pull, as recommended by the Iceberg Towing Manual. The contractors or equipment suppliers contracted for this type of operation would be expected to supply most of the rope and connectors required to undertake this type of job. The actual site may require additional client supplied materials.

Wire Towing Hawsers: In comparison with polypropylene ropes, wire ropes are safer because they store less elastic strain energy. Also wire ropes cut into the ice and make a better attachment. Synthetic ropes are more susceptible to damage which would weaken the lines. Although wire hawsers are very heavy and difficult to attach to an iceberg directly, they are used at the end of a towing hawser for safety reasons. A 6 x 37 Marine

Round Strand Wire Rope with fibre core is the type recommended. Table 3.4 lists characteristics of some wire rope sizes.

Synthetic Ropes: The synthetic rope which is recommended (Iceberg Towing Manual) for iceberg towing is 8-strand polypropylene braided rope. This rope has a 0.90 specific gravity and floats. A floating rope is simpler to deploy to attach a tow line to an iceberg. It is non-rotating and non-kinking hence easy to handle. Polypropylene rope is lower strength than nylon braidline and hence requires larger size rope to achieve an equivalent strength.

Diameter (in Inches)	Approx. Circum.	Average Breaking Strg. (in Pounds) (1)	Approx. Wgt. Per 100 Ft. (in Pounds)
3 - 5/8"	11"	188,000	190.0
4"	12"	220,000	230.0
4 - 1/4"	13"	255,000	260.0

(1) Tensile strength based on tests of new and unused rope under laboratory conditions.

Polypropylene Rope Characteristics

Table 3.5

The synthetic lines are elastic and very dangerous when broken under tension. Normally, synthetic rope is used only to encircle the berg, with wire rope completing the rest of the tow line to the supply boat winch. The minimum length of wire hawser recommended for high tension towing is about 100 m.

Ropes are available for a Bollard pull of 65 tons. The Iceberg

Towing Manual recommends 100 mm (4 in) size with a breaking strength of 99 tonne (220,000 lbs.).

Large diameter synthetic towing lines are ordered and then produced by the manufacturer. They are cost and quoted by the job. The lead time for the delivery of a tow line is about two months. Table 3.5 lists characteristics for some polypropylene rope sizes.

Marker buoys, shackles, swivels, and stay lines with equivalent strengths to the tow line are required for a tow. These items would only be a small percentage of the cost of a tow line.

Chapter 4

Mechanical Requirements for Iceberg Towing

The power and distance required to accelerate an iceberg for an impact experiment are important because they govern the choice of towing mechanisms, e.g. tractors, winches or towboats and, in the case of tractors, the length of road required. A general solution to the equation of motion for an iceberg under the action of a towing force is presented. The drag on the iceberg is assumed to be quadratic, but a more exact model could be obtained from actual towing data. The towing force is assumed to be a linear function of speed.

Nomenclature

T^* - Bollard pull or towing force - $T_0 - B_0^2 V$

T_0 - Constant component of towing force

B_0^2 - Linear (with velocity) component of towing force

M - Iceberg mass

V - Iceberg velocity

DR - Drag force - $B_1^2 V + C_1^2 V^2$

B_1^2 - Linear (with velocity) component of drag force

C_1^2 - Quadratic (with velocity) component of drag force

T - T_0 / M

B^2 - $(B_0^2 + B_1^2) / M$

C^2 - C_1^2 / M

D^2 - $T + B^4 / 4C^2$

From Newton's second law of motion:

$$MdV/dt = T^* - DR = T_0 - (B_0^2 + B_1^2)V - C_1^2V^2$$

For an iceberg accelerating in the direction of motion, the solution is:

$$V(t) = \frac{D}{C}\,\frac{(1 - e^{-2CDt-L})}{(1 + e^{-2CDt-L})} - \frac{B^2}{2C^2}$$

L is an integration constant determined from the initial conditions.

$$V(0) = \frac{D}{C}\,\frac{(1 - e^{-L})}{(1 + e^{-L})} - \frac{B^2}{2C^2}$$

The distance travelled is:

$$s = s_0 + \int_0^t V\,dt$$

$$s = s_0 + \frac{1}{C^2} \ln (e^{CDt + L/2} + e^{-CDt - L/2}) - \frac{B^2 t}{2C^2} + G$$

G is an integration constant determined from the initial conditions.

$$G = -\frac{1}{C^2} \ln (e^{L/2} + e^{-L/2})$$

Examples using tractors

Case 1 Two D8N tractors are capable of towing a 100,000 tonnes iceberg from standstill to a velocity of 0.5 m/s in a time of 85 seconds over a distance of 25m. In reality, loss of efficiency due to friction in pulleys, angle of tow, etc. will cause the time and distance to be greater. The pull available in two D8N tractors is 1.4 times that necessary to tow the iceberg at that speed. The impact has a kinetic energy of 12.5 MJ and would generate a contact area of about 15 m^2.

Calculations:

$T^* = .946 \times 10^6 - .774 \times 10^6 V$ Newton

$M = 50 \times 40 \times 50 \times 1024 = 1.024 \times 10^8$ kg

$B^2 = B_0^2 = .774 \times 10^6 / 1.024 \times 10^8 = 7.559 \times 10^{-3}$

$DR = \frac{\rho C_d A V^2}{2} = \frac{1024 \times 1.0 \times 50 \times 40 \times V^2}{2} = 1.024 \times 10^6 V^2$

$C^2 = 1.024 \times 10^6 / 1.024 \times 10^8 = .01$

$D^2 = \frac{.946 \times 10^6}{1.024 \times 10^8} + \frac{(7.559 \times 10^{-3})^2}{.04} = .01067$

$V(0) = 0 = \frac{.1033}{.1} \frac{(1 - e^{-L})}{(1 + e^{-L})} - \frac{7.559 \times 10^{-3}}{2 \times .01}$

$L = .7673$

$V_{final} = 0.5 = 1.033 \frac{1 - e^{-2*.1*.1033t-.7673}}{1 + e^{-2*.1*.1033t-.7673}} - \frac{7.559 \times 10^{-3}}{.02}$

$t = 84.5$ s

$G = -100 \ln (e^{-.7673/2} + e^{-.7673/2}) = -76.5$

$s = 100 \ln (e^{.01033*84.5+.7673/2} + e^{-1.256}) - \frac{7.559 \times 10^{-3} \times 84.5}{.02} - 76.5$

$s = 25$ m

Case 2 Two D11N tractors are capable of towing a 100,000 tonnes iceberg from standstill to a velocity of 0.84 m/s in a time of 92 seconds over a distance of 54 m. The actual time and distance will be greater. The pull available in two D11N tractors is 1.25 that necessary to tow the iceberg at that speed. The impact has a kinetic energy of 35.4 MJ and would generate a contact area of about 35 m^2.

Calculations

$T^* = 2.40 \times 10^6 - 1.80 \times 10^6 V$ Newton

$$B^2 = \frac{1.796 \times 10^6}{1.024 \times 10^8} = .0175$$

$$C^2 = .01$$

$$D^2 = \frac{2.40 \times 10^6}{1.024 \times 10^8} + \frac{.0175^2}{.04} = .03109$$

$$D = .1762$$

$$V(0) = 0 = 1.762 \frac{1 - e^{-L}}{1 + e^{-L}} - \frac{.0175}{.02}$$

$$L = 1.0896$$

$$V_{final} = .841 = 1.762 \frac{1 - e^{-2x.01762xt-1.0896}}{1 + e^{-2x.01762xt-1.0896}} - \frac{.0175}{.02}$$

$$t = 91.8 \text{ s}$$

$$G = -100 \ln (e^{1.0896/2} + e^{-1.0896/2}) = -83.47$$

$$s = 100 \ln(e^{.01762x91.8+.5448} + e^{-.01762x91.8-.5448}) - \frac{.0175x91.8}{.02} - 83.47$$

$$s = 53.8 \text{ m}$$

Chapter 5

Hydrodynamics Of Iceberg Motion And Hydraulic Model Testing

The purpose of the model tests is to establish the feasibility of the full scale tests. Specifically, it is desired to test various towing schemes, in the presence or absence of alongshore currents, and to evaluate the drag force and free drift of an iceberg in the vicinity of a cliff. The important unknown in this towing experiment is the drag, to be overcome by the towing forces. Added mass is also important, but its determination in the presence of drag is difficult and beyond the scope of this work. No attempt is made here to investigate realistic iceberg shapes or stability under tow.

5.1 Drag Force

The total force exerted by water assumed at rest at infinity on an iceberg in steady translational motion is of great practical importance in this experiment. Contributions to this total force are made by the tangential stress at the body surface, integrated over that surface, and by the normal stress. The total force due to the tangential stress will usually be approximately opposite in direction to the velocity of the iceberg, and is termed the friction drag since it is wholly or directly a consequence of viscosity or internal friction in the fluid. The total force due to the normal stress at the surface of the iceberg in steady motion has a more complex origin, and it is useful to recognize the following contributions, which are additional to the buoyancy force due to the action of gravity on the fluid:

a) the lift on the iceberg,

b) the induced drag, an accompaniment to the lift,

c) the form drag.

Of these, only the form drag is non negligible. This is the component of the resultant pressure force parallel and opposite to the velocity of the berg after the induced drag has been subtracted. The form drag depends strongly on the shape and attitude of the berg.

Two flow regimes can be distinguished.

Flow without separation of the boundary layer:

The various streamlines lying close to the body surface here proceed from an attachment point or points on the forward side of the body to some detachment point or points on the downstream side, where the boundary layer leaves the body and becomes a wake whose thickness, at positions close to the body, is of the same order as the boundary layer thickness. Such an absence of boundary layer separation can occur only when the total fall in velocity of the fluid just outside the boundary layer is small. The body must be slender, be aligned roughly with the flow at infinity and have a cusped edge at the rear. It is clear this is not the case for icebergs.

When the distribution of velocity in the irrotational flow just outside the boundary layer is known, the tangential stress at each point of the body surface can be calculated. The total friction drag is obtained by integration.

$F_{Friction} = k\ \rho A V^2\ R^{-1/2}$

k depends on the shape of the body

V = flow velocity

$R_e = LV/\nu$ = Reynolds number

L - characteristic length

ρ - fluid density

A - a measure of the area of the body.

ν - dynamic viscosity

Example Skin friction drag of a 100,000 tonne berg travelling at 1 m/s.

Assume the iceberg is a cube of 47.68m (156.43 ft) to the side. Its bottom is 42.91m below water surface and it travels at v = 1.0 m/s = 3.28 fps. Its wetted surface is

$$S_w = 4 * 47.68 * 42.91 + 47.68^2 = 10457 m^2 = 112560 \text{ ft}^2$$

$$Re = \frac{VL}{\nu} = \frac{3.28 \times 156.43}{1.968 \times 10^{-5}} = 26.1 \times 10^6$$

Friction drag coefficient $C_f = \frac{.075}{(\log R_e - 2)^2} = 2.56 \times 10^{-3}$

Friction drag

$$F = \frac{1}{2} C_f \rho S_w V^2 = \frac{1}{2} 2.56 \times 10^{-3} \times 1.9947 \times 112560 \times 3.28^2 = 3088 \text{ lbs} = 1.4 \text{tonnes}$$

Like the friction drag, the form drag is proportional to $R^{-1/2}$. This is seen by the following description: the existence of a thin boundary layer and wake has a small effect on the form of the surrounding irrotational flow and a corresponding small effect on the distribution of pressure at the body surface. The streamlines of the irrotational flow are displaced laterally by both the solid body and the boundary layer, and the thickness of the boundary layer in general increases from the leading to the trailing edge of the body; consequently, the rise in velocity and fall in pressure at the sides of the body where the streamlines are crowded together may be expected to be more marked at the rear of the body than in the absence of the boundary layer, and this greater decrease of pressure at the rear causes the total drag due to normal stresses to be

non zero and positive. The pressure at any point on the body surface differs from that in wholly irrotational flow by an amount proportional to the displacement thickness of the boundary layer, and so the form drag is proportional to $R^{-1/2}$.

Flow with separation

When the body is not sufficiently slender or is slender but not aligned with the stream, attachment of the boundary layer over the whole surface of the body is impossible because there would be considerable retardation of the external stream over the rear portion of the body and this is incompatible with a steady state of the boundary layer.

Analysis of the flow due to a bluff body moving steadily through fluid is effectively prohibited by the large scale unsteadiness of the flow behind the body. The resulting turbulence contains large eddies and co-ordinated velocity fluctuations which extend across the broad wake between the separating streamlines. On the upstream side of the field the vorticity generated at the surface of the body is confined to a thin boundary layer; outside this layer the flow is irrotational, but the part of the boundary of this irrotational region formed by the separating streamlines is of complex, fluctuating and unknown shape and as a consequence the irrotational flow cannot be determined.

Whereas friction drag makes the major contribution to the drag on a slender body, form drag is responsible for most of the drag on a bluff body.

When the boundary layer separates from the side of a bluff body, the streamlines passing downstream from the separation points enclose a wide region in which the pressure does not vary greatly, since the velocities

there are considerably smaller than V_0 (fluid velocity at ∞). The value of this approximately uniform pressure is roughly the same as that in the irrotational flow just outside the separated boundary layer. Thus over most of the rear of the body surface the pressure has the same low value as that at the side of the body, where the velocity exceeds the free-stream speed. On part of the forward face of the body, viz. near the stagnation point, the pressure is large, and the consequence of this fore-and-aft asymmetry of the pressure distribution is an appreciable form drag on the body. Also, since the pressure variations round the body surface are essentially a consequence of velocity variations of the same order of magnitude as V_0, the link being made (over the forward part at least) by Bernoulli's theorem, we may expect that the total form drag will be of the same order of magnitude as $1/2\rho V_0^2$ (which is the excess of pressure at a stagnation point over that at infinity) times the frontal area of the body. The drag of bluff bodies is customarily expressed in the form of a drag coefficient defined as

$$C_D = \frac{D}{1/2\rho V_0^2 A}$$

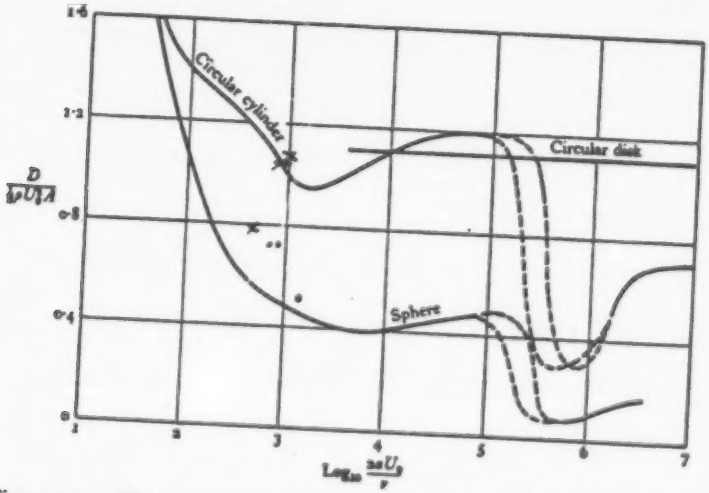

Figure 5.1 The measured drag on unit axial length of a circular cylinder ($A = 2a$), on a sphere ($A = \pi a^2$), and on a circular disk normal to the stream ($A = \pi a^2$), all of radius a. The broken curves represent results obtained in different wind tunnels.

where D is the total drag in a stream of speed V_∞ at infinity and A is the area of the projection of the body on a plane normal to the stream at infinity. The dimensionless C_D is a function of Reynolds number alone (leaving aside effects of roughness of the body surface) and is about 1.0 for Re > 100. Fig. 5.1 shows C_D versus Log Re for various shapes. The data points will be explained later.

Example Form drag of a 100,000 tonne berg travelling at 1.0 m/s.

$$D = \frac{1}{2} C_D \rho A V^2 = \frac{1}{2} \times 1.0 \times 1024 \times 47.68 \times 42.91 \times 1 = 1.047 \times 10^6 \text{ N} = 100 \text{ tonnes}$$

It is seen that the friction drag is negligible in comparison to the form drag.

5.2 Added Mass

The determination of the effective mass of a body accelerating in a fluid medium of a given density requires the consideration of the motion of the fluid as well as that of the body. The basic definition of added mass is the quotient of the additional force required to produce the accelerations throughout the fluid divided by the acceleration of the body.

A body moving at constant velocity in a fluid temporarily pushes fluid particles aside in passing, but also displaces these particles permanently in the direction of its motion. This permanently displaced mass of the fluid enclosed between the initial and final positions of fluid particles, is in fact the added mass itself. It can be shown in general that the motion of a body through an inviscid fluid media is always accompanied by a fluid-mass transport and that this mass is the added mass which unveils itself only if the body is accelerated. For an

accelerating or decelerating body (or fluid about a body) the induced mass varies with the instantaneous shape and volume of the wake or cavity as well as with their rates of change.

For the separated motion of real fluids, the added mass coefficients depend, in general, on the parameters characterizing the history of the motion, time, Reynolds number, in addition to type and direction of motion, proximity effects, etc. There is often no single mathematical or experimental procedure to separate the inertial component of the force from that attributable to the form drag. No attempt will be made in this work to do so.

Work by Hay and Co. shows that the added mass changes significantly only when the gap between the iceberg and the cliff is very small.

5.3 Theory of Similarity

Research on scale models is based on the theory of similarity between the model and the prototype. In geometric similarity, the model corresponds exactly in shape to the prototype and all dimensions are reduced in the same scale. In kinematic similarity, corresponding points of the trajectories are arrived at in proportional times. This requires similarity of velocity and acceleration. In dynamic similarity, forces are proportional. Finally, mechanical similarity includes geometric, kinematic and dynamic similarity. Dynamic similarity, on the other hand, always includes kinematic but not necessarily geometric similarity.

Hydraulic models only work with approximate mechanical similarity, based on the ratio of those forces which determine the type of motion. By working on the model according to one main and determining law and

neglecting the others, errors occur due to scale effect and the reduction of the model against reality must be chosen to make this error in the given situation negligible. In hydraulic research the main criteria of similarity are the Froude and Reynolds laws.

Froude law

The Froude law represents the condition of dynamic similarity for flow in model and prototype exclusively governed by gravity. Other forces, such as frictional resistance of a viscous liquid may be neglected. In the flow of real (viscous) fluid, however, internal friction always acts simultaneously with gravity. If the model is geometrically similar to prototype and the boundary conditions are also similar (e.g. wall roughness), then similarity not only between forces due to gravity but also to a large extent between the resistances due to friction is ensured.

Gravity force is expressed by:

$$P = \rho g W$$

where P = force

ρ = density

W = volume

If S denotes the scale factor between prototype and model:

$$S_p = \frac{P_p}{P_m} = S_\rho S_g S_l^3$$

Inertia forces are given by Newton's law:

$$F = ma$$

where F = inertia force

m = mass

a - acceleration

$$S_F = S_m\, S_a = S_m \frac{S_l}{S_t^2} = S_\rho \frac{S_l^4}{S_t^2} = S_\rho S_l^2 S_V^2$$

where the subscripts t and V denote time and velocity.

Comparison of gravity and inertia forces gives:

$S_\rho S_g S_l^3 = S_\rho S_l S_V^2$ or

$$\frac{S_V}{(S_l S_g)^{1/2}} = S_{Fr} = 1 \quad \text{or}$$

$$\frac{V_p}{(g_p l_p)^{1/2}} = \frac{V_m}{(g_m l_m)^{1/2}}$$

For $S_g = 1$, $\dfrac{V_p}{\sqrt{l_p}} = \dfrac{V_m}{\sqrt{l_m}}$

Reynolds law

Reynolds law expresses the criterion of dynamic similarity of the motion of two incompressible viscous liquids under the exclusive effect of internal friction. It is valid, for example, in modelling flow round bodies submerged in liquid without surface waves, etc....

Resistance during the flow of liquid depends exclusively on its viscosity, expressed by the coefficient of viscosity μ for an area A and change in velocity along a perpendicular dv/dr. The internal friction force is given by:

$$P = \mu \frac{dV}{dr} A$$

The ratio of these forces in the prototype and the model is expressed by:

$$S_p = \frac{\mu_p (dV_p/dr_p) A_p}{\mu_m (dV_m/dr_m) A_m} = S_\mu S_V S_l$$

Comparison with inertia forces gives:

$$S_\mu S_V S_l = S_\rho S_l^2 S_V^2$$

Therefore:

$$\frac{S_\rho S_l S_V}{S_\mu} = S_{Re} = 1$$

Use of the dynamic viscosity coefficient $\nu = \mu/\rho$ gives:

$$\frac{V_p l_p}{\nu_p} = \frac{V_m l_m}{\nu_m}$$

If the same liquid is used in the model as in the prototype (e.g. water) the relation between the velocity scale and length scale is:

$$S_V = 1/S_l$$

Comparison of Froude and Reynold's laws shows that the modelling of motion according to Froude similarity is considerably simpler, since the velocity of flow on the model is smaller than in prototype ($S_V = \sqrt{S_l}$). On the other hand in Reynold's similarity the velocities in the model are greater than in the prototype ($S_V = 1/S_l$).

References

5.1 G.K. Batchelor: An Introduction to Fluid Dynamics, Cambridge, University Press, 1970.

5.2 Hay & Co: Motion & Impact of Icebergs ESRF (COGLA) 044, Aug. 1986.

5.3 P. Novak, J. Cábelka: Models in Hydraulic Engineering, Physical Principles and Design Applications. Pitman, 1981.

5.4 T. Sarpkaya, M. Isaacson: Mechanics of Wave Forces on Offshore Structures, Van Nostraud Reinhold, 1981.

Chapter 6

Model Tests of Towing Schemes

6.1 Introduction

This feasibility study includes simple towing tank model tests that demonstrate the impact of an iceberg on a cliff and simulate various towing schemes such as the pendulum and winching systems in as realistic a manner as possible. The intent of the tests is to show the behaviour of the bergs under various towing methods rather than exact measurements. Of course the tests were done as carefully as possible, but it was clear from the start that the data collected will have to be used with great caution, since actual towing forces and other quantities will depend greatly on the actual berg shape.

The model tests were conducted in the wave tank of Memorial University during the period of March 10 to 25, 1988. Initially drag force tests were conducted on the model icebergs at various speeds. Then a total of seventy-one iceberg impact tests were performed under varying conditions. Finally a short series of free drift experiments were completed.

6.2 Model Design

Given the equipment available it was decided to model the iceberg on a scale of 1:100, which means that the speed of the iceberg and the current are scaled at 1:10 by using Froude's law.

Two regular iceberg shapes were employed in this experiment, a sphere and a cube. The model icebergs were made of paraffin which has a similar density and therefore buoyancy to ice. Each model iceberg had a small

weight placed in its base to provide greater stability at higher water speeds and to aid in model manipulation. The cube measured 0.345 by 0.350 meters in plan and 0.350 metres in height. The sphere was approximately 0.31 meters in diameter and had a flat top to allow for placement of light emitting diodes (see Section 6.3.3, Data Acquisition System).

In these model tests the icebergs were towed from the water line in order to simulate probable field conditions where either the tow line would be wrapped around the berg or anchors would be secured to the berg near the water surface. Eyebolts were placed in drilled holes and filled with paraffin to act as the anchor bolts. For the cube the bolts were placed near the middle of opposite sides.

During the course of the experiments the model iceberg was towed towards an inclined or vertical cliff. At the proposed site the impact area is at an angle of approximately 45 degrees, therefore the model was set up in a similar manner. A few tests were also conducted against a vertical face for comparison. Figures 6.1 and 6.2 show the side and plan views of the experimental set-up. The model cliff, constructed from sheets of plywood bolted together, measured 2.05 meters in width and 2.26 meters in depth. The cliff was mounted on a steel frame at the required angle and the frame was in turn bolted to the carriage on the wave tank. The width of the model cliff was dictated by the width of the carriage. The extent of the cliff above the water line, 0.39 meters, provided enough space for mounting pulleys and for preventing any overtopping from wave runup. The extent of the cliff below the water line, 1.87 metres, was adequate to reflect the conditions of the proposed site.

It is estimated that the cliff slope extends at 45° for a

considerable distance offshore of the actual proposed site. Bottom effects are likely to be negligible, therefore the water depth chosen for the experiments was the maximum of 2.0 meters. Thus, in this simplified experiment the model did not 'feel' the influence of the bottom until it was over the cliff.

6.3 Experimental Apparatus

6.3.1 Wave Tank and Carriage:

The wave tank in which the tests were conducted measured 58 meters in length, 4.5 meters in width and the water depth was 2.0 meters (Fig. 6.0). The majority of the tests were performed across the width of the tank.

The test equipment was moved the length of the tank through the use of a 4000 kg towing carriage to simulate alongshore current. The carriage was run on rails mounted on top of the tank walls and had a velocity in the range of 0.025 to 5.0 m/s.

One objective of the experiment was to test the influence of a current on the various towing schemes. As the current magnitudes or directions were not known for the proposed site, a worst case condition was chosen for the model tests. It was understood that a cross current, along the shoreline would be the greatest detriment to the controlled towing of the berg. (Admittedly a current moving perpendicular to and away from shore would be more of a problem. But this situation is unlikely, and if "brute force" is insufficient to overcome the current, the site would not be used). Therefore this former case was examined by mounting the test equipment on the carriage and running it at various speeds along

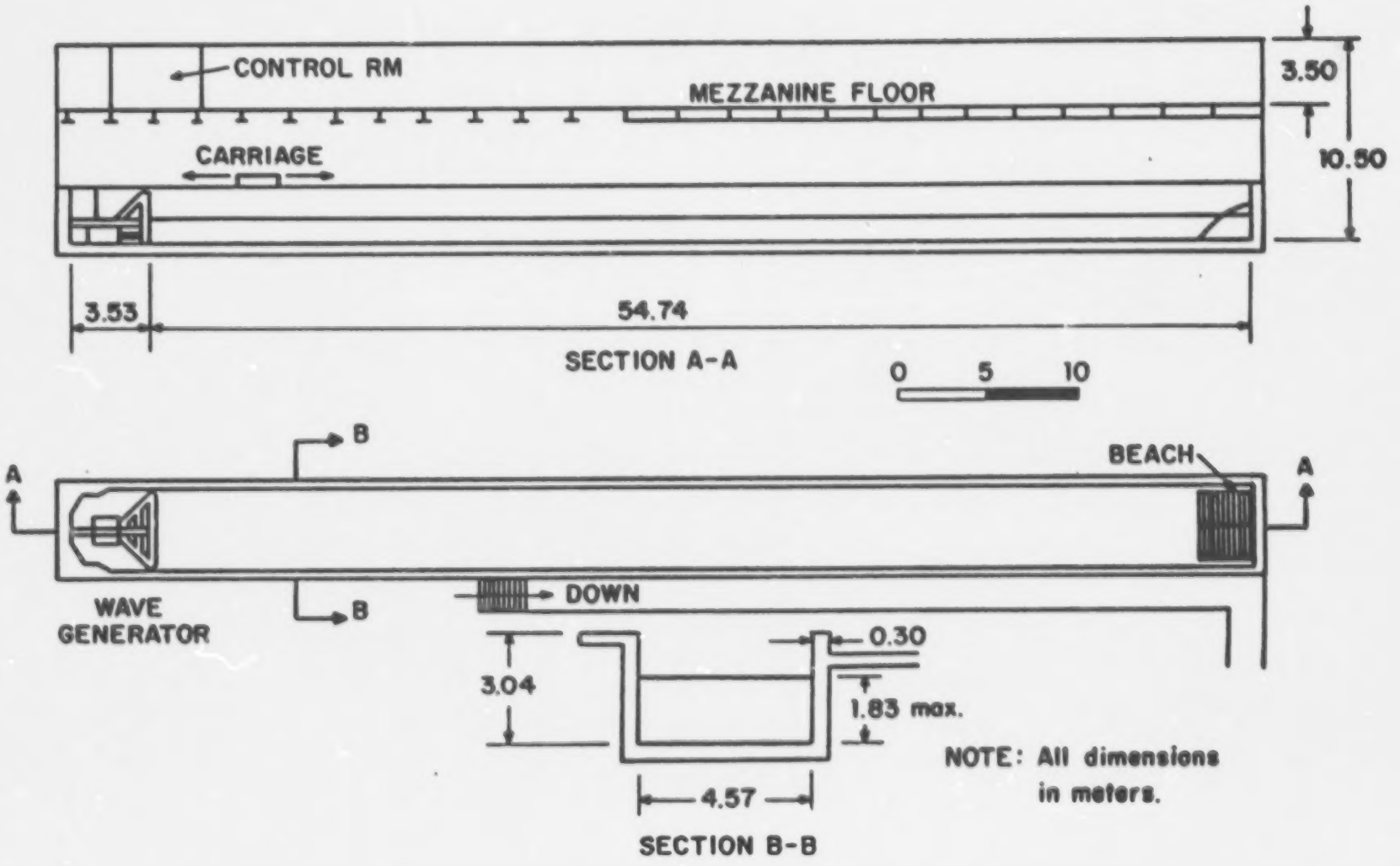

ELEVATION AND PLAN VIEW OF WAVE/TOW TANK

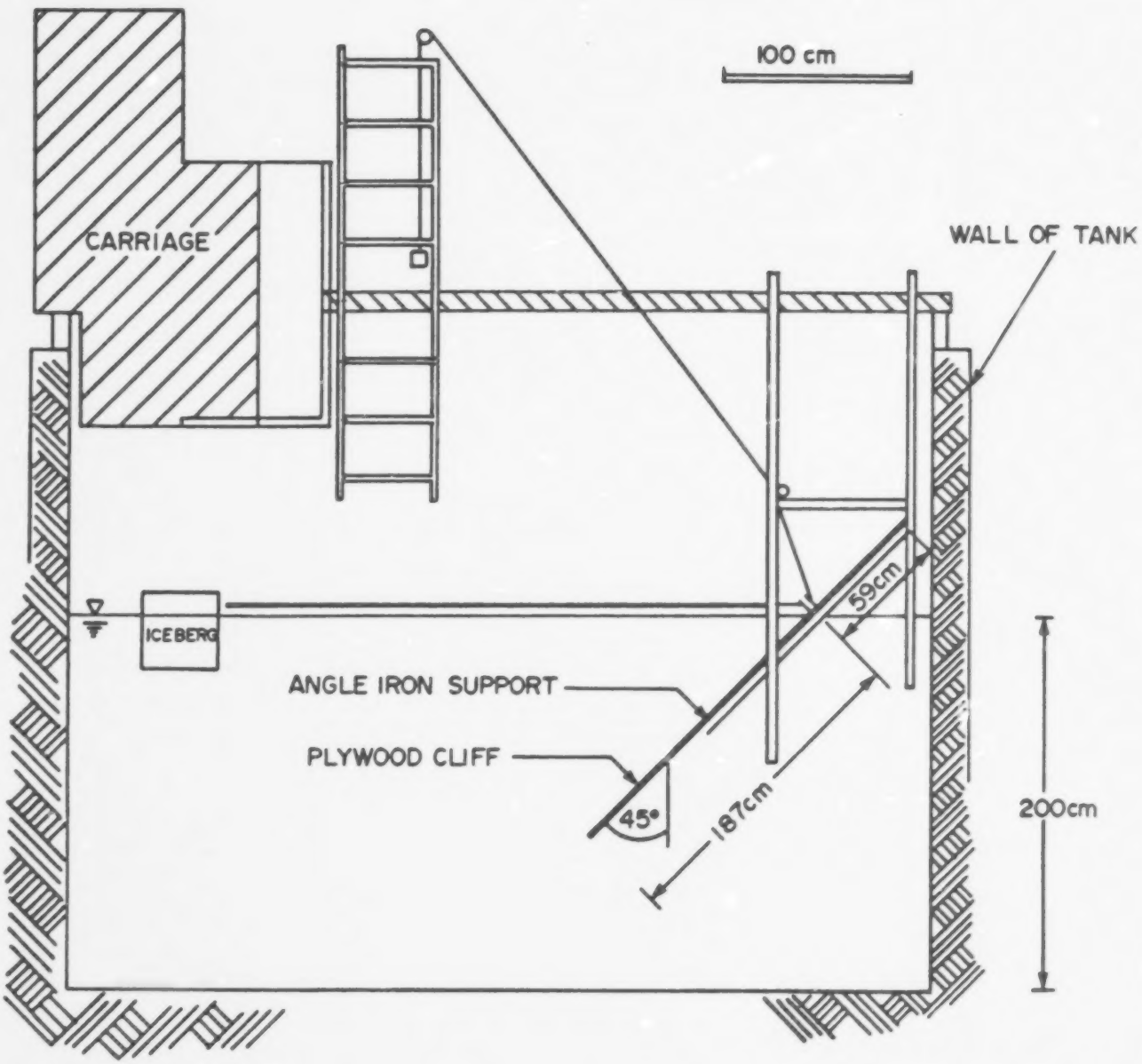

Figure 6.1 Side View of Iceberg Impact Experimental Set Up

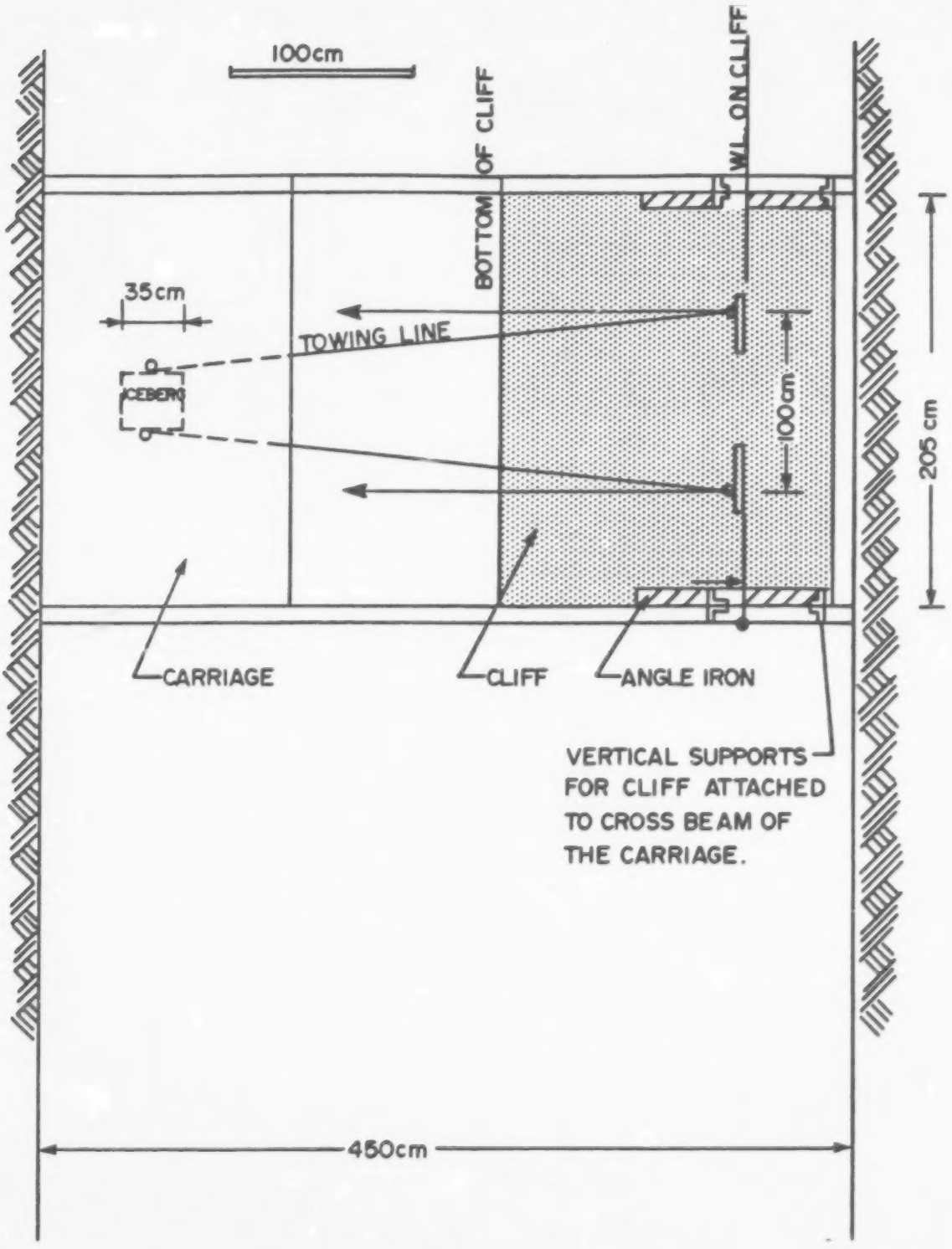

Figure 6.2 Plan View of Iceberg Impact Experimental Set Up

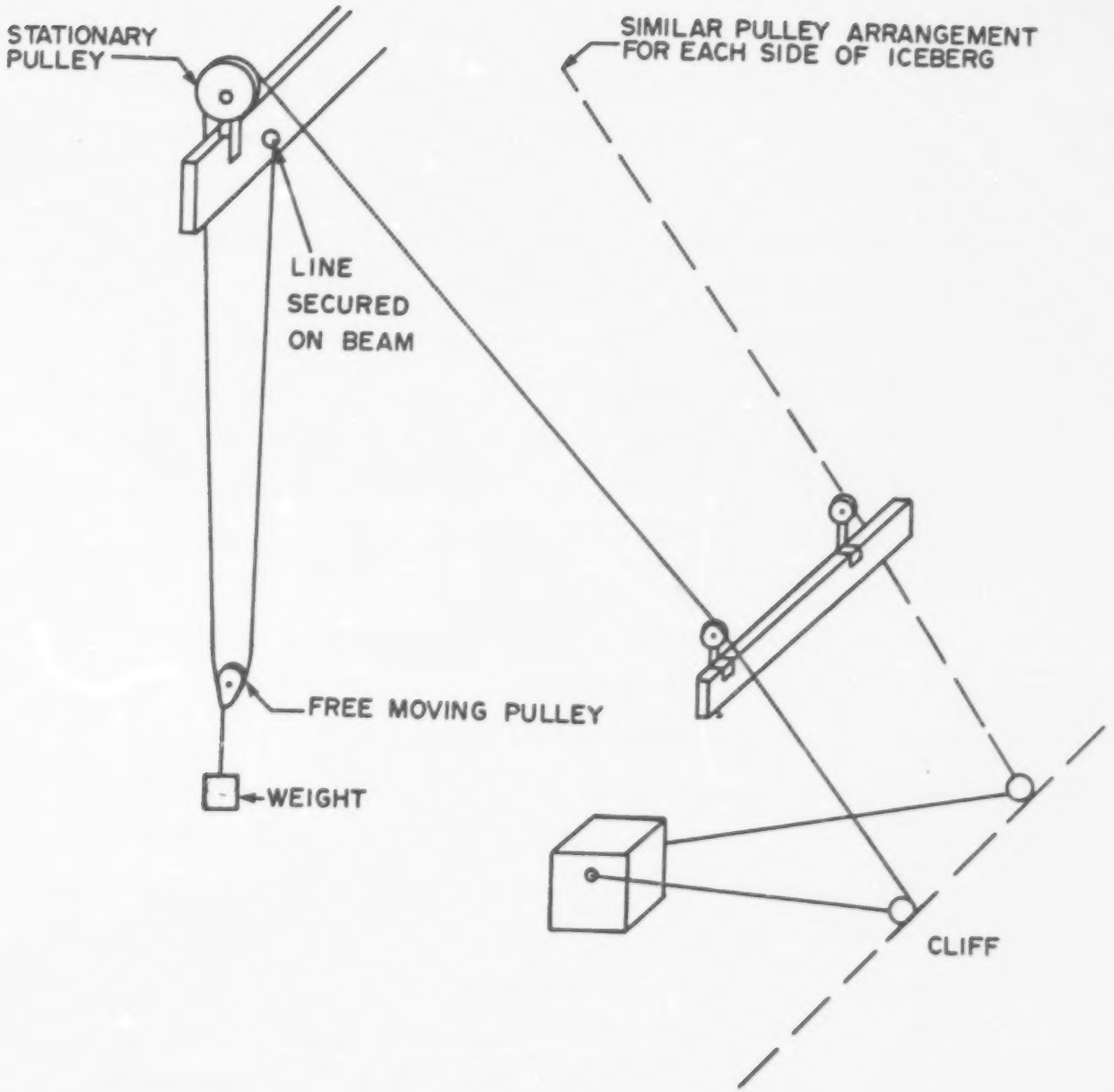

Figure 6.3 Double Pulley Configuration

the length of the tank, while the iceberg was being towed the width of the tank.

6.3.2 String and Pulley Arrangement:

A system of weights and pulleys were employed to tow the model towards the cliff. A double pulley configuration was used so that the model could be towed in twice the distance that the weight would fall. This also meant that the weight required was actually double the towing force on the model. The basic pulley system is shown in Figure 6.3.

Through experimentation it was found that the distance across the tank was adequate in the majority of cases for the model to reach its terminal velocity well before impact. This meant that the acceleration of the towing weights due to the iceberg acceleration was not a concern (see Appendix II).

Unless otherwise stated, two pulleys, located 1.0 meter apart near the waterline on the cliff, guided the model towards the proposed impact location. Initially pulleys were fixed to the cliff with their axis movable to allow for the changes in the approach angle of the iceberg during the course of a test. Due to problems caused by the fluctuating movement of the pulleys they were replaced by low friction eyebolts. The distance across the tank to the impact location was about 3.7 meters.

A flexible nylon line was used for the set up. It did not stretch significantly, was strong and had low frictional properties when wet or dry.

The pulleys were checked periodically during the course of the experiment to ensure they were freewheeling.

6.3.3 Data Acquisition System:

Data was recorded during the tests in four ways. A VHS video camera located on a stationary catwalk across the tank recorded the complete side view of the iceberg as it traversed the width of the tank. A second video camera recorded an overhead view of the berg as it approached and impacted on the cliff. This camera was able to view 1.5 meters from the edge of the cliff. A Selspot (selective spot recognition) system recorded the positional data of the berg during approximately the last meter before impact, depending on the test arrangement. As part of the Selspot system, infrared cameras were used to locate Light Emitting Diodes (LED's) secured to the model. Through a software package, the six degrees of freedom of the berg were calculated for each test period. Finally notes were recorded by hand on the motion of the berg and test conditions.

6.4 Drag Force Experiments

Two series of drag force experiments were conducted on the selected iceberg shapes. The tests were performed in order to estimate the drag coefficient for the models. In each series the iceberg was connected to a load measuring device which was mounted on the underside of the carriage. The carriage and model were then towed the length of the tank at selected constant speeds.

6.4.1 Free Moving Model:

In the initial group of tests the model was towed from a line and able to move freely in the water. The force on the iceberg was measured by a strain gauge in a force block. The voltage variations were recorded

on magnetic tape and were monitored visually throughout the tests. Prior to testing the system was calibrated with precision weights. A resistance curve for the spherical berg is shown in Figure 6.4 for speeds of .05 to 0.5 m/s. At slower speeds the models swayed approximately the width of the berg. As the towing speeds were increased above 0.5 m/s bow waves and eddies were visible around the model as it heaved across the water surface. During tests on the cubical model, the model rotated by 90 degrees after towing speeds were increased above 0.3 m/s. The tests were performed at speeds of 0.05 to 0.3 m/s. The cubical model generally heaved and surged less than the spherical one. Due to the high resistance recorded during the rotation of the cube and the change in projected area of the model, the resistance curve for the free moving model was not plotted.

6.4.2 Rigid Model:

In order to attain more accurate measurements of the resistance of the bodies at various speeds, the iceberg shapes were connected to a dynamometer. The Kempt and Rimmers R47 dynamometer was developed for determining the resistance of model ships' hulls. It is capable of measuring ±20 kgf to an accuracy of 0.1%. In this case the iceberg was held rigidly at its natural draft in the water during the tests. Only one component of force (drag) was recorded in a similar manner as the previous tests. At the beginning and end of the group of tests the calibration of the dynamometer was checked. The resistance curves for these tests are shown in Figure 6.5. As the operational speeds of the full scale iceberg is probably less than 1 m/s, that is 0.1 m/s model scale, the cube was tested in the range of 0.035 to 0.50 m/s. At the higher towing speeds

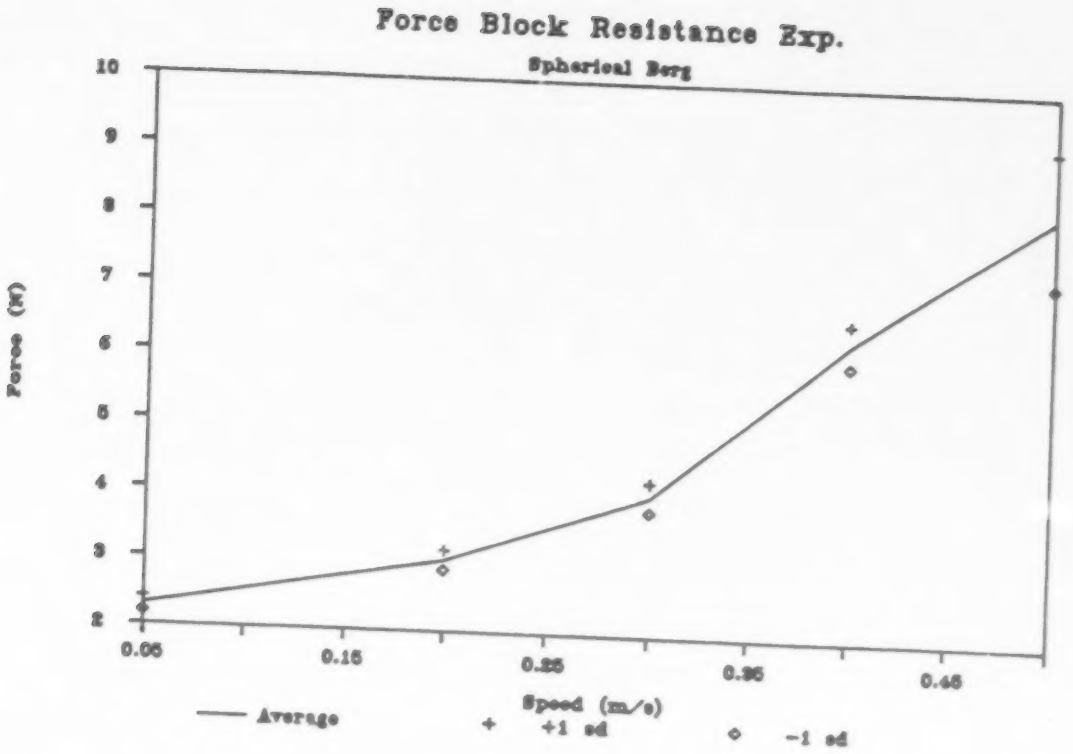

Figure 6.4 Resistance Curve for Sphere With Free Moving Model

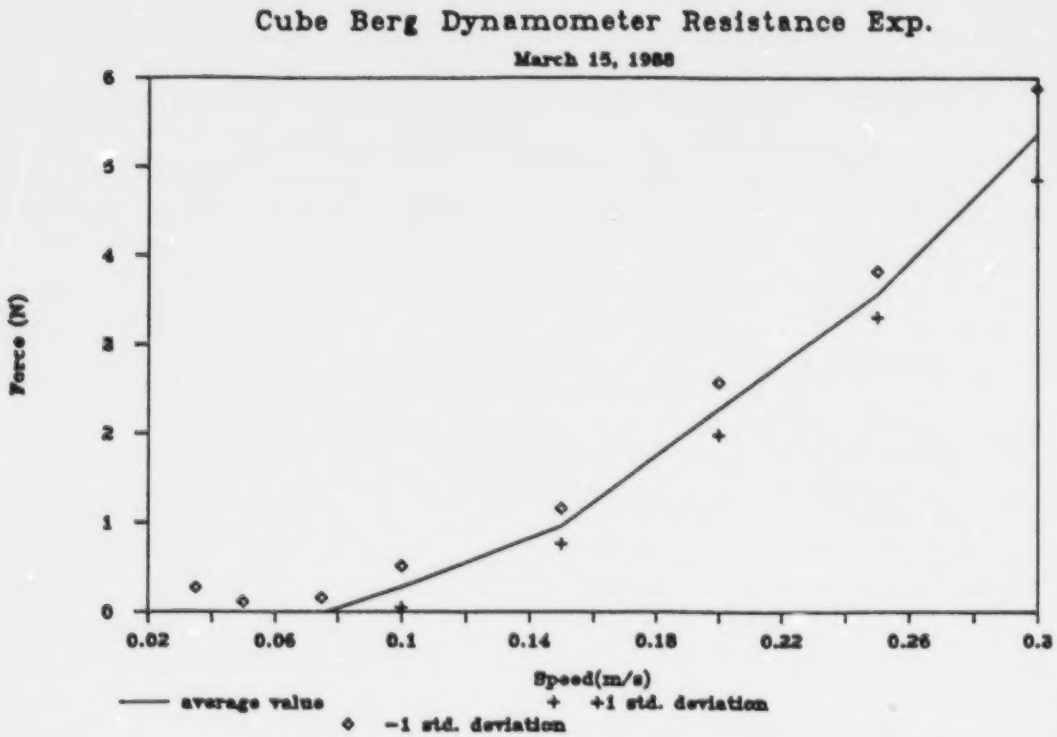

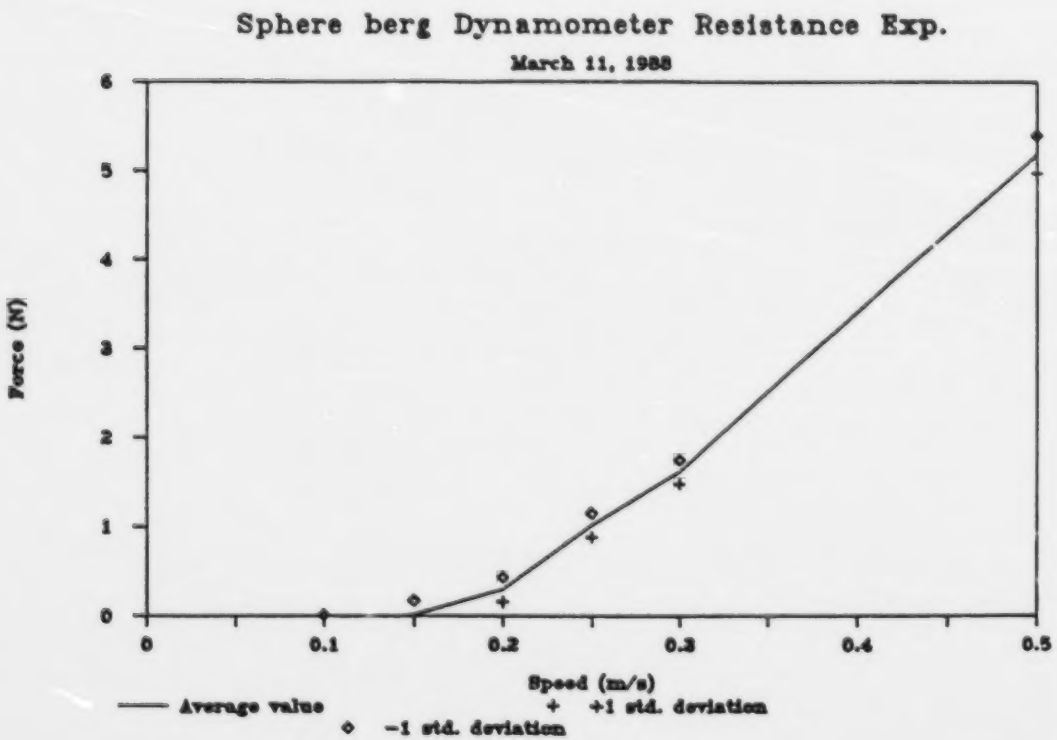

Figure 6.5 Resistance Curve for Cube and Sphere With Rigid Model

eddies were visible around the bow of the models tested. The calculated drag coefficients are shown in Table 6.1 for the cube and sphere.

$$C_D = \frac{2D}{\rho A V^2}$$

where C_D = drag coefficient
D = drag force
ρ = water density
A = projected area normal to flow
V = velocity.

Above a speed of 0.20 m/s, the drag coefficients are self consistent and in the expected range. They are plotted on Fig. 5.1 with the symbols . for the sphere and x for the cube. Note that the data from Batchelor are for totally immersed bodies. In the present tests there is a small additional resistance due to wave making. Unfortunately, the dynamometer is not accurate for loads less than 100 gram force (about 1N) and the data for slow speeds were rejected.

6.5 Iceberg Impact Tests

In this experiment an attempt was made to simulate as many towing schemes as possible. Due to time and budget constraints it was decided to perform the tests only on the cubical shaped iceberg. For the most part the tests were intended to be performed at what was deemed reasonable currents and towing speeds. The tests are summarized in Tables 6.1 and 6.2.

TABLE 6.1

Drag Coefficients at Various Model Velocities

SPHERE ($2a = 0.310m$, $\nu = 1.138\ cm^2/sec$)

$\text{Log}_{10} \frac{2aV}{\nu}$	Velocity m/s	Drag Force N	C_D
2.83	0.25	1.023	.697
2.91	0.30	1.627	.728
3.13	0.50	5.188	.515

CUBE ($2a = 0.350m$)

$\text{Log}_{10} \frac{2aV}{\nu}$	Velocity m/s	Drag Force N	C_D
2.66	0.15	0.962	0.775
2.79	0.20	2.283	1.034
2.89	0.25	3.567	1.034
2.97	0.30	5.367	1.080

6.5.1 Continuous Towing, Double Pulley:

The first tests conducted were with the model being towed into the 45 degree cliff by two tow ropes connected to two pulleys with no cross current. The towing force on the model was maintained up to and after the time of impact, and was the same for each of the pulleys. It was of interest during these tests to see if the iceberg reached a constant speed prior to impact, if so what it was and to look at the location of impact with respect to the target. It was also important to view the general motion of the model.

Tests numbered 1 through 12 were included in this series. They were performed with weights varying from 25 to 200 grams per tow line. To this weight must be added half the pulley weight. As the angle the towing line

TEST SUMMARY SHEETS

TEST	TIME sec	TYPE	WEIGHT grams	DRIFT cm	CLIFF deg	CURRENT m/s	SELSPOT	VIDEO
5	30	D	50, 50	0	45	0	G	O,S
6	30	D	100,100	0	45	0	G	O,S
7	30	D	70, 70	0	45	0	G	O
8	30	D	70, 70	0	45	0	G	O,S
9	30	D	150,150	0	45	0	G	O,S
10	30	D	200,200	0	45	0	G	O,S
11	30	D	120,120	0	45	0	G	O,S
12	30	D	50, 50	0	45	0	G	O
13	30	D,B	120,120	73	45	0	G	O,S
14	30	D,B	120,120	50	45	0	G	O,S
15	30	D,B	120,120	63	45	0	G	O,S
16	30	D,B	120,70	40	45	0	G	O
17	30	D,B	120,120	45	45	0	G	O,S
18	30	D,B	120,120	31	45	0	G	O,S
19	30	D	120,120	0	45	0.025	G	O,S
20	30	D	200,120	0	45	0.025	G	O,S
21	30	D	500,120	0	45	0.025	-	O,S
22	30	D	500,120	0	45	0.025	G	O,S
23	30	D	200,50	0	45	0.025	G	O,S
24	30	D	200,20	0	45	0.025	G	O,S
25	30	D	200,20	0	45	0.05	G	O,S
26	30	D	400,40	0	45	0.05	G	O,S
27	30	D	400,40	0	45	0.075	N	O,S
28	30	D	500,0	0	45	0.075	G	O,S
29	30	D	700,0	0	45	0.075	G	O,S
30	30	D	500,0	0	45	0.05	G	O,S
31	30	S	200	0	45	0.025	G	O,S
32	30	S	100	0	45	0.025	-	O,S
33	30	S	50	0	45	0.025	G	O,S
34	30	S	100	0	45	0.05	G	O,S
35	30	S	200	0	45	0.05	G	O,S
36	30	S	150	0	45	0.035	G	O,S
37	30	S	150	0	45	0.04	G	O,S
38	30	S	120	0	45	0.03	G	O,S
39	30	P	0	0	45	0.075	G	-
40	30	P	0	0	45	0.075	G	O
41	60	P	0	0	45	0.1	G	O
42	60	P	0	0	45	0.125	G	O
43	60	P	0	0	45	0.15	G	O
44	60	P	0	0	45	0.175	G	O
45	60	P	0	0	45	0.2	G	O

Table 6.2

TEST SUMMARY SHEETS

TEST	TIME sec	TYPE	WEIGHT grams	DRIFT cm	CLIFF deg	CURRENT m/s	SELSPOT	VIDEO
46	60	P,W	120	0	45	0.05	G	O
47	30	D	200,20	0	45	0.025	N	O,S
48	30	D	200,20	0	45	0.025	G	O,S
49	30	D	200,0	0	45	0.05	G	O,S
50	30	D	500,0	0	45	0.05	G	O,S
51	30	D	400,0	0	45	0.075	G	O,S
52	30	S	50	0	45	0.025	G	O,S
53	30	S	100	0	45	0.03	G	O,S
54	30	S	120	0	45	0.035	G	O,S
55	30	S	120	0	45	0.04	N	O,S
56	30	S	200	0	45	0.05	N	O,S
57	30	S	200	0	45	0.05	G	O,S
58	30	S	150	0	45	0.045	G	O,S
59	30	C	120	0	45	0	G	O,S
60	30	P,W	120	0	45	0.05	-	O,S
61	30	P,W	120	0	45	0.05	G	O,S
62	30	S	50	0	45	0.025	N	O,S
63	30	S	50	0	45	0.025	G	O,S
64	30	S	110	0	45	0.035	G	O,S
65	30	S	120	0	45	0.04	N	O,S
66	60	S	120	0	45	0.04	G	O,S
67	60	S	150	0	45	0.04	G	O,S
68	60	D	120,70	0	90	0	G	O,S
69	30	D	120,120	0	90	0	G	O,S
70	30	D,B	120,120	70	90	0	G	O,S
71	30	D	200,0	0	90	0.05	G	O,S
72	30	D,B	100	-	-	0	G	O,S
73	30	D,B	70	56	-	0	G	O,S
74	30	D,B	120	58	-	0	G	O,S
75	30	D,B	150	58	-	0	G	O,S
76	30	D,B	70	51	-	0	G	O,S
77	30	D,B	100	51	-	0	G	O,S
78	30	D,B	120	58	-	0	G	O,S

KEY
- S - Single weight
- D - Double weight
- B - Allowed to drift
- W - Weight added
- P - Pendulum
- C - Pulleys moved together

- G - Good data
- N - Noisy data
- O - Overhead view
- S - Side view

Table 6.3

made with the model changed during the test the towing force also changed. However, calculations show that 84 percent of the towing force was maintained up to the point of impact and 95 percent up to 1.0 meters from the target. The model reached a constant speed in all of the tests conducted. The model velocity and towing force are shown in Table 6.4.

Table 6.4

Model Velocity and Towing Force

Weight/Pulley g	Model Velocity m/s	Towing Force g
50	0.067	111
70	0.082	131
100	0.092	161
120	0.106	181
150	0.107	211
200	0.179	261

The cube did not hit the target in all of the tests, this may be due to inaccurate positioning of the model on the far side of the tank, the eyebolts on the cube being slightly asymmetrical or the drag of the LED cables. The friction of the pulleys and line was approximately identical for each side of the model.

In plotting the Selspot data the following coordinate system was maintained. The surge axis is positive towards the beach, the sway axis is positive to the left of the beach (towards the pendulum point), from the centerline of the input point and the heave axis is positive out of the water. Pitch is positive in the sense of rotation from the surge axis to the heave axis; roll is positive in the sense of rotation from the heave axis to the sway axis; yaw is positive in the sense of rotation from

the sway axis to the surge axis (Figure 6.9).

Selspot data for tests #6,#10 and #12 (Figure 6.6 - 6.8) show the model motion at speeds of 0.092, 0.179 and 0.067 m/s. From the tests it is evident that the berg heaved only slightly but swayed considerably from the right to left. Mostly the roll and pitch motion occurred after impact. This motion increased with the speed of the berg. The speed of the berg was calculated from the slope of the surge plot and is shown on the figures. An iceberg speed of 1 m/s is anticipated for the full scale project, this relates to a model speed of 0.1 m/s. This approximate speed was attained by using weights of 120 g/pulley in the model tests.

6.5.2 Drift, Double Pulley:

It was of interest to look at the drift of the iceberg after the towing had ceased. This was simulated by having the weights on the pulleys "bottom out" at selected distances from the cliff. The weight chosen for these tests was 120 g/pulley as that was the amount needed to develop the required berg velocity. In these tests the release distance from the cliff was varied from 0.73 to 0.31 (corresponding to prototype distances of 73 to 31 m) meters and no currents were simulated.

Examples of the Selspot data for these are shown in Figures 6.10, 6.11 and 6.12, in which the weights were removed at 0.73, 0.50 and 0.31 meters from the target location, respectively. During the tests it was difficult to discern the slowing down of the cube. However the selspot data clearly exhibits a flattening of the surge curve, which corresponds to a deceleration of the berg. It can be assumed that the cube had a similar initial velocity in each trial as the same weights were used. The

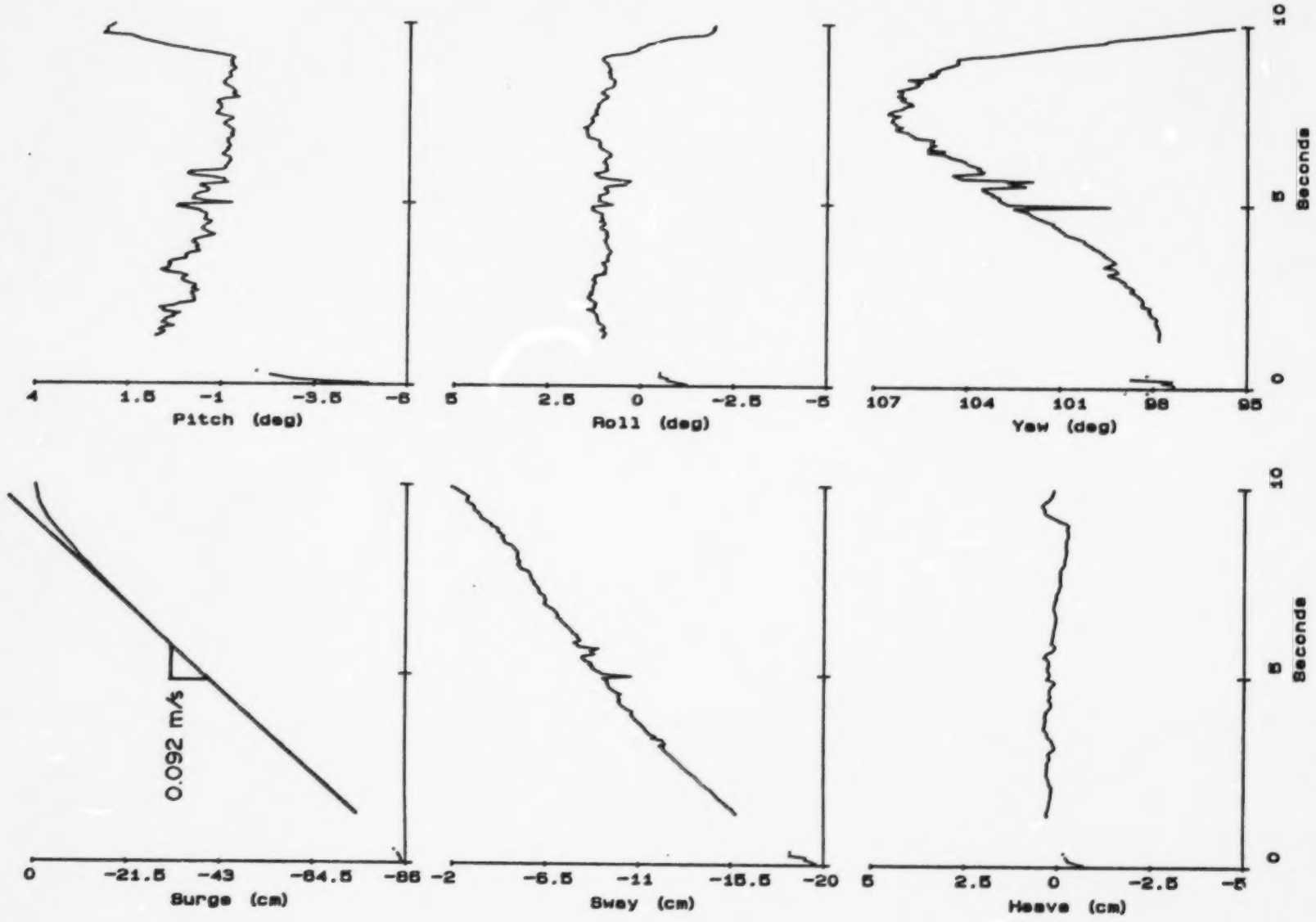

Figure 6.6 (Test #6, 10, 12) Continuous Towing, Double Pulley, Selspot Data

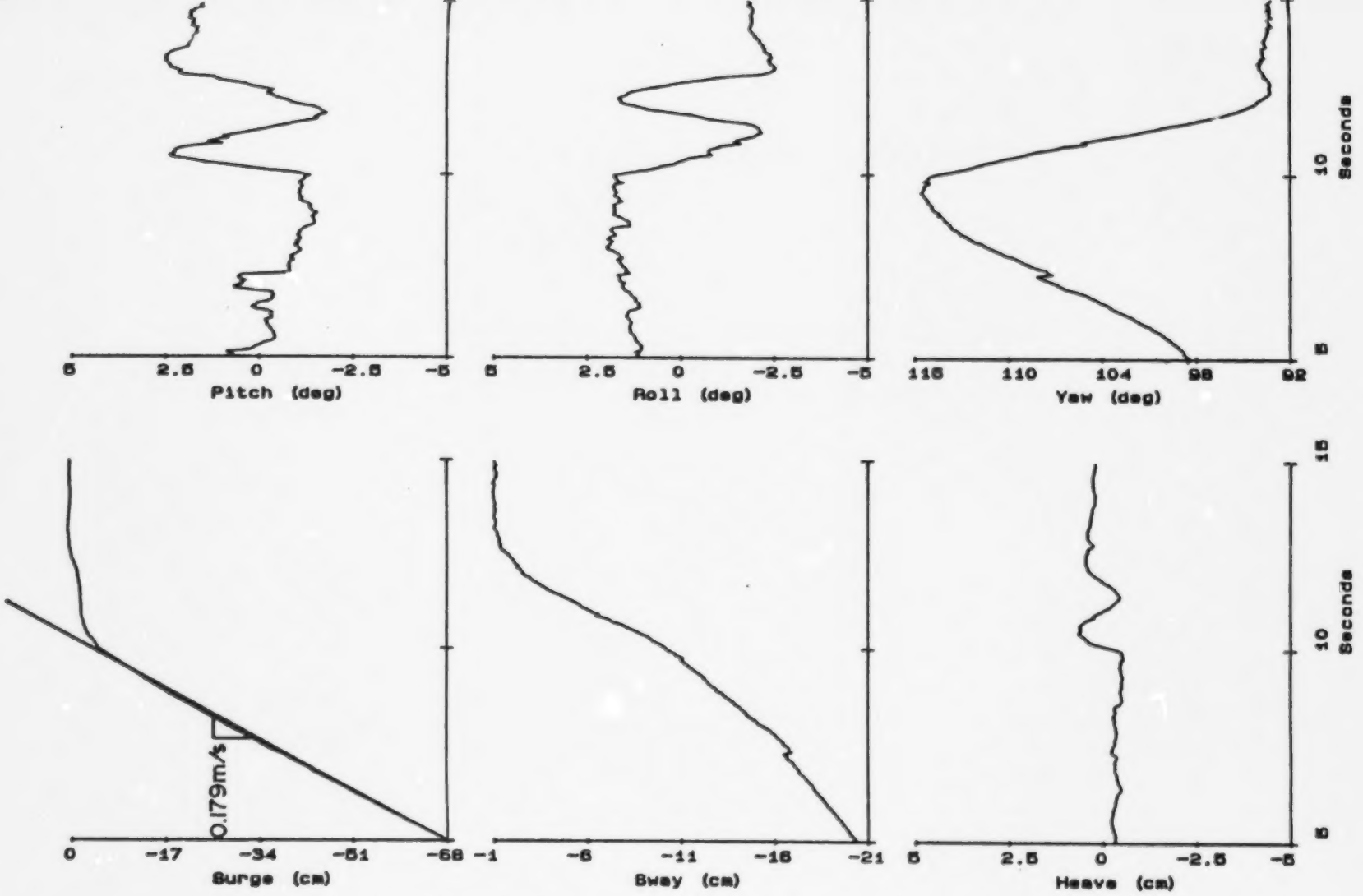

Figure 6.7 (Test #6, 10, 12) Continuous Towing, Double Pulley, Selspot Data

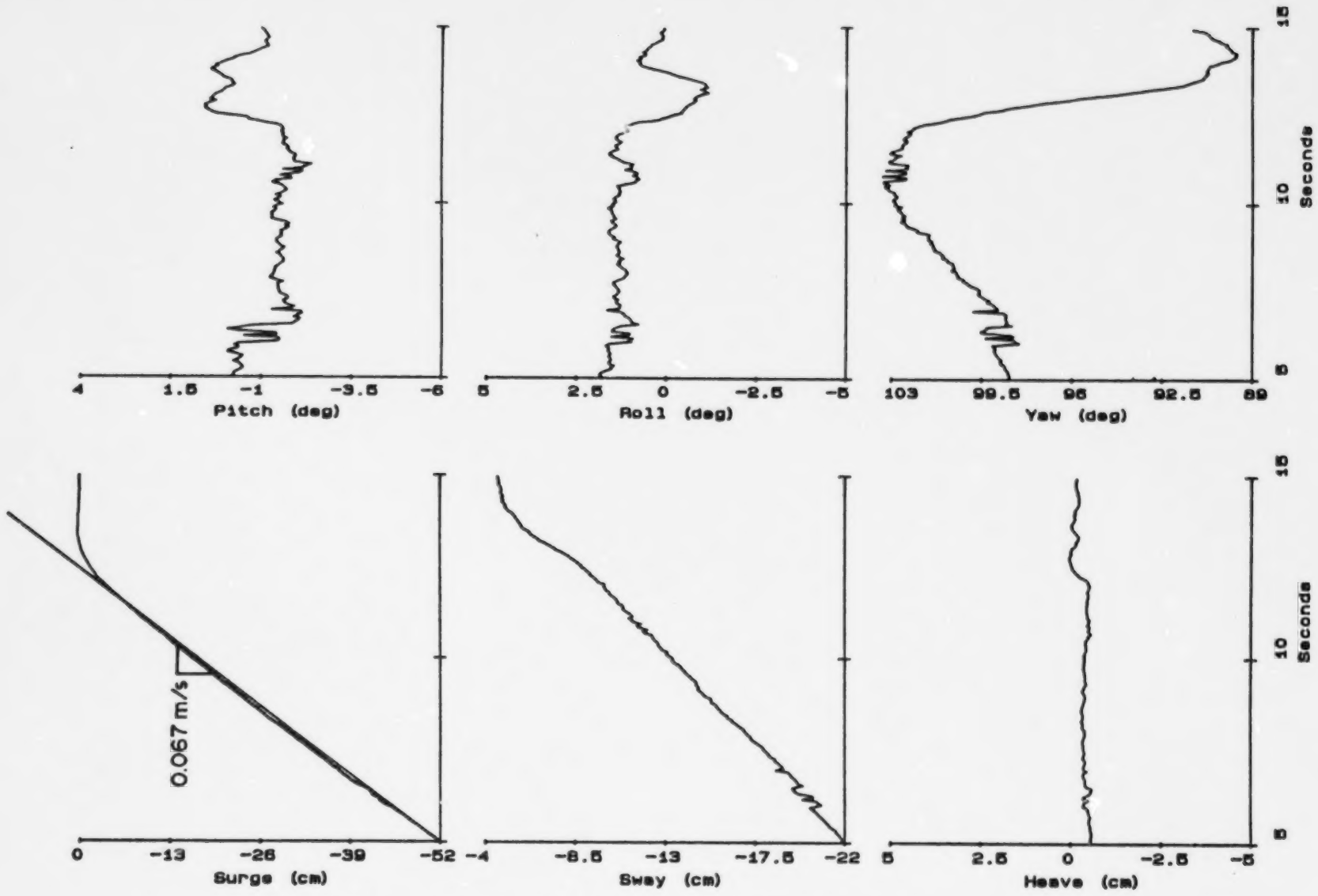

Figure 6.8 (Test #6, 10, 12) Continuous Towing, Double Pulley, Selspot Data

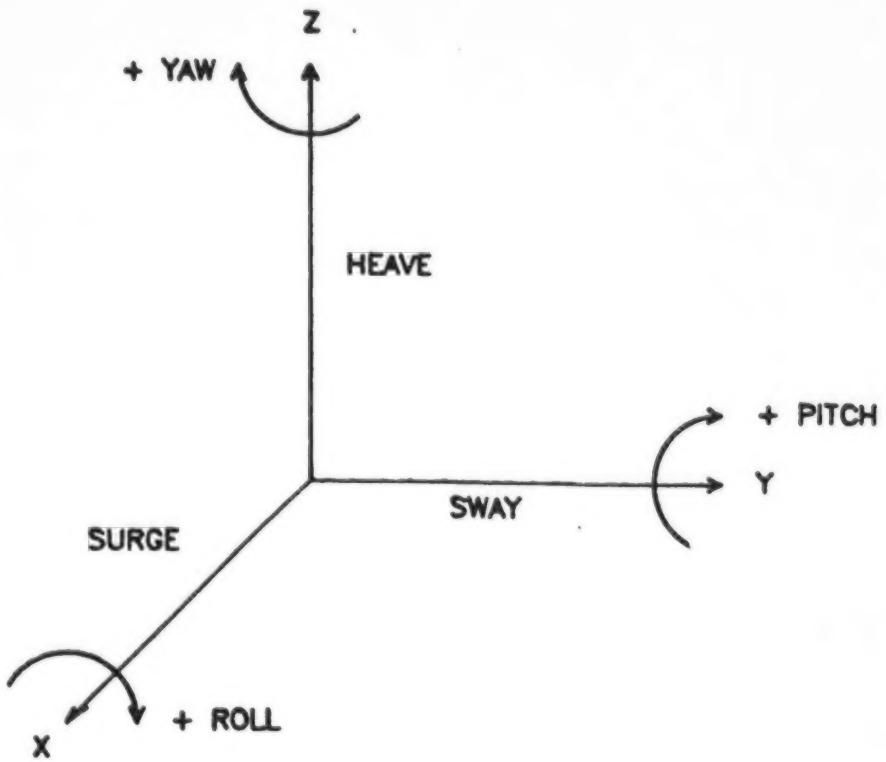

The Six Degrees of Freedom
For a Body in Motion

Figure 6.9 Selspot Co-ordinate System

curves also show a greater total decrease in model speed as the release distance is increased, as expected.

6.5.3 With Current, Double Pulley:

One of the concerns in the site selection was the strength and the direction of the current. In this series of tests various currents were simulated by moving the carriage with the test setup along the length of the tank. The model was started in line with the centerline of the 45 degree cliff. The object of these tests was to make use of two pulleys and determine if it was possible to hit the target with different current strengths, while maintaining reasonable iceberg speeds. The motion of the berg during the towing was also relevant.

A total of seventeen tests were conducted in this manner, with currents of 0.025, 0.05 and 0.075 m/s. Figures 6.13 to 6.16 show examples of the Selspot data for these tests. Generally the berg rotated a great deal with the influence of the current as seen in the yaw plots. It was carried 'downstream ' with the current initially, then gradually brought close to the target as it approached the cliff (see the sway plots). The smaller the weight used in each case, the greater the drift of the model. The control of the berg and repeatability of results also decreased with towing force. Optimum weight combinations were determined for three different speeds (Table 6.2 and 6.3). These weights brought the berg close to the target while keeping the speed to within towing capabilities.

It was found that at currents of 0.075 m/s, large towing forces and high icebergs speeds were required to hit the target. At higher speeds the berg impacted on a corner while at the lower model speeds it tended to

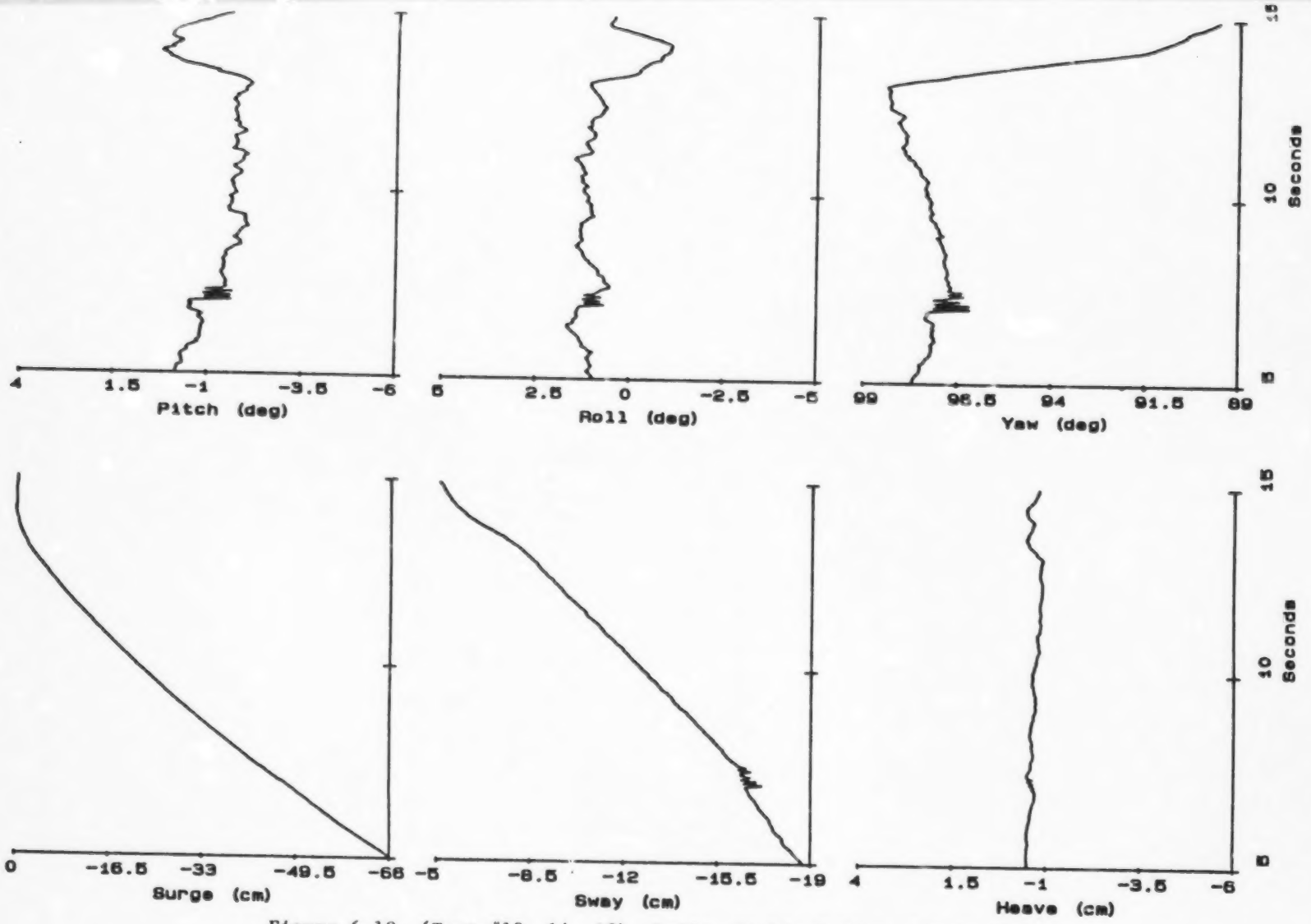

Figure 6.10 (Test #13, 14, 18) Drift, Double Pulley, Selspot Data

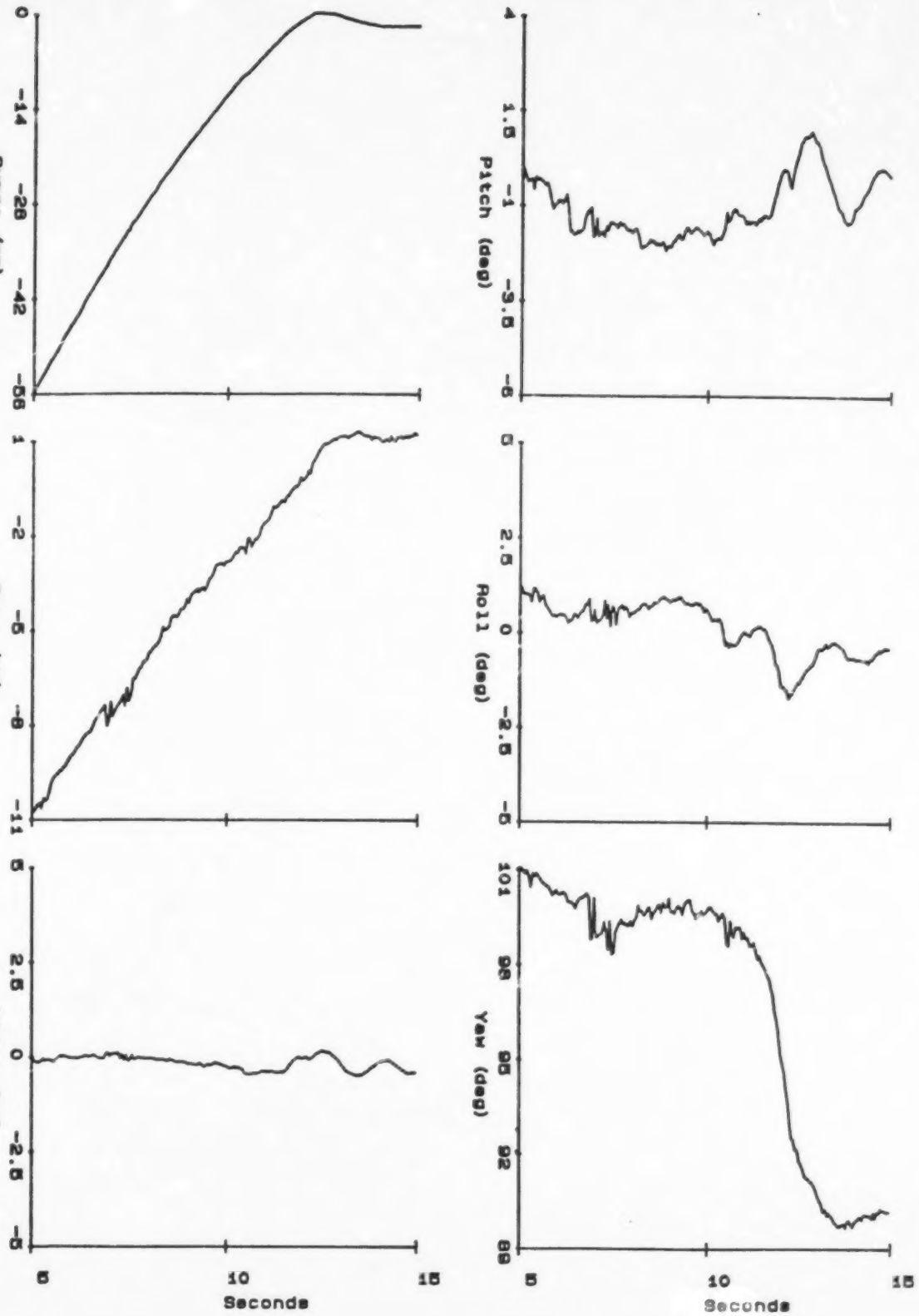

Figure 6.11 (Test #13, 14, 18) Drift, Double Pulley, Selspot Data

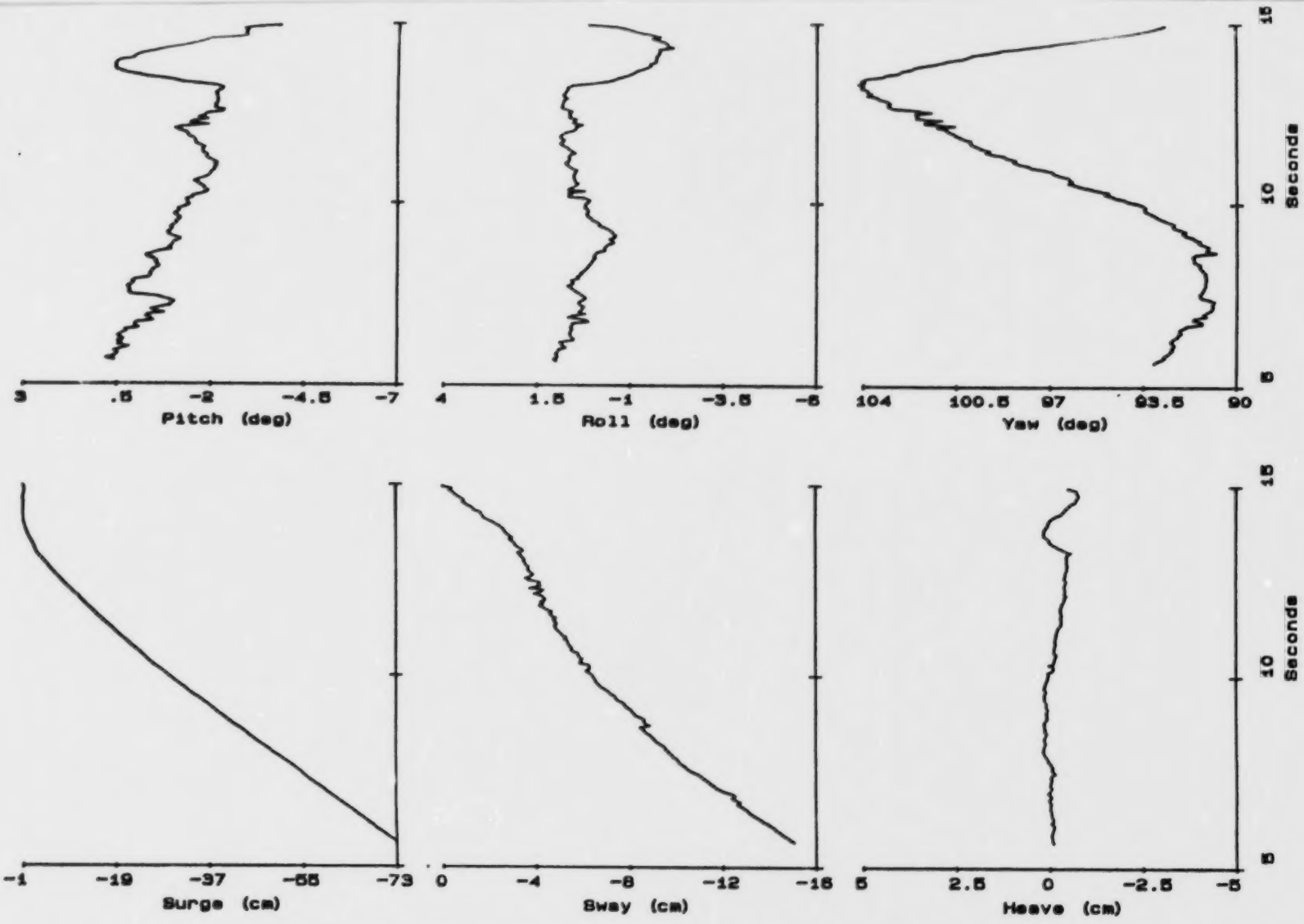

Figure 6.12 (Test #13, 14, 18) Drift, Double Pulley, Selspot Data

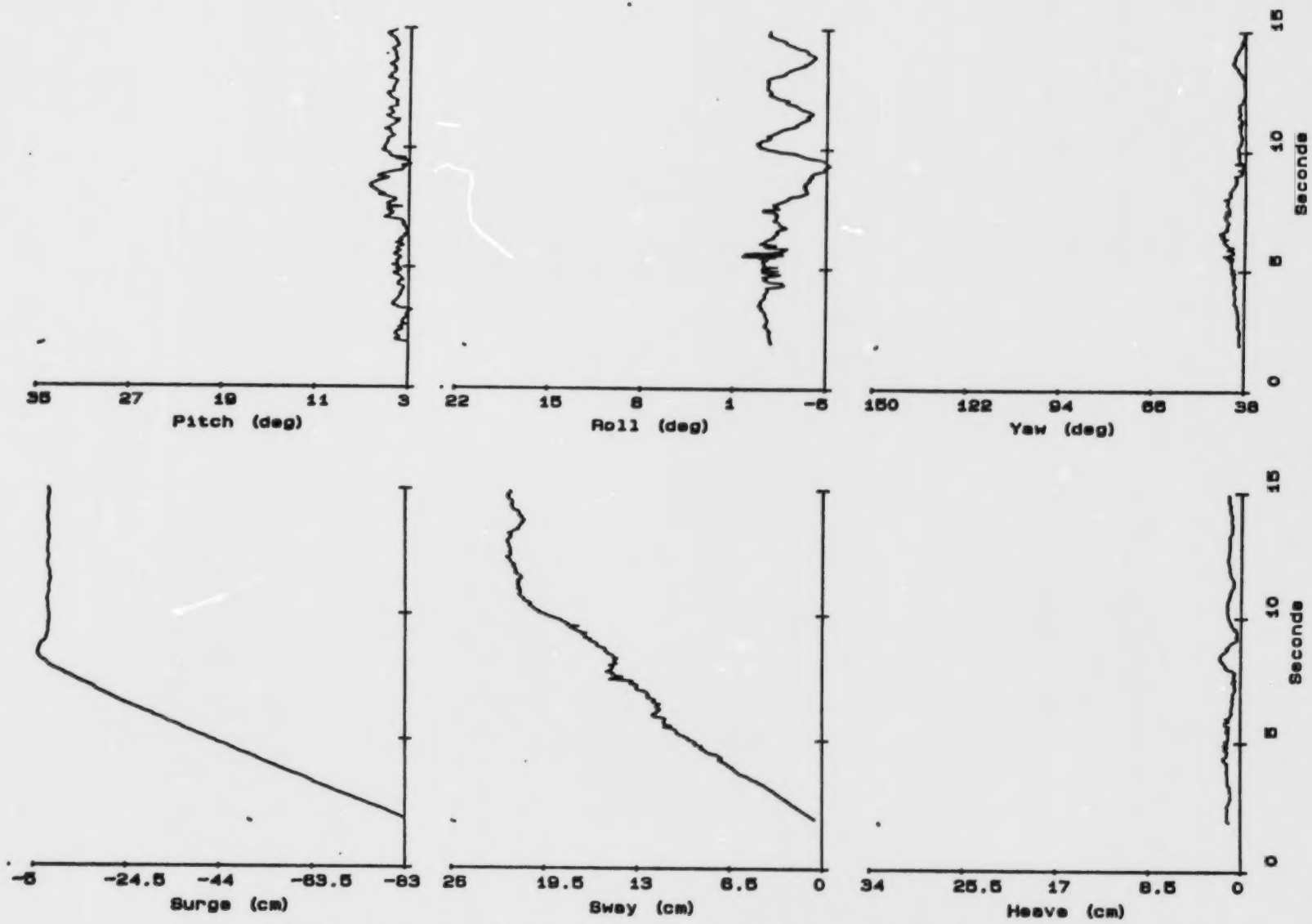

Figure 6.13 (Test #22, 23, 50, 29) With Current, Double Pulley, Selspot Data

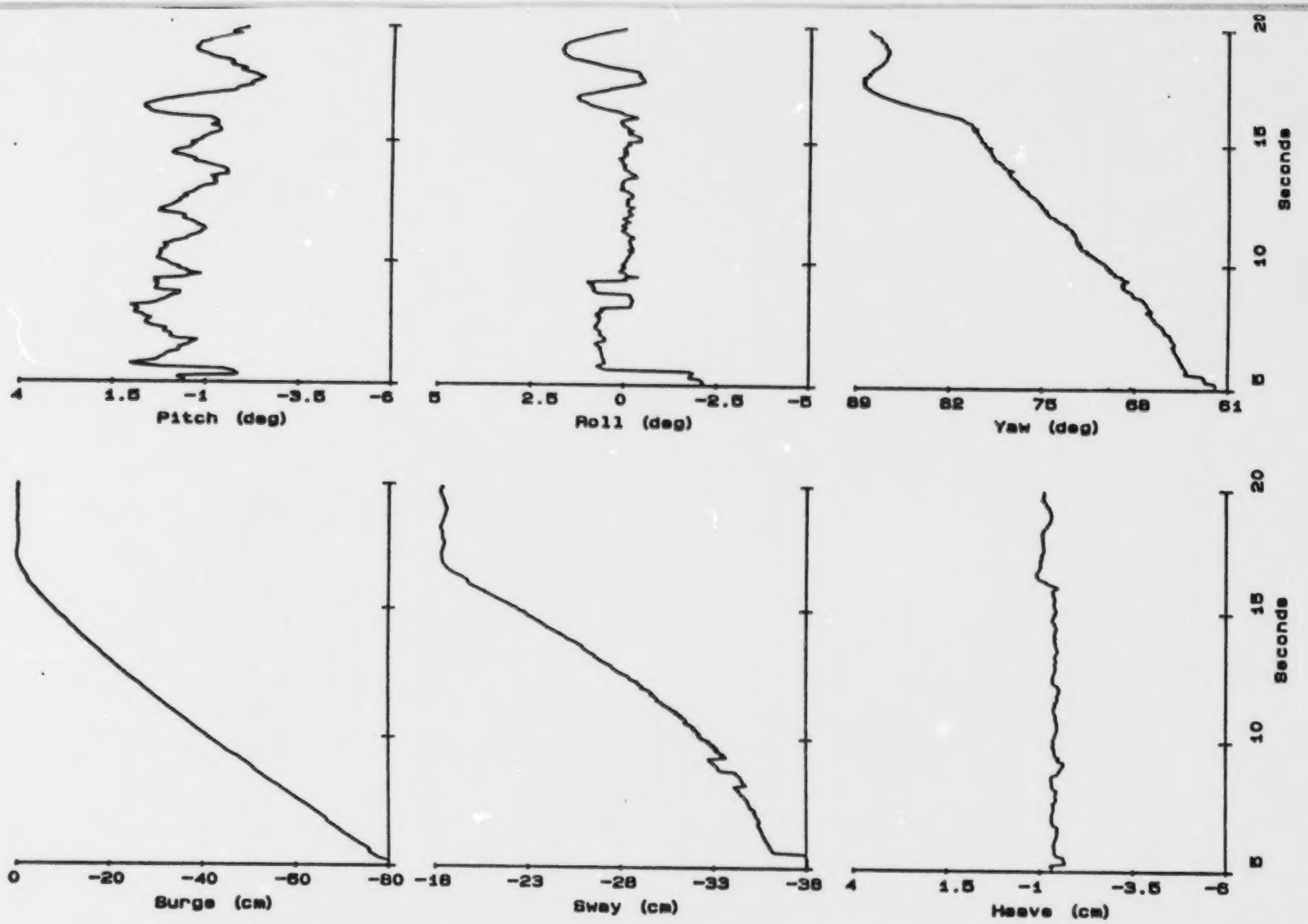

Figure 6.14 (Test #22, 23, 50, 29) With Current, Double Pulley, Selspot Data

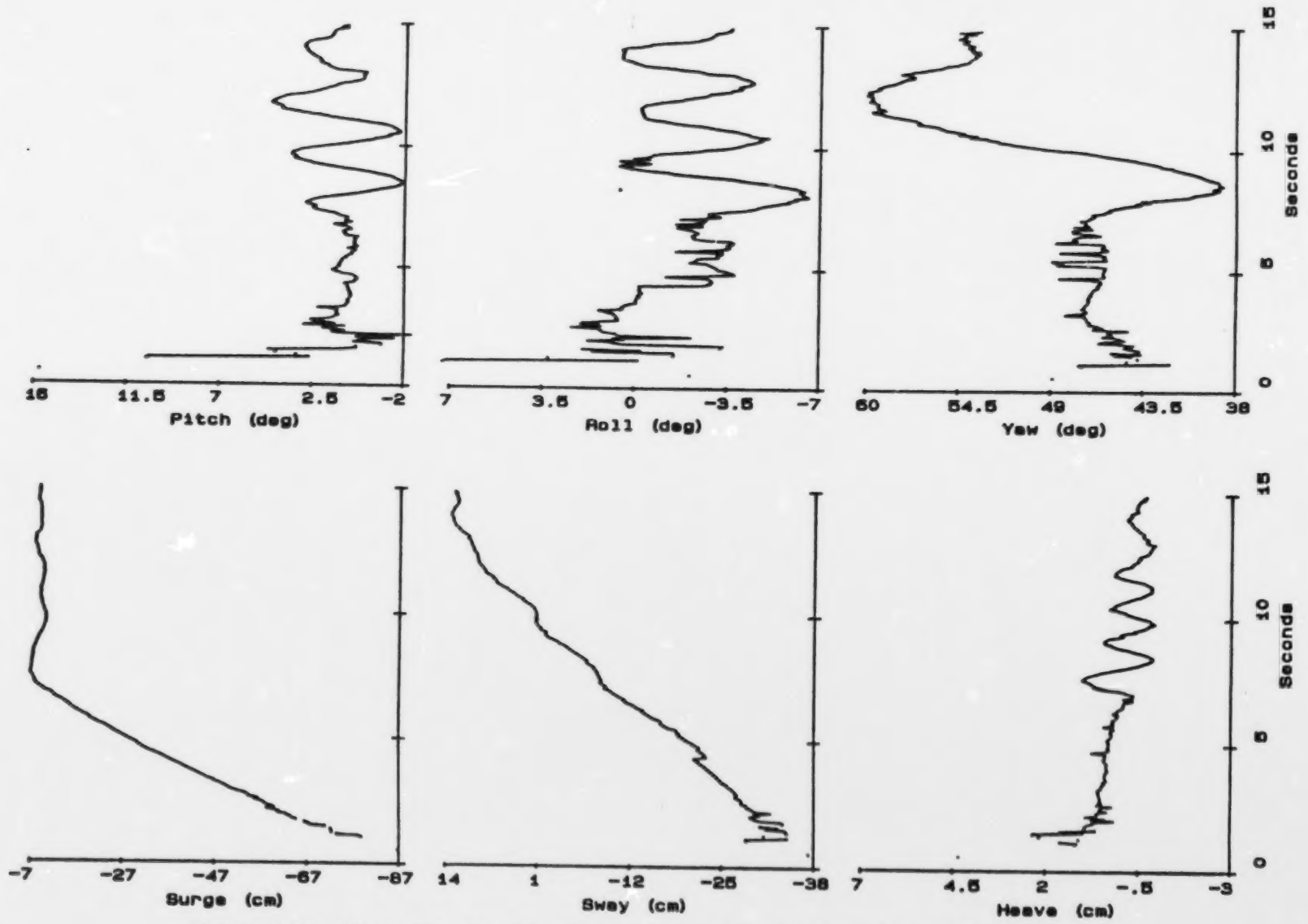

Figure 6.15 (Test #22, 23, 50, 29) With Current, Double Pulley, Selspot Data

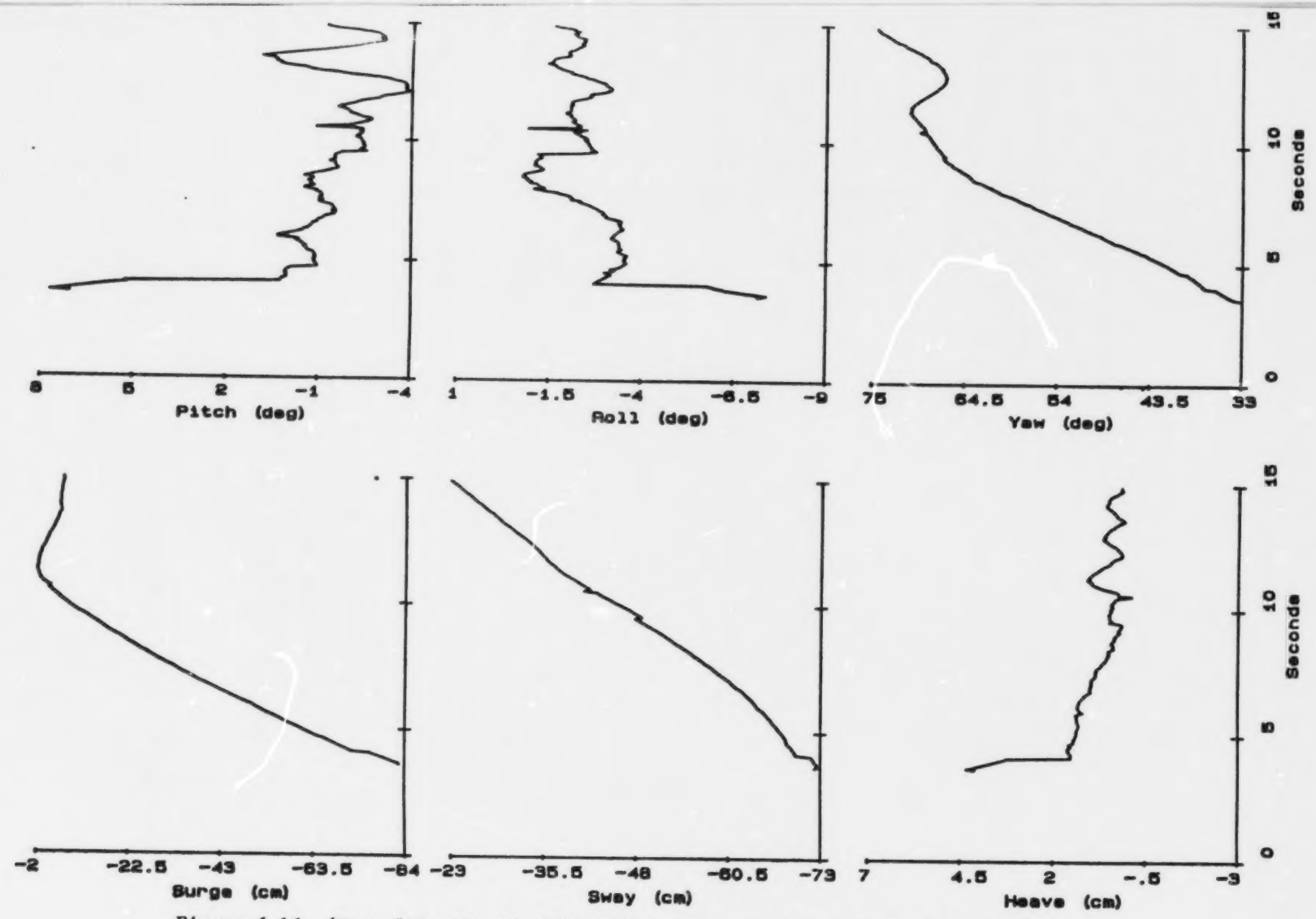

Figure 6.16 (Test #22, 23, 50, 29) With Current, Double Pulley, Selspot Data

slide slowly along the cliff before making contact. In some cases two impacts were recorded at the lower velocities.

6.5.4 Modified Pendulum, Single Pulley:

This test was similar in some respects to the previous one. The model was held on the far side of the tank and weights were used to bring the model into position. However in these tests the current was used to advantage by releasing the berg 2.25 meters upstream of the centerline of the cliff. In addition only a single pulley was used to control the model. The tests were conducted at current speeds of 0.025 to 0.05 m/s as the earlier tests indicated that this type of test was not meaningful with greater currents.

Of the twenty tests performed six have been selected to show the Selspot results at current speeds tested (Figures 6.17-6.22). Again it was important to match the weight correctly with the current so that the cube impacted directly into the cliff instead of sliding along its length. The conditions for these tests are shown in Table 6.2 and 6.3. Generally much less weight was required for these tests than the previous ones and the berg did not drift as far down stream. The majority of the impacts were with the right hand corner of the cube as seen from the water. This is shown by the yaw plots; the model enters the viewing area at 10 to 20° and rotates to 40 to 55°. In all tests the velocity of the berg decreased as it approached the cliff due to it opposing the current.

6.5.5 Pendulum, Constant Line Length:

An attempt was made to perform a pure pendulum impact test. This was

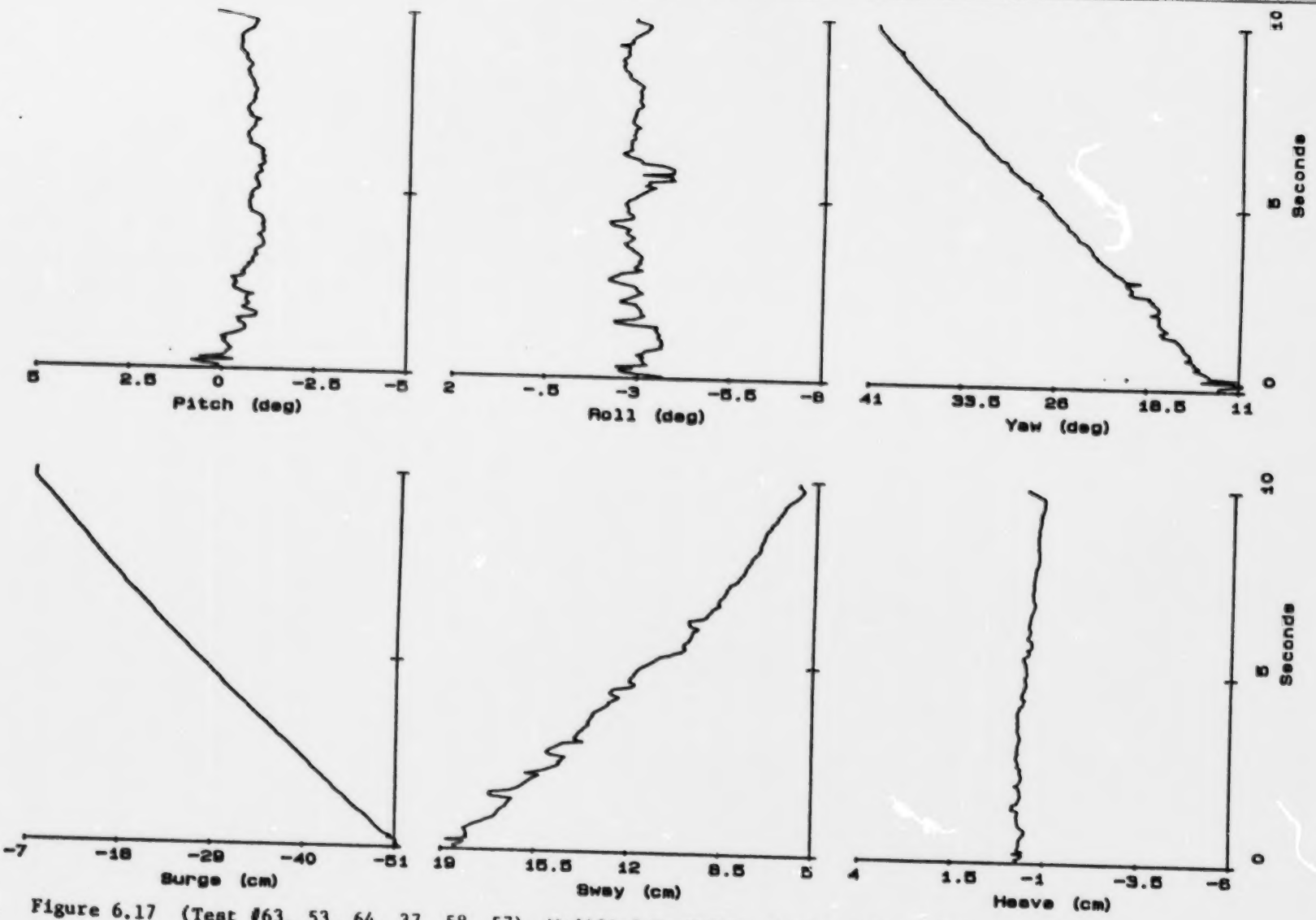

Figure 6.17 (Test #63, 53, 64, 37, 58, 57) Modified Pendulum, Single Pulley, Selspot Data

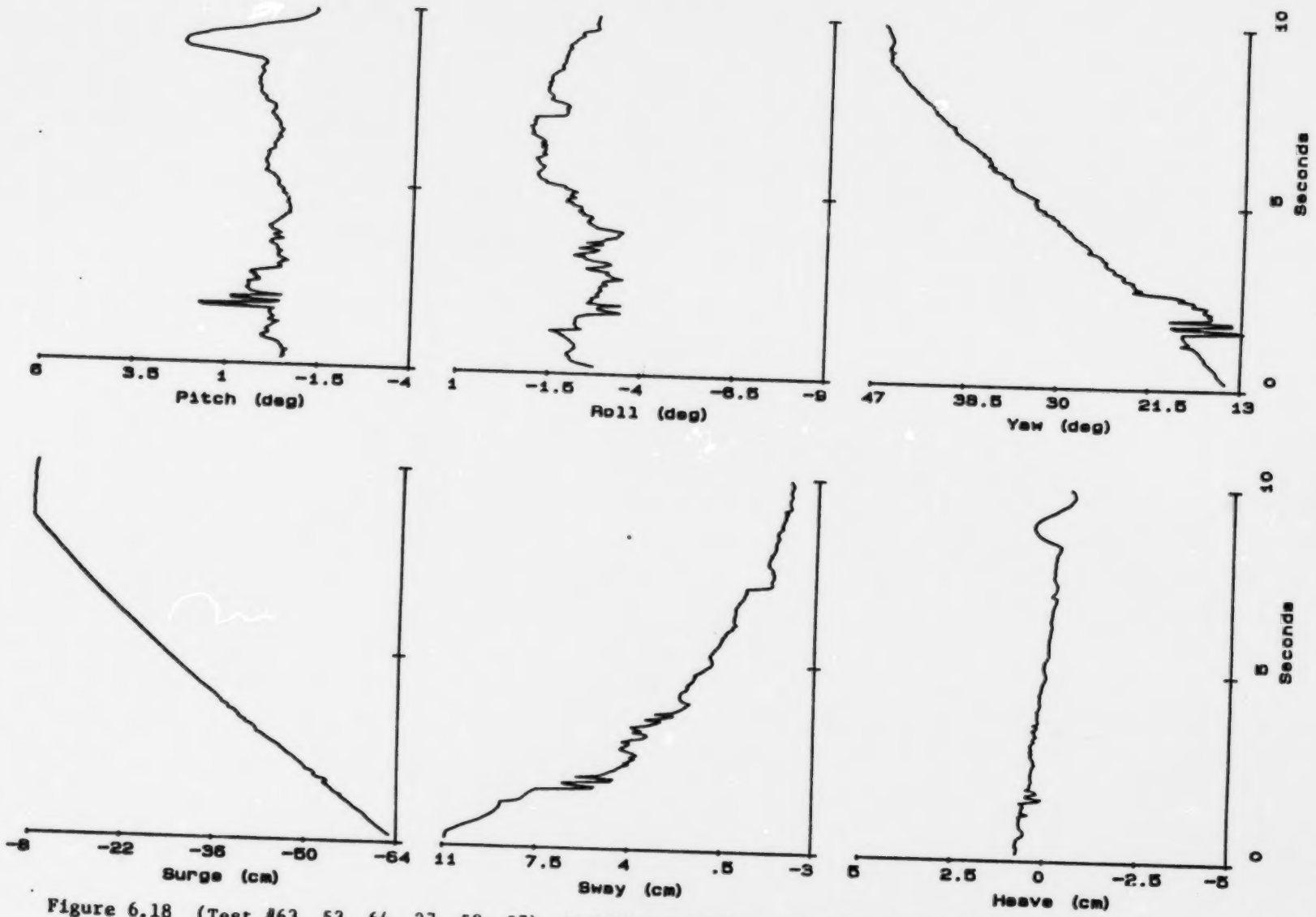

Figure 6.18 (Test #63, 53, 64, 37, 58, 57) Modified Pendulum, Single Pulley, Selspot Data

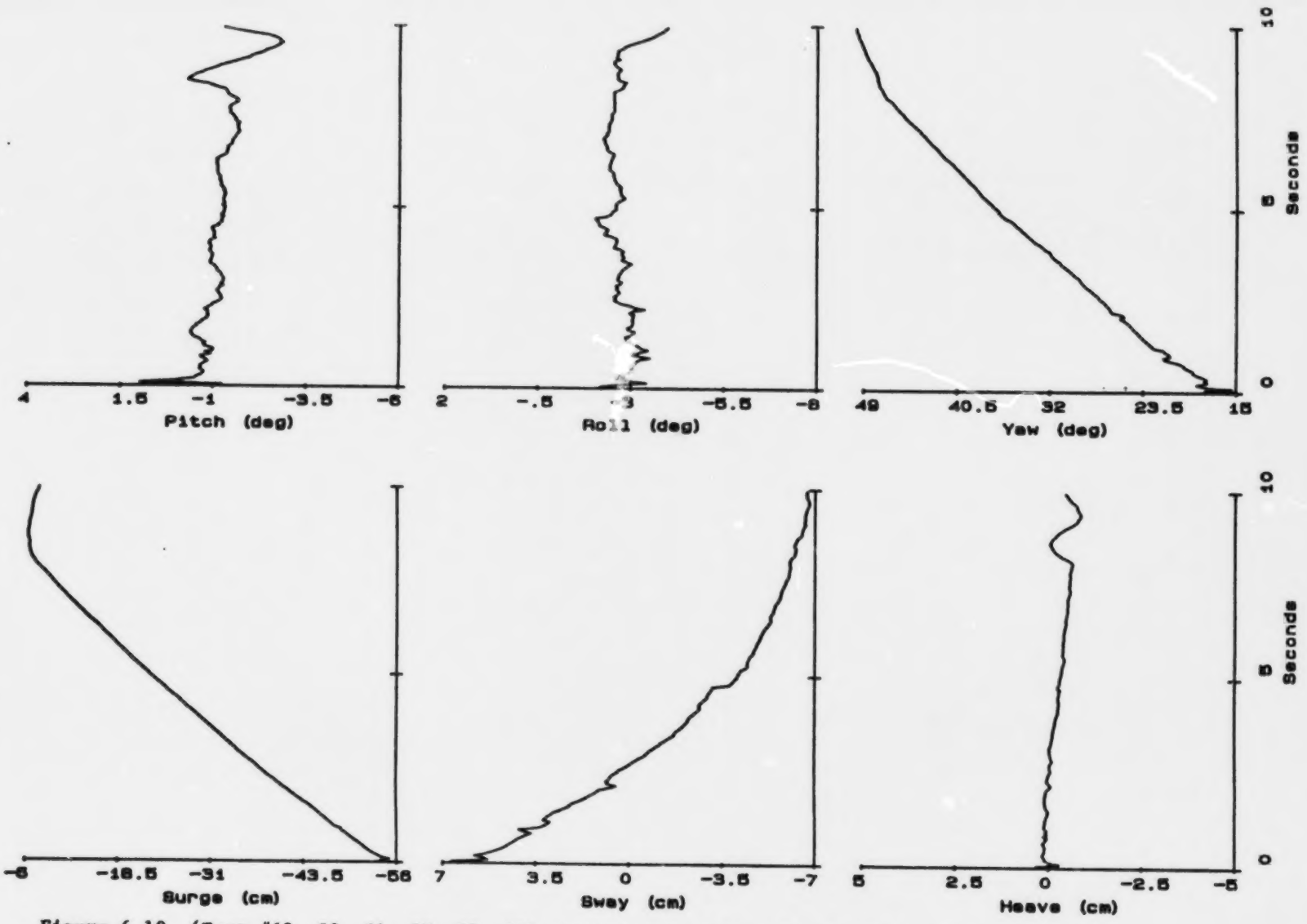

Figure 6.19 (Test #63, 53, 64, 37, 58, 57) Modified Pendulum, Single Pulley, Selspot Data

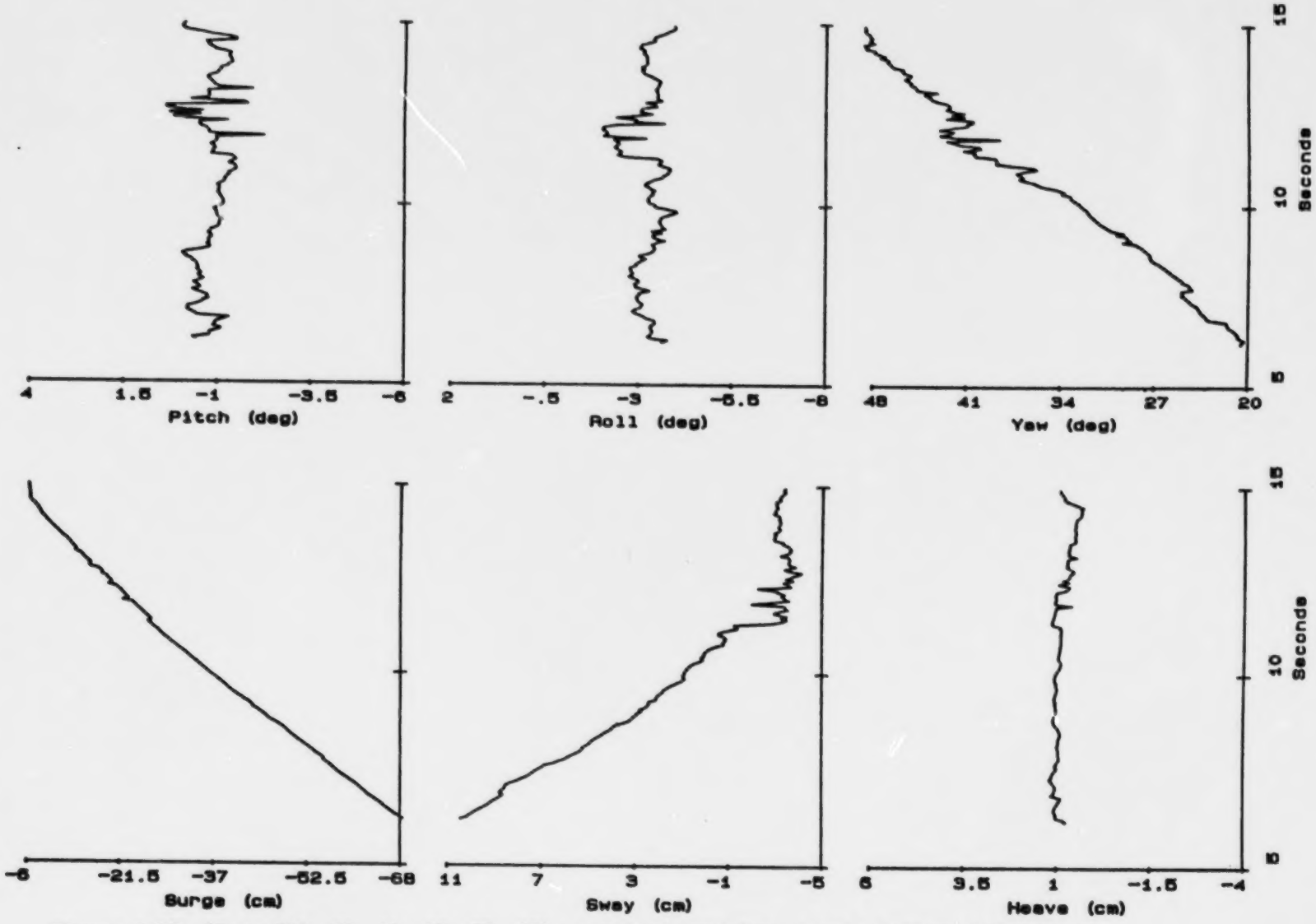

Figure 6.20 (Test #63, 53, 64, 37, 58, 57) Modified Pendulum, Single Pulley, Selspot Data

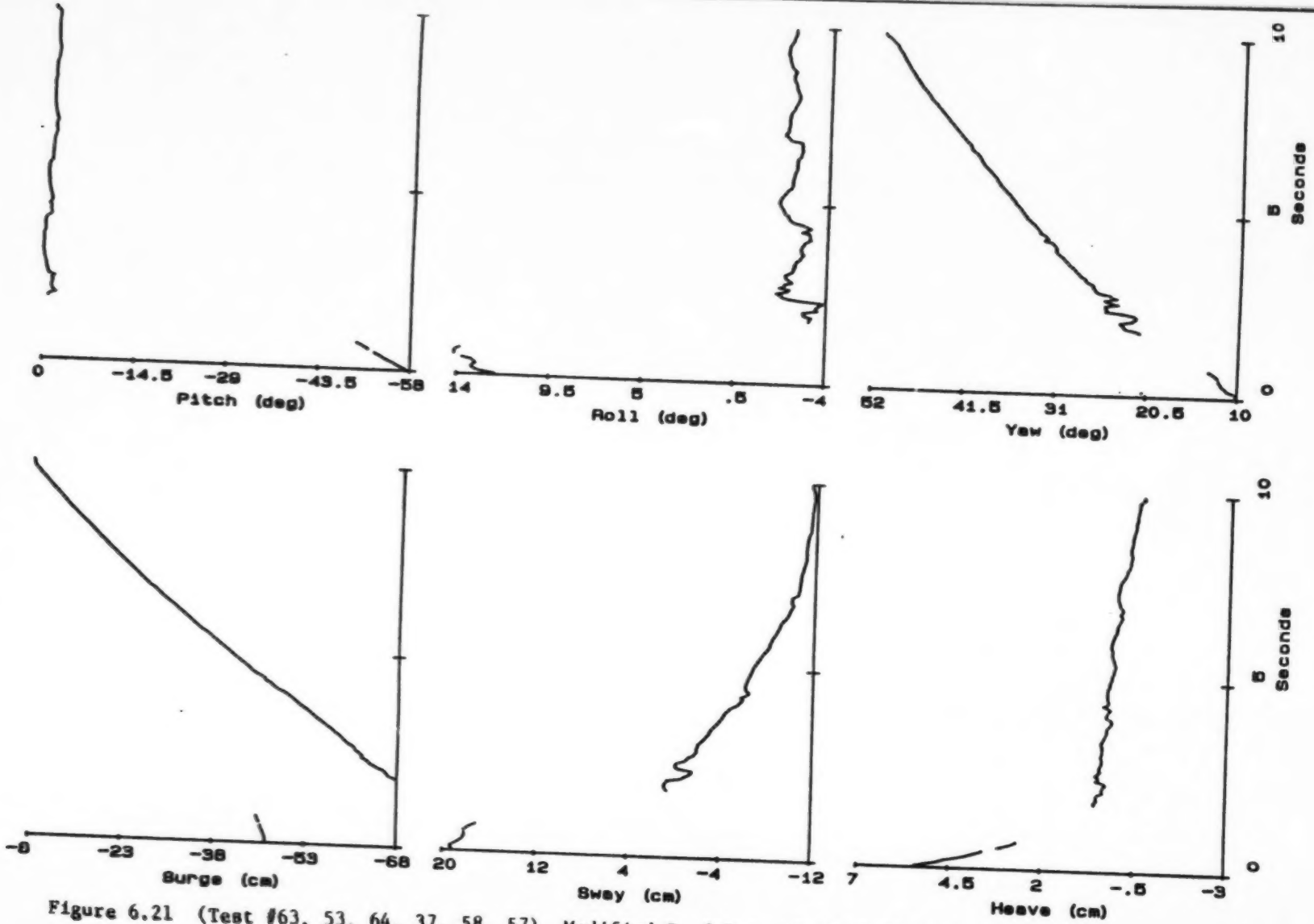

Figure 6.21 (Test #63, 53, 64, 37, 58, 57) Modified Pendulum, Single Pulley, Selspot Data

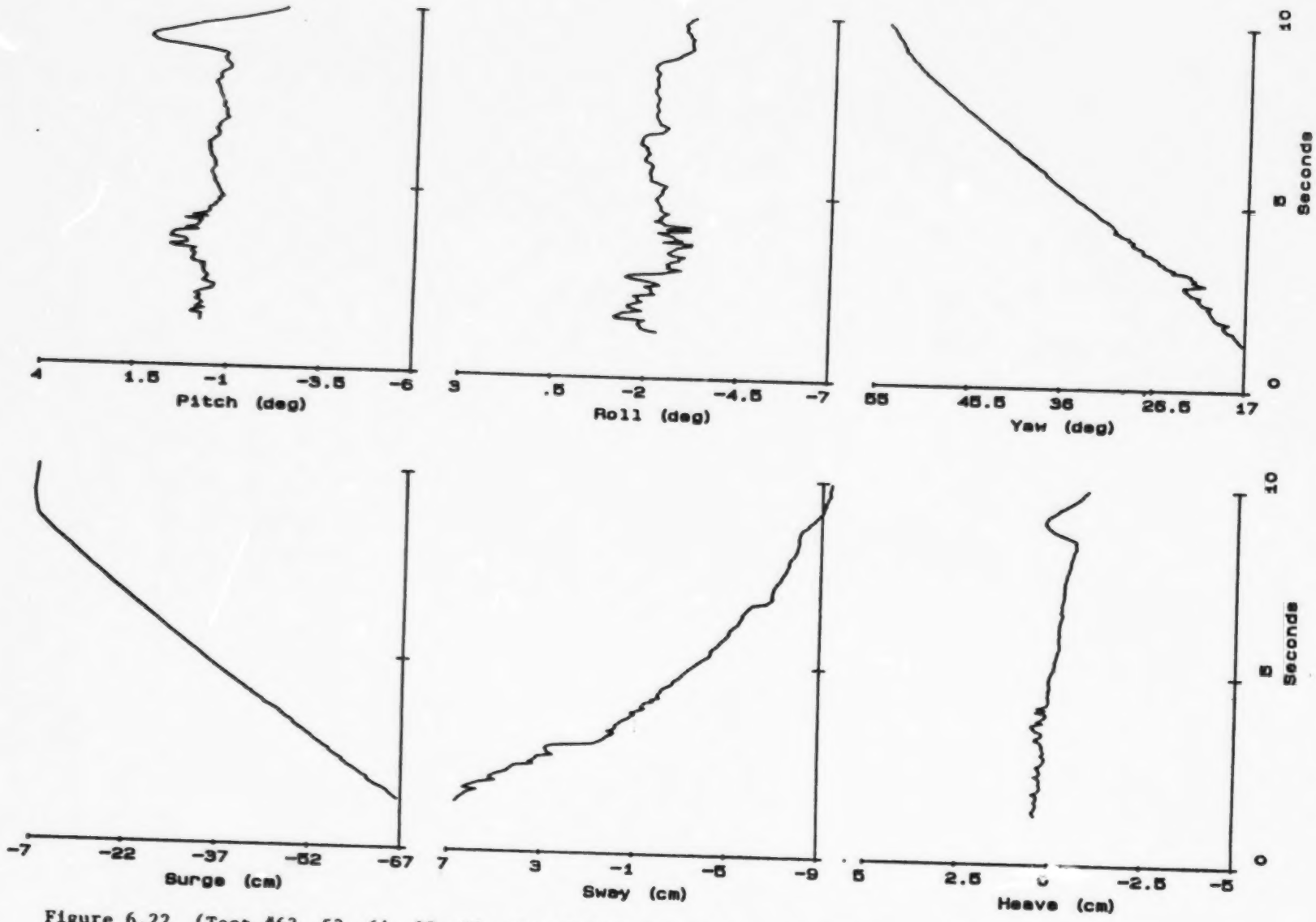

Figure 6.22 (Test #63, 53, 64, 37, 58, 57) Modified Pendulum, Single Pulley, Selspot Data

set up by securing the tow line to a pivot point located about 2.75 meters upstream of the target on the cliff. The pivot point was cantilevered over to the carriage by way of a beam, so that it moved with the carriage and was in fact 0.44 meters behind the line of the impact location (i.e the pivot is further inland than the impact target). This increased the possibility of making a 'good ' impact. To commence the tests the berg was placed perpendicular to the wall opposite the pivot point as shown in Figure 6.23.

Seven of these tests were performed at current speeds ranging from 0.075 to 0.20 m/s. At the lower speeds the cube gradually got caught by the current and moved in an arc towards the cliff and hovered near it, in some cases impacting at very slow speeds. At the higher speeds the berg impacted on the cliff and then moved off. The only impact at a reasonable speed was observed at a current of 0.2 m/s which would probably be too high to work in, due to berg instability and insufficient towing equipment. The yaw and Selspot surge plots for tests #41 and #45 in Figures 6.24 and 6.25 show the wavering of the berg at slow speeds and the impact at the highest speed.

6.5.6 Vertical Cliff Tests:

A few representative tests were performed with a vertical cliff. The set up was similar to that of the other tests but the point of impact was moved into the tank by approximately 0.12 meters. A continuous tow test, a drift test and a current with two pulleys test were completed.

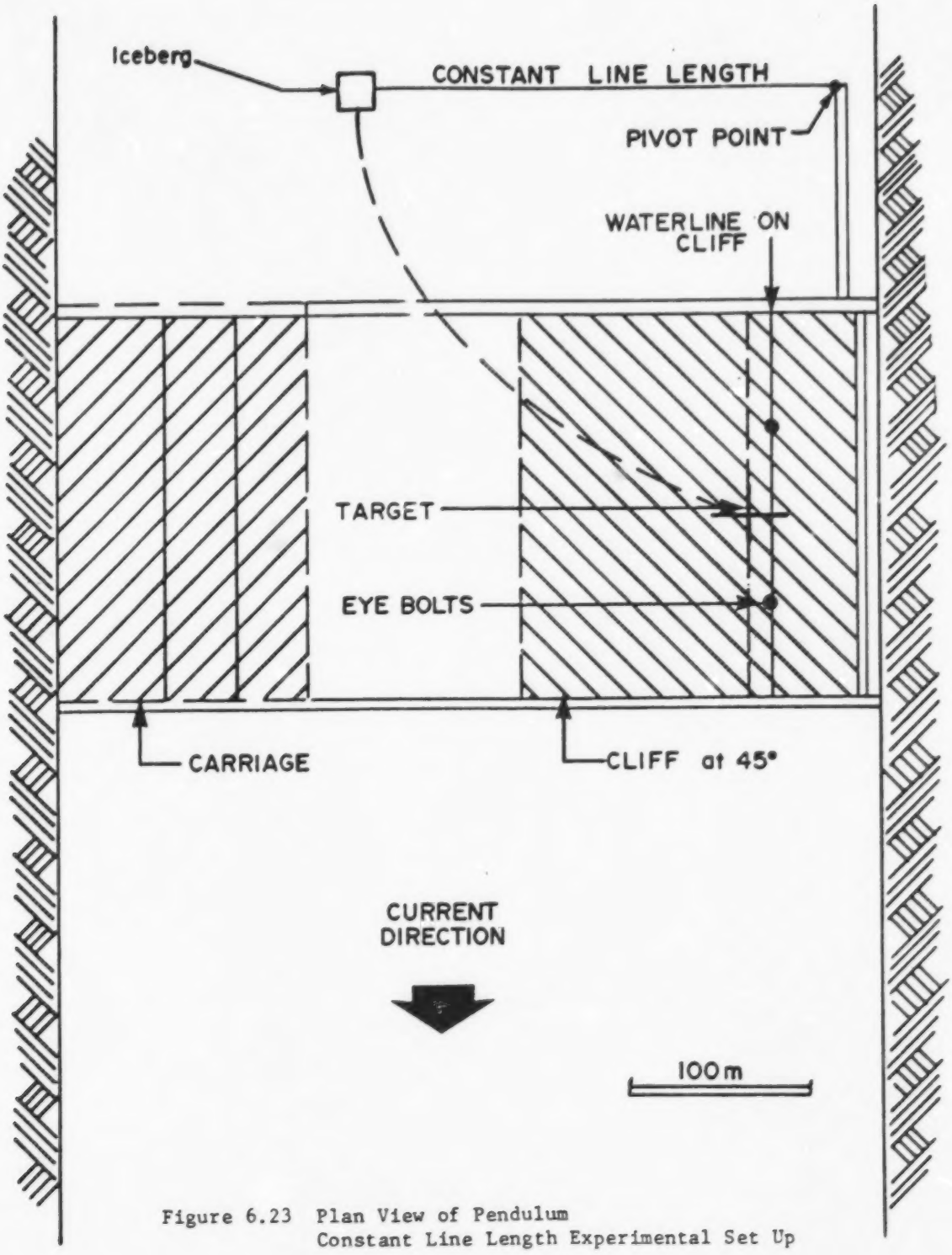

Figure 6.23 Plan View of Pendulum
Constant Line Length Experimental Set Up

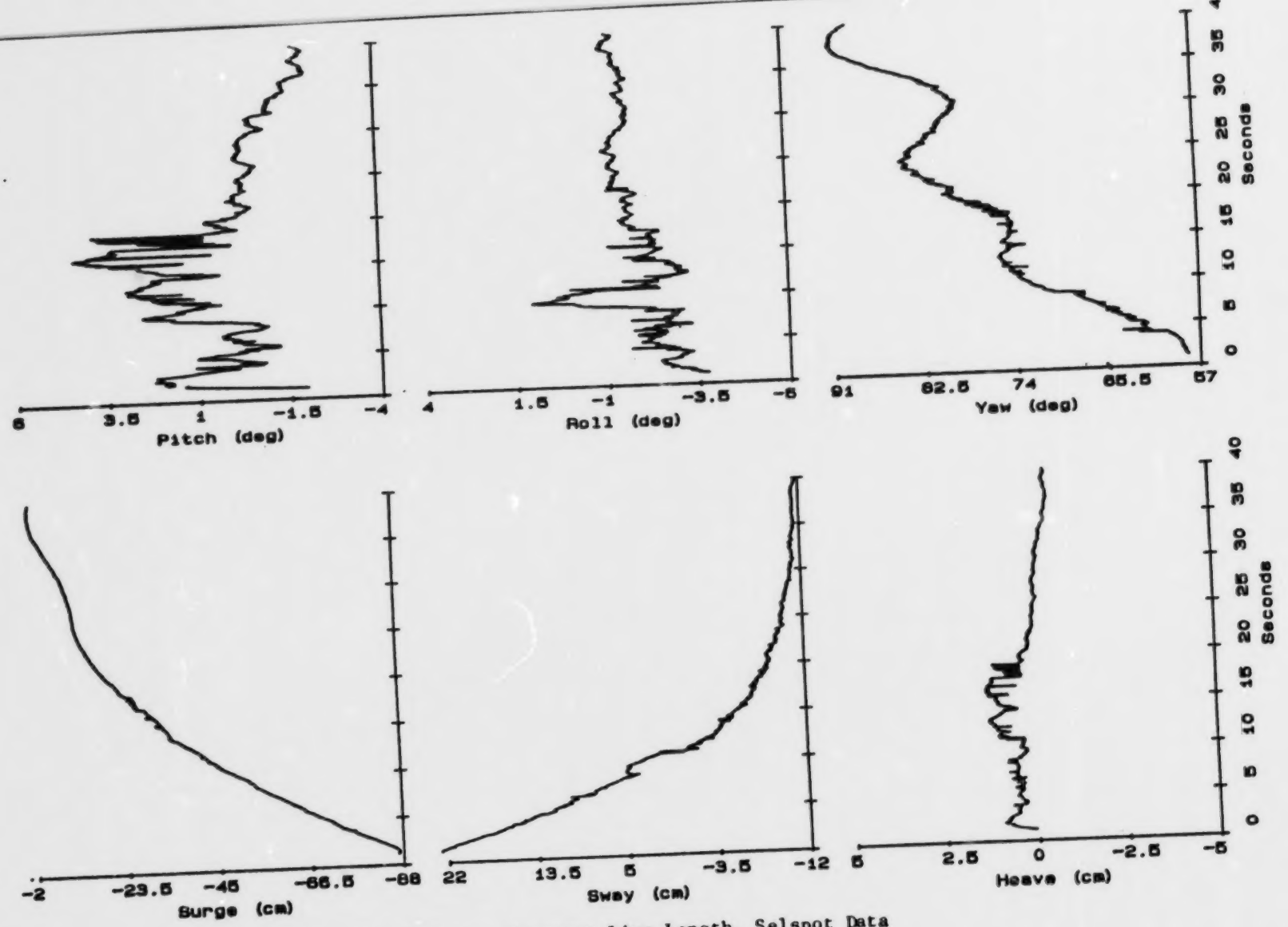

Figure 6.24 (Test #41, 45) Pendulum, Constant Line Length, Selspot Data

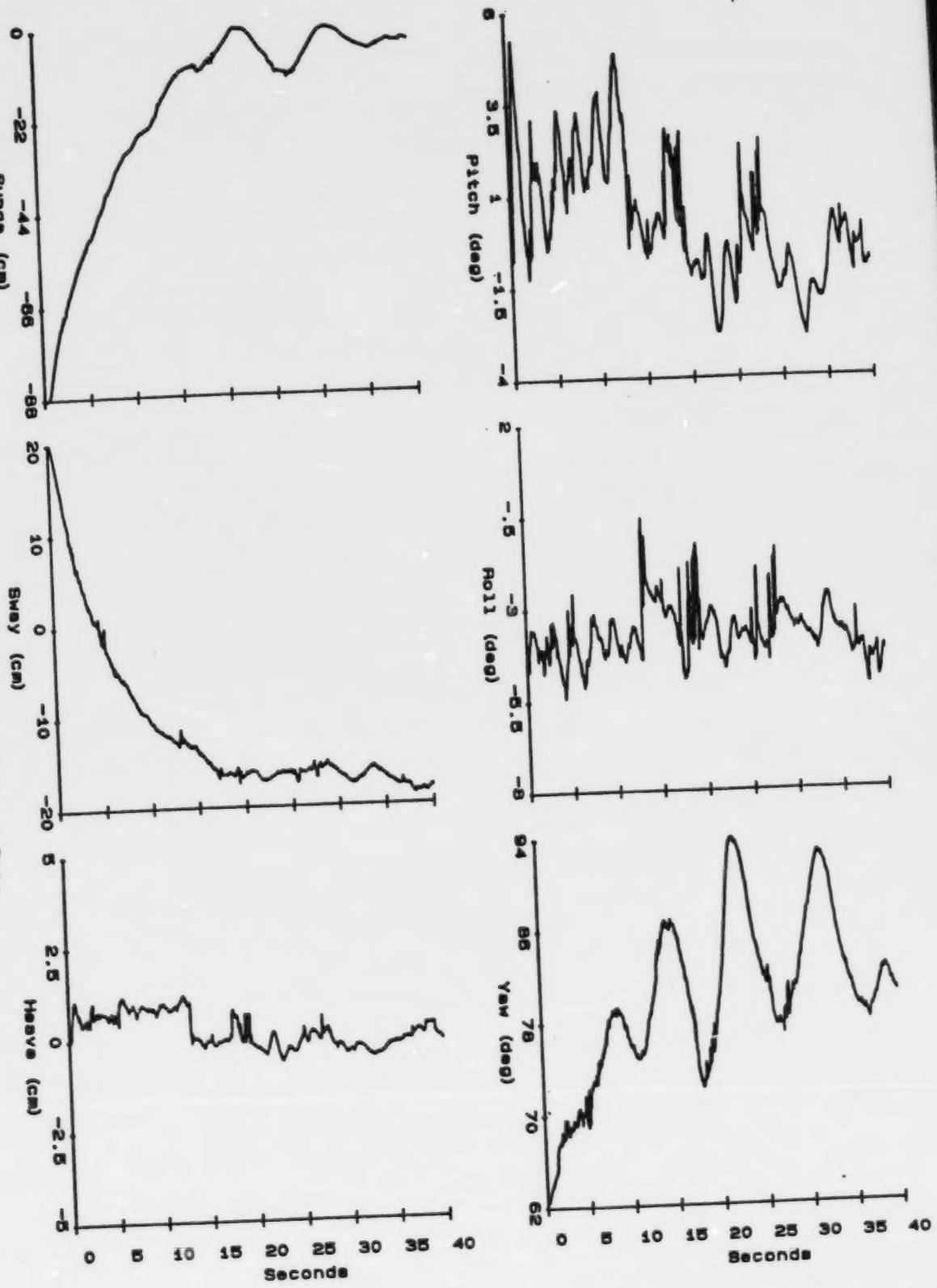

Figure 6.25 (Test #41, 45) Pendulum, Constant Line Length, Selspot Data

6.5.7 Additional Tests:

A few extra test arrangements were considered before ending this part of the experiment. The pendulum concept was expanded on by using the set up in Section 6.5 and attaching a towing line to the other side of the model. For these tests the pivot point was moved forward in line with the target, and a weight was attached to the towing line when the berg had started to decelerate near the cliff. These tests worked well but the timing of the towing was critical so that the berg had adequate speed on impact. Also, when the towing commenced, the berg rotated quickly and this could cause instability.

Another test variation checked was the effect caused by moving the eyebolts on the cliff closer together. Originally they were set at 1.00 meter; for this test they were adjusted to 0.54 meters apart, and a continuous tow, double pulley test was performed. The data recorded shows that this change had no noticeable effect on the model motion. It would perhaps have a greater influence if tested with a current.

A continuous tow, double pulley test was conducted in which the weights on the pulleys were different from one another. As expected the berg moved towards the line with the greater tension. The overhead video showed that this caused the berg to impact to the right of the target instead of to the left as in the base case.

6.6 Iceberg Free Drift Tests

If the iceberg is to be towed only part way towards the target it is important to consider how far it will drift and how it decelerates. Some of this information can be derived from the initial drag force tests, but it can be also considered from viewing the drift experiments. For these

tests it was assumed that the model reached its terminal velocity before the weights were removed, from the results of the previous tests this should be the case. The cliff was removed during these tests and the berg was towed across the tank with no current using equal weights per pulley. The weights were released from the line at approximately the same point for each trial.

Seven drift experiments were completed employing weights of 70 to 150 grams per pulley. The weights and pulleys were removed just after the model entered the Selspot viewing area. In some cases the berg did not drift far enough to reach the side wall of the tank, a distance of approximately 1.2 meters, or about three and a half berg lengths. The Selspot data for tests #76, #77 and #78 in Figures 6.26 to 6.28 shows the rotation and the deceleration of the berg with weights of 70,100 and 120 grams respectively.

6.7. Summary of Results and Conclusions

These initial experiments were used to demonstrate various pendulum and winching schemes and to examine the guidance and control of the iceberg as it approaches the target. The tests were also intended to provide an estimate of the free drift of the iceberg, and to assist in determining criteria for site selection. Finally, the data can be used to verify the theoretical calculations of iceberg motion near a large object. Listed below are the preliminary findings of this study.

- By reviewing the data from the various towing schemes it is evident that if there is a current at the site, there will be considerable problems in towing the iceberg. This is especially true if the cross

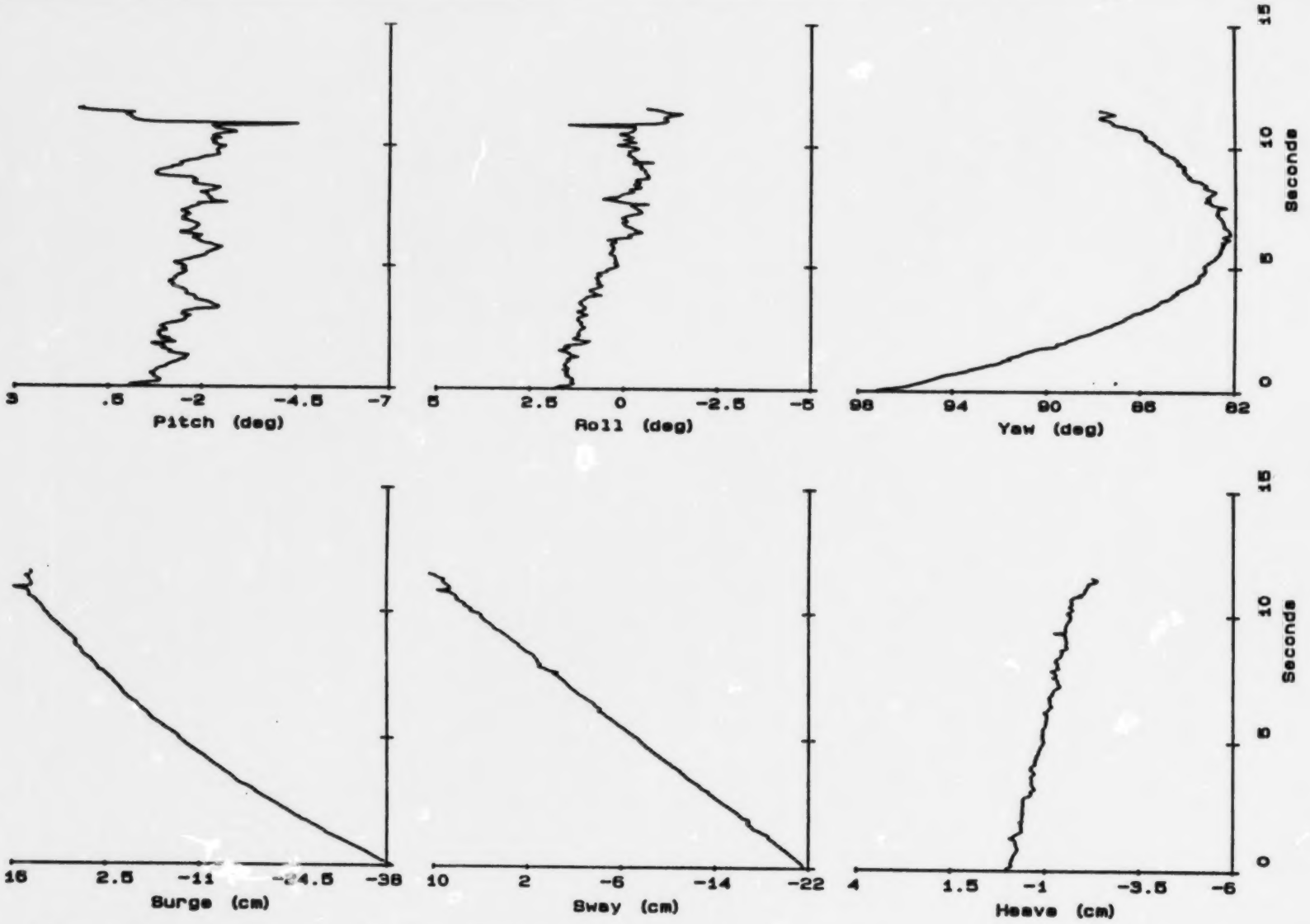

Figure 6.26 (Test #76, 77, 78) Free Drift Test, Selspot Data

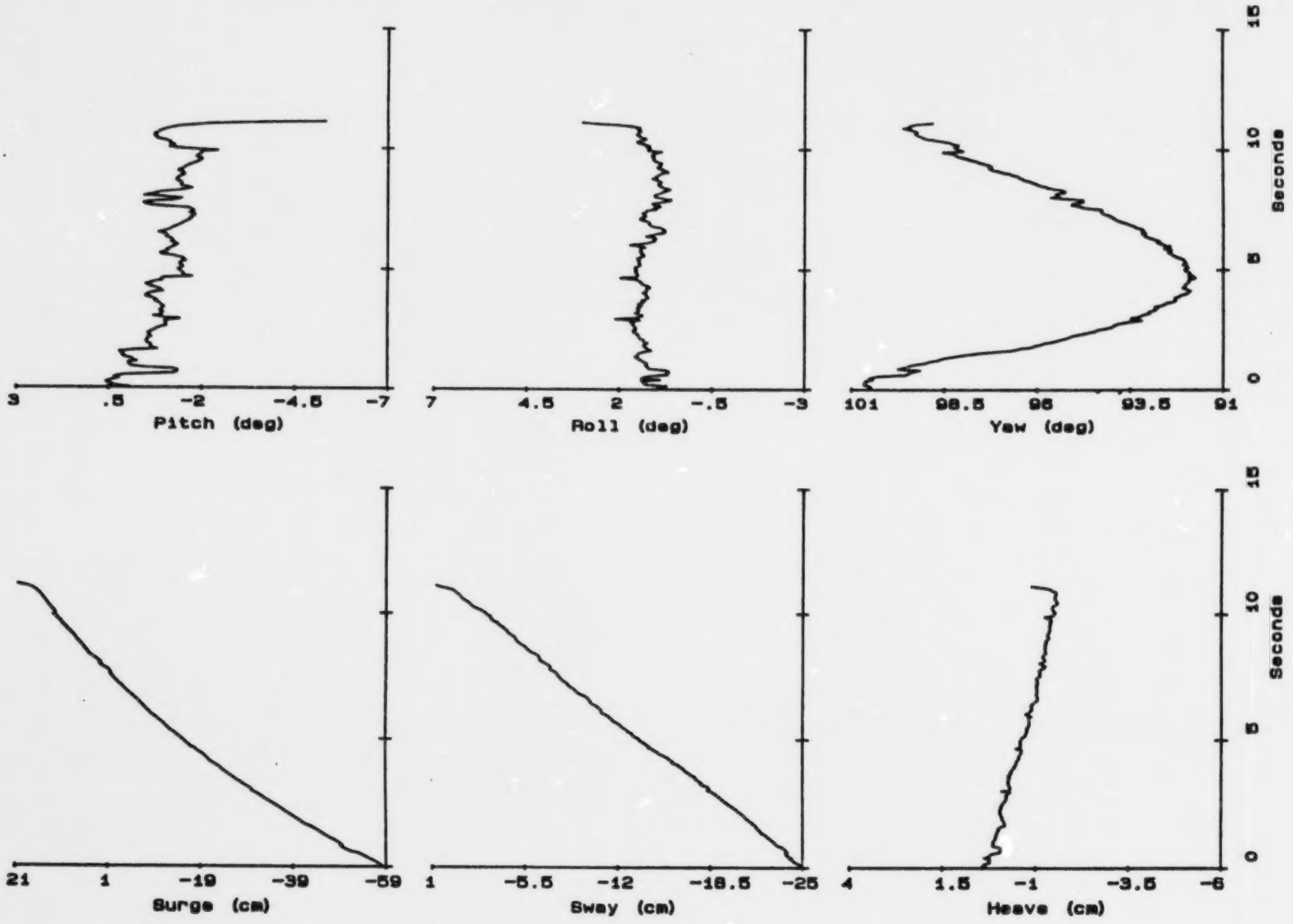

Figure 6.27 (Test #76, 77, 78) Free Drift Test, Selspot Data

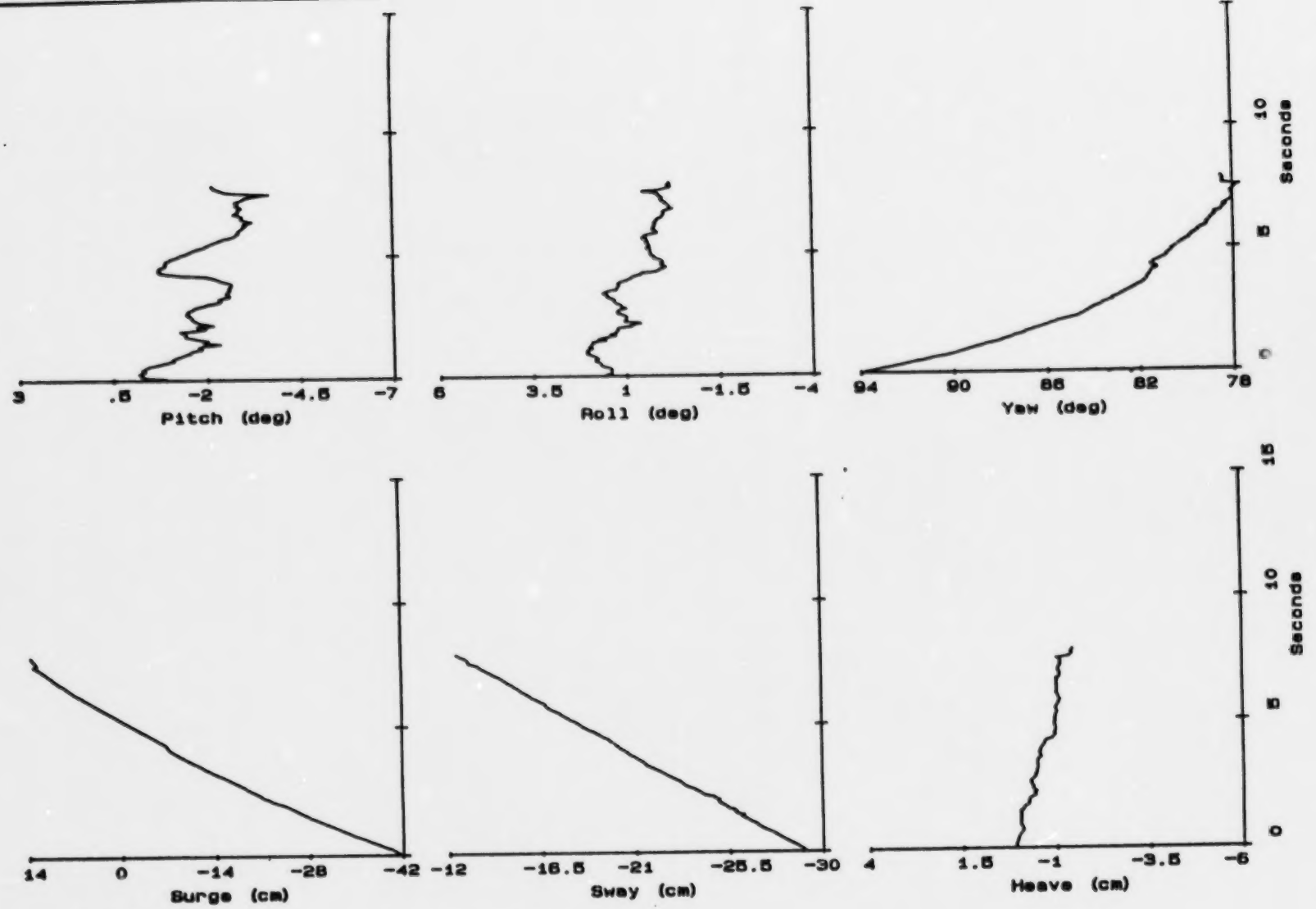

Figure 6.28 (Test #76, 77, 78) Free Drift Test, Selspot Data

current is greater than 0.6 m/s, both from the point of view of iceberg stability and the provision of adequate towing power.

- The simple pendulum system with a constant line is not a feasible alternative as the current speed required for impact is too high. However, a tow line added to this setup greatly improved the impact velocity.
- The iceberg rotates considerably when using the current to the best advantage. This may cause handling difficulties with the berg.
- It is possible to impact right on target, with sufficient coordination between the towing forces. The presence of a current makes this operation difficult. However, tugboats with varying speed and towing force offer more flexibility than the experimental set-up. Also, the modified pendulum with a single pulley reduced the required towing force.
- After release, the iceberg drifted a distance of approximately three and a half iceberg lengths at the range of speeds tested.
- The berg attained a model speed of 0.106 m/s at a towing force of 181 grams.
- The drag coefficients on the cube and the sphere fall within the expected range at velocities above 0.2 m/s.
- As the iceberg model tested was weighted slightly it was more stable than full scale. At high currents or during fast iceberg rotation there may be more stability problems than those experienced during the model tests. During these experiments the model was towed from close to the water line, it may be necessary to tow from closer to the iceberg center of gravity. Further tests could be conducted in this area.
- The Selspot system employed in these tests provided accurate and valuable information for looking at the overall motion of the model.

APPENDIX I

MECHANICAL REQUIREMENTS FOR LARGE SCALE ICE INDENTATION

Impact force, impact energy and towing force required to develop indentation areas of 30 m^2 and 300 m^2 are worked out. The ice crushing strength is assumed piecewise constant and the indentor spherical with a depth of indentation equal to 1/10 of the radius.

Let R = spherical indentor radius
x = indentation depth
α = x/R

Then:

Contact area $A = 2\pi R^2 \alpha$
Normal area $A_p = \pi R^2 \alpha\ (2-\alpha)$

Crushed volume $V = \pi R^3 \alpha^2\ (1-\alpha/3)$

If the ice crushing strength is assumed constant, then

Maximum contact force $F = \sigma A_p$
Crushing energy $E = \sigma V$

Typically assume $\alpha = 1/10$. Also assume $\sigma = 3.3$ MPa. Then

$R = (5A/\pi)^{1/2}$
$F = 2 \times 10^6\ R^2$ Newton $= (A/\pi)10^7$ N

$E = 10^5\ R^3$ Joule $= 10^5\ (5A/\pi)^{3/2}$ J

Impact force increases as A. Impact energy increases as $A^{1.5}$.

Example 1 $A = 3.0\ m^2$
$F = .95 \times 10^7$ N = 1000 tonnes $E = 10^6$ J
Comparable to POND INLET.

Required water depth, assuming a cubical berg

$$d = \frac{\rho_i}{\rho_w}\left(\frac{m}{\rho_i}\right)^{1/3}$$

$m(10^9$ kg)	d(m)
1.0	93
.5	74
.25	59
.10	43

If the berg is twice as long as wide or deep, above draft can be halved.

Drag force $D = \frac{1}{2}C\rho_w AV^2 = \frac{1}{2}C\rho_w A\, 2E/m$

Again, assume a cubical berg of side L

$$A = \frac{\rho_i}{\rho_w}L^2 \qquad m = \rho_i L^3 \qquad A = \frac{\rho_i}{\rho_w}\left(\frac{m}{\rho_i}\right)^{2/3}$$

$$D = \frac{1}{2}C\rho_w \frac{\rho_i}{\rho_w}\left(\frac{m}{\rho_i}\right)^{2/3} \frac{2E}{m} = CE\left(\frac{\rho_i}{m}\right)^{1/3}$$

Example 2 $A = 30\ m^2$ $\sigma = 3.33$ MPa $C = 1.0$

$R = 6.91$ m $F = 9.5 \times 10^7$ N = 10,000 tonnes $E = 33 \times 10^6$J

Tow Iceberg

m (10^6kg)	V(m/s)	Drag (kN)
500	.36	400
250	.51	500
100	.81	700

Ram Ship

m (10^6kg)	V(m/s)
2.6	5.0
10.6	2.5

Example 3 $A = 90\ m^2$ $R = 6.91$ m

$A(m^2)$	$\sigma(10^6$ Pa)	$\Delta E(10^6$J)	$\Delta F(10^6$N)
30	3.0	30.06	85.5
60	2.8	28.06	79.8
90	2.6	26.05	74.1
		84.17	239.4

Tow iceberg

m(10^6kg)	V(m/s)	Drag(10^6N)
500	.58	1.02
250	.82	1.29
100	1.3	1.75

Example 4 $A = 300\ m^2$ $R = 6.91\ m$

$\Delta(m^2)$	$g(10^6\ Pa)$	$\Delta E(10^6 J)$	$\Delta F(10^6 N)$
30	3.0	30.06	85.5
60	2.8	28.06	79.8
90	2.6	26.05	74.1
120	2.4	24.05	68.4
150	2.2	22.04	62.7
180	2.0	20.04	57.0
210	1.8	18.04	51.3
240	1.6	16.03	45.6
270	1.4	14.03	39.9
300	1.2	12.02	34.2
		210.42	598.5

Tow iceberg

$m(10^6\ kg)$	V(m/s)	Drag$(10^6 N)$
500	.92	2.55
250	1.3	3.22
100	2.0	4.37

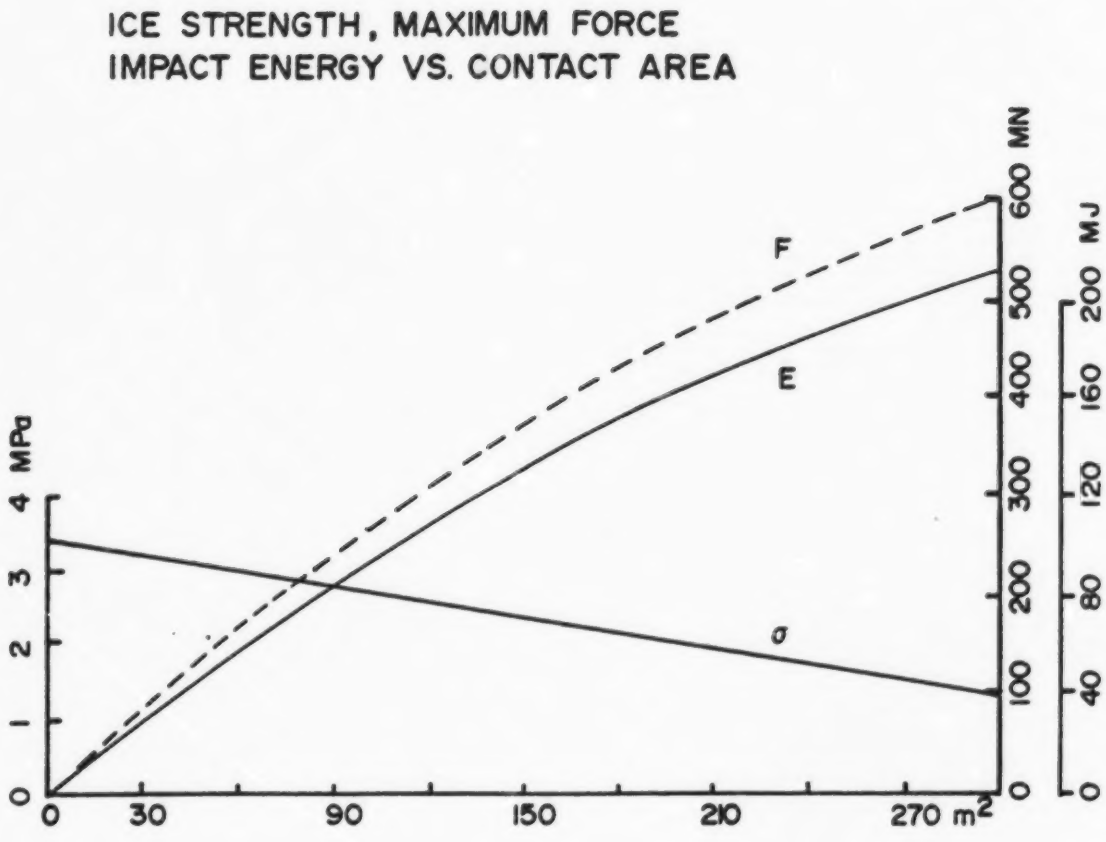
ICE STRENGTH, MAXIMUM FORCE
IMPACT ENERGY VS. CONTACT AREA
F
E
σ
0 1 2 3 4 MPa
0 100 200 300 400 500 600 MN
0 40 80 120 160 200 MJ
0 30 90 150 210 270 m²

Figure 1.1 Ice Strength (σ - MPa), maximum force (F - MN), and impact energy (E - MJ) versus contact area (m^2).

APPENDIX II

CALCULATION OF TOWING FORCE CAUSED BY FALLING WEIGHTS

Let $x(t)$ and $u(t)$ be the instantaneous positions of points on the iceberg and the tow rope. α is the angle between the tow rope and the direction of motion of the iceberg. d is the distance between the impact target and the point of attachment (pulley) of the tow rope.

$$u(t) = x(t)/\cos\alpha(t) = x(t)\,(1 + \tan^2\alpha)^{1/2} = x(t)\,(1 + d^2/x^2(t))^{1/2}$$

$$\dot{u}(t) = \dot{x}(1 + d^2/x^2)^{1/2} - \dot{x}(d^2/x^2)\,(1 + d^2/x^2)^{-1/2}$$

$$\ddot{u}(t) = \ddot{x}(1 + d^2/x^2)^{-1/2} + (\dot{x}^2/x)\,(d^2/x^2)\,(1 + d^2/x^2)^{-3/2}$$

$$\ddot{u}(t) = \ddot{x}\cos\alpha + (\dot{x}^2/x)\sin^2\alpha\cos\alpha$$

Towing force $T = m(g - \ddot{u})$

Example: $d = 0.50\text{m}$ $x = 1.0\text{m}$ $\dot{x} = 0.1\ \text{m/s}$ $\ddot{x} = 0.01\ \text{m/s}^2$

$$\ddot{u} = .01(1 + .25)^{-1/2} + .01 * .25(1 + .25)^{-3/2} = 1.07\text{x}10^{-2}\ \text{m/s}^2$$

Negligible in comparison to $g = 9.81\ \text{m/s}^2$.

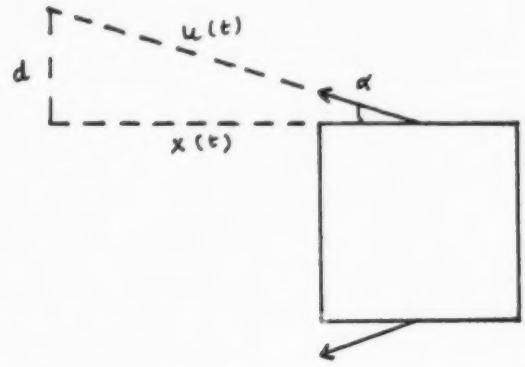

APPENDIX III

STATEMENT OF WORK FROM THE DEPARTMENT OF PUBLIC WORKS

Title: Testing of Iceberg Impact

Background:

At present iceberg impact forces are calculated using iceberg strength values based on small scale tests. Even industry's latest work using indentor equipment on a grounded iceberg in Pond Inlet only tested crushed areas up to three square metres. Experience with the loading of sea ice on arctic structures, however, indicates that the effective strength of ice is reduced as the contact area is increased. It is very plausible that iceberg ice would be affected in the same manner. If a large iceberg were to strike a fixed platform, the contact area of the crushed ice would be in the range of 300 to 600 square metres. The effective strength of this large contact area would probably be much lower than the results from small scale tests suggest. But before an engineering team can use this information in the design of platforms, real loads resulting from large scale iceberg failures must be measured.

Relation to Energy Development, Departmental Mandates and Industrial Activities:

Iceberg impact force is one of the main design considerations for offshore structures located in the East Coast and Grand Banks area. It is critical in terms of its impact on the safety and cost of the individual structures. Up to now, accurately predicting iceberg impact force on offshore structures is one of the major uncertainties in the same and efficient design of such structures. The laboratory and field simulation

efficient design of such structures. The laboratory and field simulation of iceberg impact on offshore structures as proposed in this project will lead to an improved estimation of iceberg impact forces.

Public Works Canada, as the design and construction agency of the Federal Government, has a mandate to conduct applied research and transfer new technology to design and construction units within PWC and other government departments engaged in architectural and engineering activities through its appropriate product lines. This mandate also includes the transfer of technology to industry which provides architectural and engineering services to the Federal Government.

The results of the work will have immediate applications both to design and regulatory work. The ice force prediction methods developed in the course of this study will be made available to the private sector for designing offshore structures in ice infested water.

Statement of Work:

In order to achieve the above objectives, a four-year research program has been developed. Each succeeding phase will only be undertaken depending on the recommendations of the proceeding phase.

1987/88 Phase 1

Will be a detailed feasibility study which will define the requirements for the experiment, in relation to the hardware specifications, the site location, operational methods, instrumentation and analysis. This phase will also include simple model testing in a test flume in order to

demonstrate the pendulum/winching system. Also during this phase, prospective sites will be identified based on iceberg flux data, bathymetric charts and logistic infrastructure. A preliminary cost estimate will be prepared.

1988/89 Phase 2

Will only be undertaken if Phase 1 is successful. Included will be an actual site survey, consisting of detailed bathymetry and current measurements. Detailed engineering and planning, including measurement and recording techniques, will be carried out.

1989/90 Phase 3

Will consist of equipment procurement, installation and the first seasons experiments. The first season's experiments will be designed to be implemented at minimum cost. Instrumentation and recording devices will be low cost. Possibly consisting of motion packages on the iceberg and distance meters (to measure deceleration), plus high-speed cameras to capture the iceberg failure process.

1990/91 Phase 4

Will be implemented if Phase 3 is successful. It will involve building and testing and instrumented structure on the cliff face which better simulates an actual structure, and can be instrumented for both global and local ice forces.